8-2015

A Century of Geomorphic Change of the San Rafael River and Implications for River Rehabilitation

Stephen T. Fortney
Utah State University

A CENTURY OF GEOMORPHIC CHANGE OF THE SAN RAFAEL RIVER AND IMPLICATIONS FOR RIVER REHABILITATION

by

Stephen T. Fortney

A thesis submitted in partial fulfillment
of the requirements for the degree

of

MASTER OF SCIENCE

in

Watershed Science

Approved by:

_____	_____
Dr. John C. Schmidt Major Professor	Dr. Janis L. Boettinger Committee Member
_____	_____
Dr. Joseph M. Wheaton Committee Member	Dr. Mark R. McLellan Vice President for Research and Dean of the School of Graduate Studies

UTAH STATE UNIVERSITY
Logan, Utah

2015

ABSTRACT

A Century of Geomorphic Change of the San Rafael River and Implications for River Rehabilitation

by

Stephen Tinley Fortney, Master of Science

Utah State University, 2015

Major Professor: Dr. John C. Schmidt
Department: Watershed Sciences

Beginning in the early 20th century and continuing into the 21st century, the lower 87 km of the San Rafael River in central Utah underwent rapid geomorphic changes. Extensive water development in the headwaters, invasion of the non-native tamarisk shrub, and man-made perturbations to the channel-floodplain system have been responsible for the changes that we documented in this study. We used a combination of spatially robust and temporally precise methods to reconstruct the modern history of channel change and identify the processes responsible for those changes. These methods include analysis of historic aerial photographs, analysis of USGS gage data, dendrogeomorphic analysis of floodplain stratigraphy, and comparison of historic and modern longitudinal profiles.

The San Rafael River changed from a wide, shallow, heterogeneous channel to a narrow, deep, homogeneous channel. Specifically, between 1938 and 2009, the San

Rafael River along the length of the entire study area narrowed 83%. Additionally, the floodplain vertically accreted between 1.0 and 2.5 m. The majority of the channel narrowing occurred during two distinct time periods - 1952 to 1979 and 1987 to the present - when low, mean annual stream flow was low. Channel narrowing is primarily due to the reduction in transport capacity, but when coupled with tamarisk establishment, channel narrowing and floodplain aggradation has been rapid.

We documented the spatial extent of channel bed changes over the course of the 20th century. We found that the channel bed aggraded in five segments, lowered in one segment, and remained the same in the other portions of the study area. Analysis of historic, precise measurements of bed elevation at the USGS gage 09328500 revealed that the channel bed incised between Hatt's Ranch and MacMillan Lower Ranch Dam during two time periods: from 1952-1965 and 1983 to the present. Both episodes of incision were caused by unequal amounts of scour and fill. This imbalance in bed fluctuation was induced by human modification of the channel during the first episode and lowering of the local base control during the second episode of incision.

The changes to the physical template of the San Rafael River have implications for the management of three endemic fish – the roundtail chub (*Gila robusta robusta*), the bluehead sucker (*Catostomus discobolus*), and the flannelmouth sucker (*Catostomus Latipinnis*) – which currently utilize the study area. Future management of the river will benefit from the results of our study, which reveal the physical processes that are responsible for the historic and current condition of the river.

(211 pages)

PUBLIC ABSTRACT

A Century of Geomorphic Change of the San Rafael River and Implications for River Rehabilitation

Stephen T. Fortney

Suspended-load rivers are subject to rapid geomorphic changes. In particular during the Holocene Epoch, arroyos of the Colorado Plateau experienced several periods of rapid erosion and aggradation. The most recent period of entrenchment occurred around the turn of the 20th century. The mechanisms responsible for the modern period of aggradation that has followed the most recent period of entrenchment have not been well documented. The research presented in this thesis reveals the mechanisms responsible for modern alluviation of the San Rafael River, which drains the Colorado Plateau

The lower 87 km of the San Rafael River, which enters the Green River south of the town of Green River, UT has experienced rapid geomorphic changes during the last 100 years. To quantify these changes, we used a complement of temporally precise and spatially robust methods. By understanding the rates, magnitudes and types of geomorphic changes, we could then identify the mechanisms of these channel changes.

The San Rafael River narrowed by 83% between 1938 and 2009 and the floodplain aggraded 1.0 to 2.5 m. Channel narrowing was caused by a reduction in the transport capacity of the river, and was accelerated by the establishment of vegetation, including the non-native tamarisk shrub, on active channel surfaces and the floodplain. Significant water withdrawals during the 20th century have primarily been responsible for the reduction in transport capacity by decreasing the magnitude and duration of the annual snowmelt flood. During this time period, monsoon floods continued to deliver large quantities of fine sediment to the channel.

During the 20th century, the channel bed incised in one segment and aggraded in five segments. The two periods of incision that we documented were related to human modifications of the channel and floodplain.

With the knowledge of the physical processes that have been responsible for the channel changes in the San Rafael River, prediction of future channel conditions can then be made. The changes to the physical template of the San Rafael River have implications for the management of three endemic fish – the roundtail chub (*Gila robusta robusta*), the bluehead sucker (*Catostomus discobolus*), and the flannelmouth sucker (*Catostomus latipinnis*) – which currently utilize the study area.

ACKNOWLEDGMENTS

I would like to thank the Natural Resources Conservation Services for funding this study. I would like to thank Jack Schmidt for giving me the opportunity to work on an amazing project in a beautiful part of the world. I cannot thank Jack enough for his guidance as well as his patience while I learned the skills that were necessary to complete the project. Jack's knowledge of the Colorado Plateau and the hydrology and geomorphology of the rivers that cross this spectacular landscape is unsurpassed, and my work greatly benefited from this. Also, the excellent work that Jack's former students have completed on projects similar to mine in places such as the Green River, Colorado River, Duchesne River, and Rio Grande River provided a great foundation of knowledge on which to build my work.

During my time at Utah State University, I had the privilege of working among an amazing group of people that were Jack's lab. In particular, my research greatly benefitted from the mentorship of my lab mates: Dave Dean, Milada Majerova, Susannah Erwin, and Rebecca Manners. Dave Dean deserves special attention, for he got me on track when I first started and he took the lead on digging and interpreting the Hatt's Ranch trench. He also provided logistical support for my research as well as technical advice to me as I analyzed, what seemed like, an insurmountable amount of data. Other folks who deserve attention for either helping me in the field or conducting grain size analysis in the lab include Alan Saltzman, Ashton Montrone, Jon Harvey, Michelle Summa-Nelson, Ryan Dutson, Martin Schroeder, and Amrith Gardihewa. Also, I would like to thank my committee members Dr. Joseph Wheaton and Dr. Janis Boettinger for

their unique perspectives on geomorphology and for providing friendship and professional support during my work. Dr. Peter Wilcock also provided guidance during the process of untangling the story of channel change of the San Rafael River.

Our collaborators - USU Fish Ecology Lab, USU Luminescence Laboratory, Utah Division of Wildlife Resources, and Bureau of land Management - deserve recognition for their support and help with the project.

Last but not least, I would like to thank my family who have been supportive of me (or at least faked it well enough for me to believe it) throughout the duration of the time that it took to complete my degree. My wife, Mijanou, deserves the most amount of appreciation. Finally, I want to thank my kids, Elias and Sally, for being wonderful. I look forward to the time when they get the opportunities to learn more than I know about the rivers and the places of this world.

Stephen Fortney

CONTENTS

Page

LIST OF TABLES

LIST OF FIGURES

CHAPTER 1

INTRODUCTION

The size and shape of a stream channel is determined by the balance in the supply of water and sediment, as well as the erodible character of the channel banks. Lane (1954) expressed the balance of channel forming forces in the following proportional relation:

$$Q_s d \propto Q_w S$$

where Q_s is the sediment supply, d is the diameter of the bed material, Q_w is the stream flow, and S is the slope of the channel. Later in Borland (1960), Vitaliani illustrated Lane's proportional relation as a channel stability balance (Figure 1.1). The relation is useful in a qualitative manner to predict the type of change that will occur if one of the variables in the equation is altered. For example, if there is a reduction in stream flow and/or channel slope and the supply of sediment remains constant, the channel stability balance predicts that the river will accumulate sediment. On the other hand, if there is a reduction in the supply and/or caliber of sediment, the equation predicts that the channel would degrade or evacuate sediment. When transport capacity equals sediment supply, the stream channel is considered to be in equilibrium, and a 'natural' range of channel adjustment would be expected. Recently, Schmidt and Wilcock (2008) have shown that when Lane's relation is quantified, it can provide more utility than a just conceptual or hypothetical understanding of channel response to changes in flux boundary

conditions. In particular, Schmidt and Wilcock (2008) proved it can be used to quantitatively assess the downstream effects of dams on the geomorphology of rivers.

Perturbations in the sediment mass balance may manifest in changes to a channel in four ways: bed material, channel slope, channel cross-section geometry, and planform. The adjustment of each of these characteristics takes place over different time scales. For example, a perturbation would yield a response in channel geometry such as width and depth in the least amount of time, whereas channel slope would require the greatest amount of time to respond to a perturbation (Knighton, 1998).

Changes in channel characteristics may result in changes to the type and distribution of aquatic habitat. A change in planform from a braided channel to a single-threaded, meandering channel may result in the reduction of the quantity and quality of complex aquatic habitat i.e., off-channel habitat, pool frequency, etc. In rivers where aquatic habitat has been homogenized, a decrease in habitat suitability may result in a decrease in the survival, growth, and abundance of riverine species. For example, in the Colorado River Basin where dams have cut off the supply of sediment one of the factors currently limiting the viability of the population of endangered Razorback Suckers is the lack of warm food-rich floodplain habitat (Wydoski and Wick, 1998). More specifically, in the San Rafael River, a tributary located within the Colorado River Basin, Bottcher (2009) found that that lack of pools in the lower 90 km is currently restricting the viability of the Roundtail Chub; and the lack of riffles, which are normally associated with gravel substrates and higher water velocities, is affecting the viability of the

Bluehead Sucker. Understanding what changes to the aquatic habitat have occurred and how they have occurred will yield important insight into how to best manage these "sensitive" fish populations.

The San Rafael River, which drains a portion of the northern Colorado Plateau, has experienced both natural and anthropogenic perturbations during the 20th century. The non-native tamarisk shrub has colonized many areas of the alluvial valley. Also, in the headwaters, there has been extensive water development for agricultural and industrial purposes. In the lower 90 kilometers of the river, a diversion dam acts as a barrier to the upstream movement of endemic fish. These 20th century perturbations have influenced the current form and function of the San Rafael River, which is currently lacking in complex aquatic habitat (Bottcher, 2009). An historical assessment of the river will help elucidate the magnitude, rate, and style of channel changes, and the mechanisms responsible for the changes.

There are four steps involved in an historical assessment of a river. The first step is to describe the character and behavior of the current condition of the river. In this step it is important to not only characterize the channel but also the floodplain and the geomorphic organization of the alluvial valley (see Chapter 2). The second step is to describe the historic condition of the river (see Chapter 3). By describing the current and historic condition of the river, it will be possible to diagnosis the physical processes that are responsible for the current and historic conditions, as well as any channel changes

that have occurred. Ultimately, an understanding of the processes responsible for channel changes can then be used to predict the future condition of the river (see Chapter 3).

An historical assessment must be conducted over a broad enough spatial area in order to account for the diversity of channel morphologies encountered in various valley settings. Valley segments may differ in a variety of characteristics including valley width, valley slope, base level control, human impacts; these differences may manifest in different types of channel morphology. In addition to the influence of valley setting, the position within the network may result in a diversity of channel morphologies.

The time span over which an historical assessment is conducted must be long enough to diagnose the capacity for a channel to adjust not only in recent time periods but also historical time periods. If changes to the sediment regime, stream flow regime, or bank properties have occurred, an analysis of the historical data will provide insight into the style of channel responses, as well as illuminate differences between river behavior and channel change.

The definition of river behavior is different from the definition of channel change. Specifically, channel change is a wholesale shift in channel behavior (Brierley and Fryirs, 2005). For example, along the length of a river, a range of channel forms may occur. These forms are the result of the "behavior" of a river. During this time period, the flux boundary conditions that are operating on the river i.e., sediment flux and water flux do not change (Figure 1.2). However, when there is a change in these fluxes either in the frequency, magnitude, or duration of these fluxes, then a wholesale shift in the

occurrence and type of channel forms may occur. This is referred to as a channel change. Channel changes will often result in changes to the quality and quantity of aquatic habitat.

In addition to understanding changes to aquatic habitat, an historical assessment of the San Rafael River will contribute to the knowledge of how similar types of Colorado Plateau rivers behave. The San Rafael River is similar to many rivers that flow across the Colorado Plateau, which have undergone several cycles of erosion and aggradation during the Holocene Epoch (Bryan, 1925; Bailey, 1935; Antevs, 1952; Cooke and Reeves, 1976; Graf, 1983; Webb, 1985; Hereford, 2002; Webb etal., 2007). Following the most recent, historical period of entrenchment, researchers have documented a modern period of alluviation in many of these rivers (Emmett, 1974; Love, 1979, 1983; Leopold, 1976; Patton and Schumm, 1981; Hereford, 1984; Hereford, 1986; Hereford, 1987; Graf etal., 1991; Webb and Hereford, 2010). It is generally agreed upon that the modern period of alluviation has been characterized by some degree of channel narrowing, tamarisk establishment, and floodplain development. However, there has been no consensus on the mechanisms responsible for these changes and the magnitude, rates, and style of alluviation have been poorly described. Since many of these Colorado Plateau streams have relatively similar hydrologic regimes and sediment supply characteristics, and they have all been invaded by the non-native tamarisk shrub, then determining the mechanisms responsible for modern alluviation will aid in the prediction of future channel responses, as well as inform how these rivers have behaved in the

recent geologic past. Also, by documenting the pattern, rates, and magnitude of alluviation, it is possible to estimate the amount of sediment stored – these estimates are useful to managers of downstream dams where sedimentation in reservoirs is a concern.

More specifically, results from an historical assessment will inform the management and proposed rehabilitation of the San Rafael River. A plan to rehabilitate the river should be guided by an understanding of the processes that govern the present-day channel form as well as the future trajectory of the river. For example, knowledge of the historic and present channel-forming processes will help the "restoration" community determine which projects will have the best chance for success, what to expect during the implementation of a project and following the completion of a project, and how to achieve the greatest amount of benefit for a given amount of investment. Furthermore, managers must decide on the pathway of action, whether it be restoration of a pre-disturbed ecosystem, rehabilitation of certain attributes of the river, or just mitigating future undesired changes (Figure 1.3) In the San Rafael River, there are ongoing efforts to remove tamarisk and determine the minimum stream flow necessary to sustain aquatic habitat - both efforts will benefit from a scientific investigation of historical channel adjustments. Finally, this study will contribute to the general understanding of how a suspended-load river behaves and be useful for management of similar types of rivers.

1.1 References Cited

Antevs, E. 1952. Arroyo cutting and filling. Journal of Geology, 60, 375-385.

Bailey, R.W., 1935, Epicycles of erosion in the valleys of the Colorado Plateau province. J. of Geology 43, 337-355.

Borland, W. M., 1960. Stream channel stability. United States Bureau of Reclamation, Denver Lane.

Bottcher, J.L., 2009. Maintaining population persistence in the face of an extremely altered hydrograph: implications for three sensitive fishes in a tributary of the Green River, Utah. M.S. Thesis, Utah State University, Logan, UT,

Brierley, G. J., Fryirs, K. A. (2005). Geomorphology and river management: Applications of the River Styles framework. Blackwell Science, Oxford, UK. (398 pp.).

Bryan, K., 1925. Date of channel trenching (arroyo cutting) in the arid southwest. Science 62, 338-344.

Cooke, R.U., Reeves, R.W., 1976. Arroyos and environmental change. Clarendon Press, Oxford, UK. (213 pp.).

Emmett, W.W., 1974. Channel aggradation in western United States as indicated by observations at Vigil Network sites: Zeitschrift fur Geomorphologie, Supplement Band 21, v. 2, 52-62.

Graf, J.B., Webb, R.H., Hereford, R., 1991. Relation of sediment load and flood-plain formation to climatic variability, Paria River drainage basin, Utah and Arizona. Geol. Soc. Amer. Bull. 103, 1405-1415.

Graf, W.L., 1983, The arroyo problem-Paleohydrology and paleohydraulics in the short term, in Gregory, K.J., (Ed.), Background to paleohydrology, John Wiley and Sons, New York, pp 279-302.

Hereford, R. 1984. Climate and ephemeral-stream processes: Twentieth-century geomorphology and alluvial stratigraphy of the Little Colorado River, Arizona: Geol. Soc. Amer. Bull. 95, 654-668.

Hereford, R., 1986. Modern alluvial history of the Paria River drainage basin. Quaternary Research 25, 293-311.

Hereford, R., 1987. The short term: fluvial processes since 1940, in, Graf, W.L., ed., Geographic systems of North America: Boulder, Colorado, Geological Soc. of America Centennial Special Paper, 2, 276-288.

Hereford, R., 2002. Valley-fill alluviation during the Little Ice Age (Ca A.D. 1400-1880), Paria River basin and southern Colorado Plateau, United States. Geol. Soc. Amer. Bull. 114, 1550-1563.

Knighton, A.D., 1998. Fluvial forms and processes: a new perspective. Arnold, London, UK. (383 pp).

Lane, E.W., 1954. The Importance of fluvial morphology in hydraulic engineering. U.S. Bureau of Reclamation Hydraulic Laboratory Report No. 372, 1-19.

Leopold, L.B., 1976. Reversal of erosion cycle and climatic change. Quaternary Res. 6, 557-562.

Love. D.W., 1979. Quaternary fluvial geomorphic adjustments in Chaco Canyon,. New Mexico. In: Rhodes D. D. and Williams, G.P., eds., Adjustments of the fluvial system: Kendall/Hunt, Dubuque, Iowa, pp. 277-308.

Love, D.W., 1983, Quaternary facies in Chaco Canyon and their implications for geomorphic-sedimentologic models, in Wells, S.G., Love, D.W., and Gardner, T.W., eds., Chaco Canyon Country, Albuquerque, New Mexico: Field Trip Guidebook, 1983 Conference, American Geomorphological Field Group, p. 195-206.

Patton, P.C., Schumm, S.A., 1981. Ephemeral-stream processes: implications for studies of Quaternary valley fills. Quaternary Res. 15, 24-43.

Schmidt, J.C., Wilcock, P.R., 2008. Metrics for assessing the downstream effects of dams. Water Resour. Res. 44, W04404, (19 pp.).

Webb, R. H., Leake, S. A., Turner, R.M., 2007. The ribbon of green: change in riparian vegetation in the southwestern United States. University of Arizona Press, Tucson, AZ (462 pp).

Webb, R.H., 1985. Late Holocene flooding on the Escalante River, south-central Utah. Ph.D. Thesis. University of Arizona, Tucson, AZ (204 pp.).

Webb, R.H., Hereford, R., 2010. Historical arroyo formation: documentation of magnitude and timing of historical changes using repeat photography. In: Webb, R.H., Boyer, D.E., Turner, R.M., (Eds.), Repeat Photography: Methods and Applications in the Natural Sciences, Island Press, Washington D.C., USA. pp. 89-104.

Wydoski, R. S., Wick, E.J., 1998. Ecological value of floodplain habitats to razorback suckers in the Upper Colorado River Basin. USFWS. Upper Colorado River Basin Recovery Program, Denver, Colorado. 55 pp.

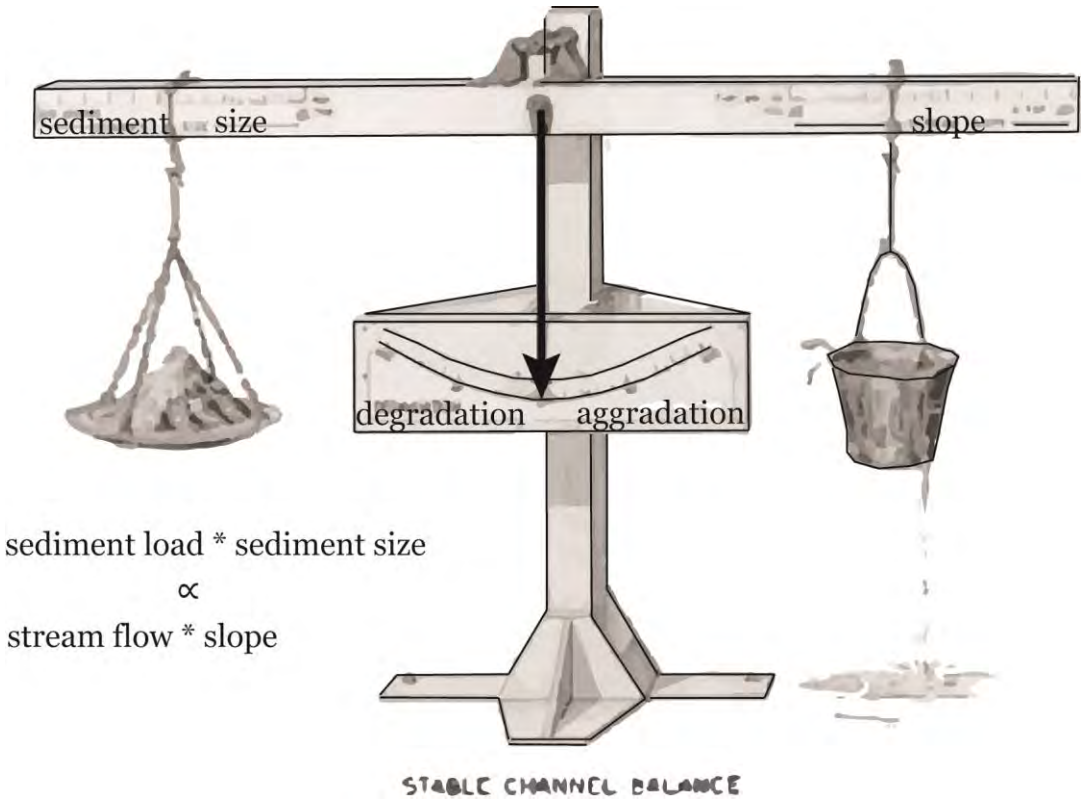

Figure 1.1. Channel stability balance, modified from Vitaliani's illustration and conceived by Borland (1960) and Lane (1954).

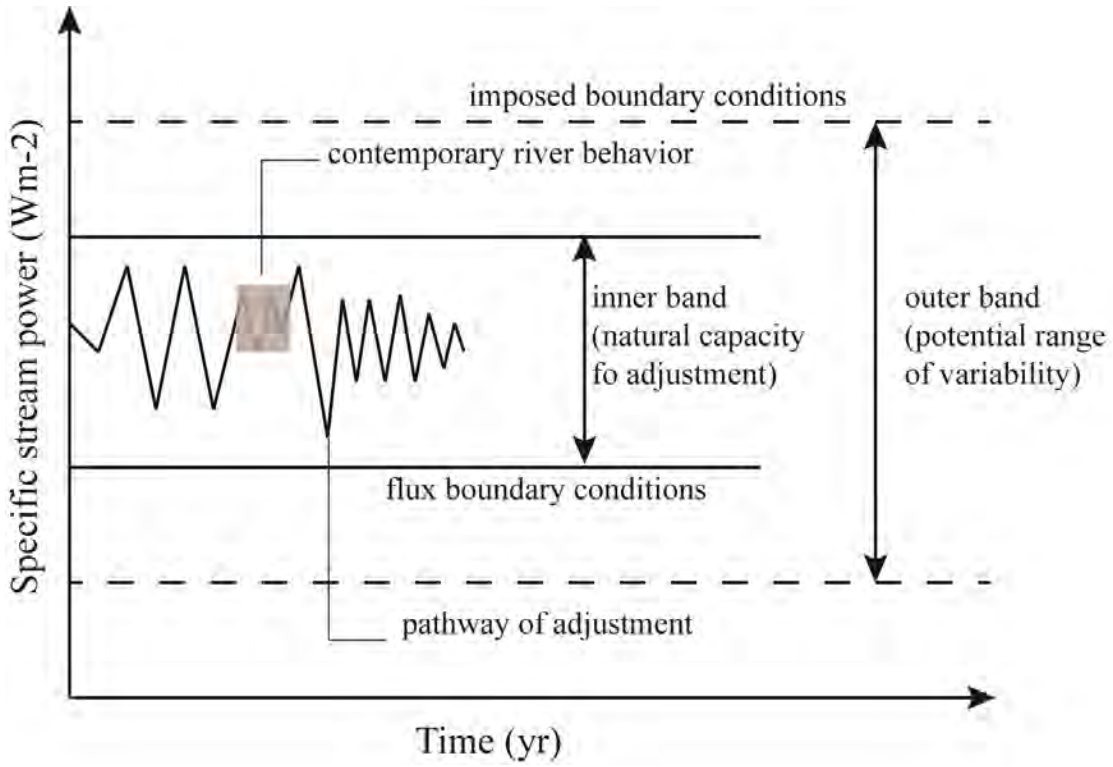

Figure 1.2. River evolution diagram [modified from Brierley and Fryirs (2005)]. The natural capacity of adjustment includes all of the possible morphologies of a river that could occur in a period of time when flux boundary conditions have not changed. The contemporary behavior of a river is a snapshot in time of the natural capacity of river adjustment. Channel change is induced by a change in the flux boundary conditions e.g. sediment load and stream flow. But, the range of potential adjustment, even during wholesale shifts in channel form, is limited by the imposed boundary conditions, which include the river reach's position in the watershed, geology and tectonics, valley width, valley slope, and base level.

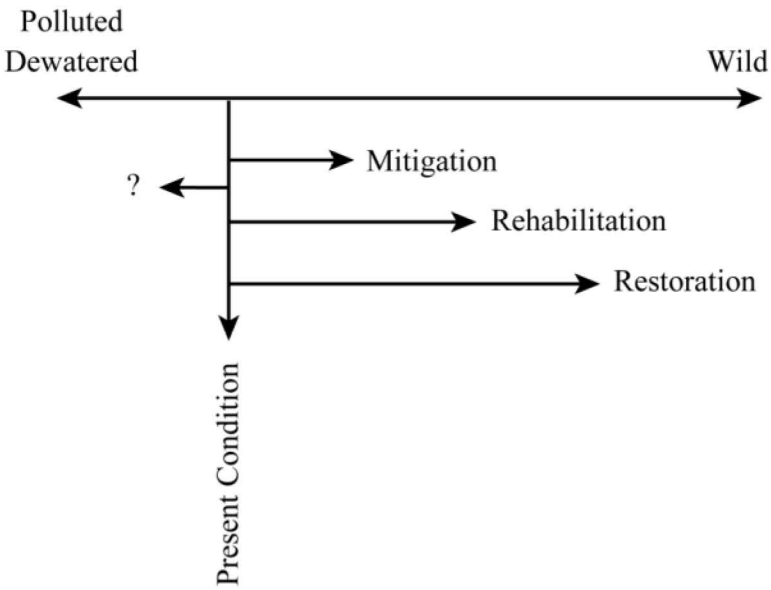

Figure 1.3. Restoration is the return of an ecosystem to its pre-disturbance condition. Rehabilitation is the reestablishment of some attributes of the ecosystem to their pre-disturbance condition. In the case of the San Rafael River, complete restoration is impossible, and policy choices must be made to identify which attributes should be partly restored.

CHAPTER 2

GEOMORPHIC ORGANIZATION OF THE LOWER 87 KILOMETERS OF THE SAN RAFAEL RIVER, UTAH

2.1 Introduction

Alluvial rivers are dynamic systems and are influenced by geomorphic processes and disturbances that vary across spatial and temporal scales. For example, types of channel morphology occurring across a physiographic province may be similar, because a province may experience similar geologic and climate processes. On the other hand, channel morphology within an individual river system may differ because it is subject to local processes such as man-made channel modification, or log jams or other hydraulic features. A geomorphic unit, such as a pool or a riffle, is not only subject to local processes but is influenced by the spatial hierarchy of processes acting at the scale of a channel reach, valley segment, entire watershed, or geomorphic province (Frissell et al., 1986; Montgomery and Bolton, 2003). Furthermore, the processes that influence channel morphology are active over a range of temporal scales. For example, tectonic uplift occurs over geologic time scales and may influence the distribution and character of aquatic habitat over the length of a valley segment. On the other hand, an individual flood may scour and fill the channel and rearrange aquatic habitat over the time period of less than a day. In general, broad-scale controls ultimately determine channel morphology, which in turn governs the distribution and character of aquatic habitat (Figure 2.1).

In this chapter, we describe the geomorphic organization of the lower San Rafael River between the San Rafael Reef and the confluence with the Green River. The lower San Rafael River is organized into five valley segments. We use several data sources in our determination and characterization of the valley segments including results from GIS analysis, a longitudinal profile survey, geomorphic mapping, and dendrogeomorphic analysis of floodplain deposits.

Our characterization of the geomorphic organization of the lower San Rafael River is intended to assist investigators in the ongoing effort to manage populations of three "sensitive" (UDWR, 2006) fish species. Recently, researchers have documented the behavior, habitat preferences, and limiting factors of roundtail chub (Gila robusta), flannelmouth sucker (Catostomus latipinnis), and bluehead sucker (Catostomus discobolus), and found that low availability of complex habitat may be limiting the distribution and abundance of these endemic fish in the lower San Rafael River. In particular, the paucity of pools is currently restricting the growth, survival, and recruitment of roundtail chub (Bottcher, 2009). Furthermore, the lack of riffles, which are normally associated with gravel substrates and higher water velocities, is affecting the viability of the bluehead sucker (Bottcher, 2009). The disconnection between the channel and the floodplain is further limiting access to the large amount of biological activity, organic matter, and nutrients typically found in the channel/floodplain system (Sparks et al., 1990). Presently, work is being conducted to determine minimum stream flows that might benefit these endemic fish populations.

Characterization of the geomorphic organization of the study area also contributes to a catchment-framed understanding of the relevant spatial and temporal scales that control channel morphology and thus arrangement of aquatic habitat. In combination with an analysis of river evolution (see Chapter 3), the results presented here provide a starting point for both the prediction of future river change and determination of the potential for river recovery. Specifically, results from this chapter may be used to determine appropriate reaches where river recovery efforts could be targeted.

2.2 Geologic Setting and Description of Study Area

The San Rafael River watershed (6255 km^2) is located in the northern Colorado Plateau (Figure 2.2). The shape of the watershed is a northwest oriented ellipse. Regional tectonics, as indicated by the dip of bedrock strata, has forced the mainstem river to the northern edge of the watershed (Williams and Hackman, 1971; Trimble and Doelling, 1978). Consequently, the longest tributaries enter the mainstem from the south and southwest.

The headwaters of the San Rafael River drain the east side of the Wasatch Plateau where maximum elevations are 3000 to 3400 m. Three primary headwater streams - Cottonwood Creek, Ferron Creek, and Huntington Creek - join at the eastern edge of Castle Valley to form the San Rafael River. In its downstream course, the river carves through the San Rafael Swell then flows across the San Rafael Desert before joining the Green River, approximately 20 km south from the town of Green River, UT.

The entire length of the San Rafael River (approximately 175 km) can be divided into five major valley segments, based on distinct breaks in slope in the longitudinal profile (Figure 2.3). A description of the 1925 longitudinal profile is presented in Chapter 3. The valley segments alternate between alluvial and bedrock valley types. Valley segments A, C, and E are alluvial valley units where the degree of valley confinement varies from confined to partly confined (Brierley and Fryirs, 2005; Bisson et al., 2006;). Valley segments B and D are primarily bedrock valleys, where there is only a narrow alluvial valley.

Valley segments A, B, C, and D are located within the San Rafael Swell, and valley segment E, the focus area of this study, is located in the San Rafael Desert. The river in valley segment A is 53 km long and begins at the confluence of the three headwater streams in Castle Valley and ends at the upstream end of Black Box Canyon in the Swell. The slope of the channel in valley segment A is consistently 0.0019 (Figure 2.3), however, valley width varies within this valley segment. There are notable parts of valley segment A: Fuller's Bottom, the 23-km long Little Grand Canyon, and the segment where the BLM campground and confluence with Buckhorn Wash are located (Figure 2.2). Downstream from valley segment A is valley segment B, where the river cuts through Permian bedrock – this segment is also known as the "Black Box". Within the Black Box, the canyon walls are as narrow as 5 m and as tall as 150 m. The channel gradient in segment B is 0.0079, a four-fold increase from the channel gradient in valley segment A. Downstream in alluvial valley segment C, the channel slope (0.0026)

decreases as the river winds around Mexican Mountain in a partly confined valley. The valley walls narrow again in a second bedrock valley segment classified as valley segment D. At the downstream end of valley segment D, the river carves an exit from the Swell through he steeply dipping monocline, known as the San Rafael Reef, where bedrock strata dip 45° to 85° to the east (Witkind, 1991). The Reef defines the eastern edge of the Swell and also the upstream boundary of the study area (valley segment E). The average slope of the 90-km long study area (also known as the "lower river") is 0.0011.

2.3 Hydrologic Setting

Three types of floods can occur in the San Rafael River. The snowmelt flood occurs in the spring and early summer. The snowmelt flood originates in the upper elevations of the Wasatch Plateau. Flash flooding is the second type of flood. In the San Rafael River, there are two types of flash floods (hereafter referred to as warm season floods); one type usually occurs in the summer and the other type usually occurs in the fall. The summer floods are caused by convective thunderstorms as a result of the North American Monsoon – these storms may occur anywhere over the watershed but are usually localized. The summer floods usually last just 1 or 2 days and may occur in July, August, or September. The second type of flash flood occurs in October and November as a result of cut-off low pressure cells or dissipating tropical cyclones, or a combination of the two. The fall season floods may last as long as a week and usually occur over

larger spatial areas than monsoon storms. A third, less significant type of flood occurs in the winter and early spring as a result of low intensity precipitation during frontal storms that originate over the Pacific Ocean.

There has been a major shift in the hydrologic regime of the San Rafael River during the 20th century. During the first half of the century, the snowmelt flood was the dominant feature of the annual hydrograph. Analysis of stream-flow measurements made at USGS gage 09328500 (San Rafael near Green River) during the early 20th century show that the median spring snowmelt flood lasted approximately 70 days, and the peak was approximately 37.4 m^3/s. Over the course of the 20th century, extensive water development in the Wasatch Plateau and Castle Valley, in conjunction with decadal scale climate shifts (Webb and Betancourt, 1992; Hereford et al 2002), drastically decreased the magnitude and duration of the annual snowmelt flood (see Chapter 3). Consequently, the median annual snowmelt flood for the period 2000-2008 lasted only 23 days, and the magnitude of the peak flow was approximately 9.8 m^3/s, a respective 67% and 93% reduction from the early 1900's.

Not only has the magnitude of the snowmelt flood decreased but the magnitude of warm season floods has also decreased. There has been a noticeable lack of large magnitude, short duration floods since the late 1950s (Figure 3.10 in Chapter 3). In general, the removal of the snowmelt flood in addition to the decline in the magnitude of warm season floods has resulted in a suppressed annual hydrograph.

2.4 Methods

We mapped the perimeter of the alluvial valley along the entire study area on orthorectified aerial photographs taken in 2009 (1-m resolution). Analyses of stereo-pairs of both the current and the historic aerial imagery (1938, 1962, 1974, and 2010) helped in the determination of the valley perimeter. The scale for each photograph series is shown in Table 3.1 in Chapter 3. We validated in the field the initial results of our geomorphic mapping conducted in a GIS. We delineated the perimeter of the valley based on two criteria: (1) the boundary which exerts controls on the movement of the river channel over the Holocene Epoch, and (2) the differentiation between non-mainstem deposits and mainstem alluvium. Once we mapped the perimeter of the valley, we divided the valley into 1-km increments and computed the area within each 1-km increment. We computed the width at each 1-km increment by dividing the valley floor area by the increment length.

A variety of surfaces including bedrock, tributary fans, slope wash, and aeolian deposits constitute the perimeter of the valley. Areas of slope wash, tributary fans, and aeolian deposits were included within the valley when determined that these deposits did not exert control on the movement of the river channel over geologic time scales. These surfaces were delineated in a GIS and subtracted from the total area of the valley in order to compute the area of mainstem alluvium. Under the current hydrologic regime, some of these types of surfaces exert control on the movement of the channel. Portions of side

canyons, where floodwaters have reentered and recently deposited mainstem alluvium were excluded from the mainstem valley.

We also mapped the geomorphic surfaces in detail in two segments of the study area. The upstream segment is located in the vicinity of Hatt's Ranch and is 3.6 km long. The second segment is located in the vicinity of Frenchman's Ranch and is 4.0 km long. We interpreted the boundaries between the geomorphic surfaces by viewing 2010 imagery (1:10,363) stereoscopically. In October 2011, we field checked our aerial photographic interpretations. The surfaces were mapped based on four criteria: (1) break in slope; (2) elevation above base flow channel; (3) topographical expression including the occurrence of features indicative of a particular map unit; and, (4) topographic slope orientation. In addition, seven attributes were used to characterize each surface: (1) sedimentology, including grain size; (2) soil development; (3) surface topography including description of floodplain features; (4) vegetation; (5) elevation above low discharge water surface; (6) processes responsible for deposition; (7) position with respect to the river. Additionally, soil data collected by the Natural Resource Conservation Service (Dyer, 2008) and interpretation of floodplain stratigraphy assisted in the description of the map units.

Dendrogeomorphic and stratigraphic analysis of floodplain sediments were conducted in three trenches that we excavated in 2009 and 2010. We excavated one trench on Hatt's Ranch, and two trenches on Frenchman's Ranch. The Hatt's Ranch trench (35-m long and 2 to 3-m deep) was excavated on the left bank perpendicular to the

flow of the river. The two trenches on Frenchman's Ranch were excavated on each side of the river, directly across from each other. The left bank trench was 18.5-m long and 1 to 2-m deep, and the right bank trench was 21-m long and 1 to 2-m deep.

Additionally, we used cross section geometry to characterize the geomorphic organization of the study area. We delineated the boundaries of the active channel on orthorectified aerial imagery taken in 2009, from which we computed channel width at 1-km increments (see Chapter 3 for details). Furthermore, we measured three cross sections, one at the abandoned cableway on Hatt's Ranch (Figure 3.3 in Chapter 3), one at the trench site on Hatt's Ranch, and at the trench site on Frenchman's Ranch.

In 2008 and 2010, we measured the longitudinal profile of the entire study area. This survey effort was led by two organizations: the NRCS surveyed the water surface elevation on the Hatt's Ranch in 2008; and in 2009 and 2010, the Fluvial Geomorphology Lab at Utah State University (USU) surveyed the water surface elevation and bed elevation of the remaining portion of the study area. Both the NRCS and USU surveyed elevations precisely, using a Real Time Kinematic Global Positioning System (RTK GPS). USU collected measurements approximately every 30 m along the centerline of the channel at a predefined horizontal precision of 1.5 cm and a predefined vertical precision of 3.0 cm. Both of the NRCS and the USU survey efforts were conducted during low flow discharge, when discharge varied between 0.31 m^3/s and 0.96 m^3/s. All of the survey data was post processed with orthometric elevations.

We calculated the slope of the valley in the study area. The valley centerline was sampled from a 5 m Auto-Correlated DEM, which was generated from the 2006 NAIP imagery, every 50 m to 100 m along the valley centerline. Imprecision in the determination of valley slope is based on two factors. First, there is 4-m elevation uncertainty in the DEM, as a result of the auto-correlation process. Second, the type of surface that was sampled along the valley centerline sometimes produced significant difference in elevation between sampled points. The types of valley surfaces that we sampled included the channel bed, floodplain, terrace, tributary fan, and slope-wash.

We compared the valley elevation to the water surface elevation at 1-km increments. In the comparison, we identified several anomalous valley elevations, so we substituted adjacent points that were sampled from a more representative valley floor elevation to correct for the anomalous points. Also, we subtracted the difference in valley floor elevation from the 2008-2010 water surface elevation at 1-km increments. These differences were computed after the corrections for aberrant valley floor elevations were made. The following equation was used to calculate the slope of both the channel and the valley centerline

$$m = \frac{rise}{run} = \frac{y_1 - y_2}{x_1 - x_2}$$

where y_1 is the elevation at x_1, which is the upstream end of the valley centerline, and y_2 is the elevation at x_2, which is the downstream end of the valley centerline.

2.5 Results

2.5.1 Valley Slope and Valley Width

The slope of the alluvial valley in the study area is similar shape and to that of the water surface slope, but slightly steeper. The slope of the valley floor is 0.0016 (Figure 2.5). The slope of the water surface measured in 2008-2010 is 0.001. Both the valley profile and the water surface profile are broadly convex. On average, the valley floor is approximately 6 m above the water surface, the maximum relief is 9.1 m, and the minimum relief is 2.9 m.

Within the relatively straight valley profile there are local variations in elevation. Specifically, three abrupt decreases in elevation occur in the valley floor profile (Figure 2.6). In distances along the centerline of the valley downstream from the San Rafael Reef, the first drop occurs at 12 km, the second occurs at 30 km, and the third occurs at 50 km. The first drop occurs at the Hatt's Ranch Diversion Dam, which is located close to an abrupt change in valley width. The second and third drops occur at tributary confluences. The second drop occurs near the mouth of Cottonwood Wash. The third drop, approximately 1 km in length, is located in the vicinity of the confluence of Moonshine Wash. Immediately downstream of the Moonshine Wash confluence, the valley centerline elevations are not representative of the average valley elevation – they are probably channel elevations. Consequently, the third drop in the valley slope appears larger than if these points along the valley centerline were sampled from higher surfaces within the valley.

Valley width varies by almost an order of magnitude in the study area. The average width of the valley measured at 57 valley cross sections is 390 m. The maximum valley width is 928 m and the minimum is 83 m. In light of the variation of valley width in the study area, there appear to be parts of these segments (longer than several km in valley distance) that alternate between narrow and wide. Furthermore, there are abrupt changes in valley width between the alternating narrow and wide segments. Three of the five noted abrupt changes in valley width correlate to changes in the bedrock lithology present at the elevation of the valley (Figure 2.7 and Figure 2.8).

2.5.2 Alluvial Valley Geomorphology

Geomorphic surfaces of the alluvial valley are comprised of both alluvial deposits (mainstem and non-mainstem) and non-alluvial deposits. Mainstem alluvial deposits include the active river channel, floodplains, and terraces. Tributary alluvium, which has been deposited by fluvial processes, occurs in the form of fans. Non-alluvial deposits include slope-wash and aeolian deposits. Appendix 2 contains descriptions of each of the map units found in the study area.

The floodplain is comprised of two units. A variety of surfaces bound the upper floodplain surface (FP2), including bedrock, tributary alluvium, terraces, and slope wash. Minor escarpments define the boundary between the upper floodplain and the terrace. The lower floodplain surface (FP1) occurs between the active channel and the upper floodplain surface. In most places, distinct breaks in slope define the boundary between the lower floodplain unit and the upper floodplain unit. FP1 is topographically complex;

topographic features include a near channel bench, levee, floodplain trough, floodplain channels, and crevasse splays. Topographic complexity of the lower floodplain surface represents the ongoing reworking by overbank flood events, and the floodplain landforms represent the processes of both aggradation and erosion. On the other hand, the surface expression of FP2 is primarily flat.

Tamarisk (*Tamarisk spp.*) is prevalent on both floodplain units, however, the proportion of tamarisk coverage varies between floodplain surfaces. For example, tamarisk is the primary vegetative cover on FP2, where few cottonwoods are present. In contrast, galleries of Fremont cottonwoods are prevalent on FP1, apparent in the vicinity of Frenchman's Ranch; the composition of these cottonwood galleries includes multiple age classes which are intermingled with grasses, forbs, and willows. The spatial pattern of the occurrence of cottonwood galleries varies. Specifically, cottonwood galleries are prevalent from Greasewood Draw to the confluence, as seen on aerial photographs taken in 2010. On the other hand, there are but a few cottonwood galleries in the upstream portion of the study area, between the San Rafael Reef and Hatt's Ranch diversion dam.

The proportion of geomorphic deposits differs between the two alluvial valley segments that were mapped in detail. The most notable difference is the amount of area covered by terrace T1. Approximately 37% of the valley area in the Frenchman's Ranch segment is comprised of T1, and only 5% of the valley area in the Hatt's Ranch segment is comprised of the T1 surface. Additionally, aeolian deposits comprise a significant portion (18%) of the valley area in the Frenchman's Ranch segment, whereas aeolian

deposits are nearly absent in the Hatt's Ranch segment. Further, FP2 comprises 15% more area in the Hatt's Ranch segment than in the Frenchman's Ranch segment, 39% and 24%, respectively. We could not determine the genetic surface of one quarter of the area of the Hatt's Ranch segment, where land has been cultivated recently. On the other hand, irrigated agriculture on Frenchman's Ranch has not occurred for at least 25 years, so we were able determine the genetic surface for most of the previously cultivated land there.

2.5.3 Planform

The San Rafael River is an actively meandering river. Point bars and cut banks are present throughout the study area. However, the degree of meandering, or sinuosity, varies throughout the study area. The degree of sinuosity appears to be correlated to the width of the valley. For example, in the segment between Dugout Wash and Moonshine Wash, meander migration is restricted by valley confinement, and the channel impinges on the valley margin frequently. On the other hand, between the San Rafael Reef and Dugout Wash, there are highly sinuous reaches where the river flows up-valley in some instances. In addition to meandering reaches, straight reaches are present throughout the study reach. The channel in 22% of the study area is straight (Table 2.1).

2.5.4 Channel Geometry

In general, the shape of the channel is homogenous throughout the study area. The channel is compound, and includes a smaller channel that is inset within a larger channel. The compound channel is a result of both erosion and depositional processes. For

example, a vegetated bench - which is usually found along each bank, adjacent to the base flow channel, and defines the boundary between the inner channel and the bankfull channel, is the result of both stripping and constructive geomorphic processes. In general, the width and height of the bench above the low flow water elevation are 2-4 m and 1-1.5 m, respectively. Along much of the study area, levees define the outer boundary of the bankfull channel. Channel shape diverges from the compound form in places, notably at meander bends. In meander bends, the channel is asymmetric and is comprised of a point bar on the inside convex bank and typically a steep, concave outer bank. Active channel width is greatest at the apex of meander bends.

Channel width varies throughout the study area. However, variation in channel width is not correlated to valley confinement, nor does channel width increase in the downstream direction. The average width of the channel in the study area in 2009 was 8.8 m (Table 3.12 in Chapter 3). The maximum channel width measured at 57 1-km increments was 11.7 m, and the minimum width was 5.6 m. The average width-to-depth ratio measured at USGS streamflow gage 09328500 for the period 1958 to 2010 was 22.4 (see Table 3.11 and Figure 3.23 in Chapter 3).

Geomorphic units, both in-channel units and floodplain units, are the fundamental constructive elements of a river (Brierley and Fryirs, 2005). Geomorphic units may be either depositional or erosional features and are the product of the interaction between stream flow and sediment flux. Thus, geomorphic units are indicative of the formative processes that shape a particular river reach (Brierley and Fryirs, 2005). Bank-attached

bars are the most common type of in-channel geomorphic units present in the study area. Two types of bank-attached bars commonly occur along the length of the lower river: point bars, and lateral bars. Point bars occur on the convex bank of a meander bend, and lateral bars occur in relatively straight segments. Lateral bars typically alternate from bank to bank, thus causing the thalweg to shift position from bank to the other bank. Furthermore, there are only a few instances of un-vegetated mid-channel bars and only a handful of vegetated, mid-channel islands along the length of the lower river.

The influence of tributaries alters the organization of hydraulic units in the study area. In-channel hydraulic units are patches of similar flow and substrate characteristics (Thomson et al., 2001; Bisson et al., 2006), and are adjustable in less time than a geomorphic unit. Types of hydraulic units that occur in the study area include riffles, runs, pools, and backwaters. Two distinct hydraulic zones occur in the vicinity of a tributary confluence (Figure 2.9). Upstream from a tributary confluence, a pool occurs, where commonly deposition of fines has resulted in bed aggradation. Downstream from a tributary confluence, the addition of tributary sediment typically creates a sequence of coarse-grained, alternate bars. The water surface gradient is steeper below a tributary confluence than it is upstream of the tributary. Additional hydraulic controls such as beaver dams and places where the bed is bedrock (Figure 2.10) cause disruptions in the typical pattern of hydraulic units and produce local channel slopes similar to those that occur at tributary confluences. In the reaches between hydraulic controls, in general, the bed is mostly comprised of sand and mud. In general, portions of gravel bed are sparse

throughout the study area, and occur mostly in the vicinity of tributaries or where the channel impinges on the bedrock perimeter or Pleistocene terraces.

2.5.5 Longitudinal Profile

The shape of the longitudinal profile in the study area is broadly convex (Figure 2.10). At close inspection, a very slight increase in channel slope occurs in the downstream direction. Local variations in the overall shape of the profile are controlled by both natural and anthropogenic influences. The Hatt's Ranch diversion dam exerts the greatest influence in the present-day longitudinal profile. Immediately downstream from the Hatt's Ranch diversion dam, the water surface elevation drops 5.6 m over the distance of 170 m. There are smaller hydraulic controls in the profile that are caused by natural forces – these include tributary confluences, beaver dams, and places where the bed is bedrock. In total, there are three places where the bed is bedrock. Also, eight beaver dams were observed in the study area during fieldwork conducted in 2009 and 2010.

2.6 Discussion

Based on observed shifts in average valley width, we have segregated the study area into five valley segments. The five valley segments can be seen in Figure 2.6, which shows the valley area calculated in 1-km increments along the length of the valley, and also in Figure 2.11, which shows average valley width for each 1-km increment. Valley segments alternate between narrow and wide. Valley segment four is the most narrow

(165 m), and valley segment three is the widest (692 m). The width of the valley varies not only among segments but also within an individual valley segment. For example, valley width varies significantly in segment three, where maximum and minimum width is 928 m and 255m, respectively (Figure 2.11). On the other hand, there is minimal variation in the width of valley segments two and four.

Lithology and tectonics control the orientation of the valley, as well as valley width. Valley segment one begins at an abrupt change in valley width where the San Rafael River exits the San Rafael Reef as it dissects hogbacks of Navajo Sandstone and flatirons of the Carmel Formation (Figure 2.7). The valley quickly widens upon exiting the reef and is bounded on the east by the Curtis Formation and on the west by a mix of the Carmel Formation, terrace gravels, and pediment gravels (Trimble and Doelling, 1978). The relatively wide valley (average valley width equals 446 m) in segment one continues south for 5.8 km before making a sharp turn to the west where it cuts through the Curtis Formation, then abruptly narrows when it enters the Morrison Formation approximately 775 m downstream from the I-70 crossing. The Morrison Formation confines valley segment two to an average width of 267 m for approximately 7.6 km. The valley re-widens at the upstream end of Hatt's Ranch (valley segment three) where the Summerville Formation comprises the perimeter of the valley on both sides. Valley segment three is relatively wide (average width is 692 m) and continues for approximately 19.5 km as it cuts through the Curtis Formation and the Entrada Formation. Valley segment three is bounded by aeolian sands and slope-wash in places.

At the confluence of Dugout Wash (enters on river right) and an unnamed tributary (enters on river left), the valley narrows abruptly. Downstream in valley segment four (average valley width is 164 m and length is 21.1 km), the valley irregularly meanders through the Carmel Formation then the Navajo Formation in a partly confined setting where vertical cliffs10-80 m tall border the valley on either side. Valley segment five is the most downstream segment and is the shortest valley segment (2.4 km long). Valley segment five begins a short distance downstream from the confluence with Moonshine Wash and ends at the confluence with the valley of the Green River.

The length of the channel that impinges on the bedrock perimeter of the valley is directly correlated to the average width of the valley. For example, the channel rarely impinges on the bedrock valley perimeter in valley segment three (22.4 m/km), which has the widest average valley width (Table 2.2). In contrast, approximately 170 m of channel per kilometer of channel impinges on the bedrock valley perimeter in the narrow valley segment four (Table 2.2). The amount of channel confinement used to be much greater. Channel confinement by bedrock and other surfaces has reduced by nearly 60% since 1938 (Table 2.3). In addition to the valley perimeter, within valley deposits restrict the movement of the channel. For example in Figure 2.12, it can be seen that a terrace restricts channel movement a short distance downstream from Frenchman's Ranch. Other types of cohesive surfaces within the valley including tributary fans and slopewash also restrict channel migration. Furthermore, tamarisk has stabilized recent floodplain deposits, which likely reduces bank erosion rates.

The width of the channel is relatively constant throughout the study area. Channel width does not increase in the downstream direction in the study area, nor does channel width increase in wide valley segments, or decrease in narrow valley segments (Figure 2.11). Also, the shape of the channel is relatively the same throughout the study area; it is not correlated to changes in valley width among valley segments. Rather, variations in both channel width and channel geometry are local in nature. For example, active channel width is greatest at the apex of meander bends. In general, local hydraulic controls influence channel shape and channel width, rather than segment-scale, geologic controls, such as valley width.

The differences in the arrangement and distribution of geomorphic surfaces between the Hatt's Ranch area and the Frenchman's Ranch area, both of which have relatively similar valley width, suggests that factors other than valley confinement control the distribution of floodplain assemblages and the occurrence of terraces. Detailed geomorphic mapping within valley segment three shows that the proportion of the valley covered by the upper floodplain unit (FP2) differs between Hatt's Ranch and Frenchman's Ranch (Figure 2.12, Figure 2.13, and Table 2.2). Furthermore, a terrace, which is nearly absent in Hatt's Ranch, comprises 37% of the valley in the vicinity of Frenchman's Ranch.

Each floodplain unit, FP1 and FP2, represents a unique style of floodplain formation. The two floodplain units combined comprise 58% and 39% of the valley surface in the vicinity of Hatt's Ranch and Frenchman's Ranch, respectively. The lower

floodplain unit (FP1) is an obliquely accreting fine sand and mud unit inset within FP2. The oblique accretion (a combination of vertical and lateral accretion) of FP1began in the late 1940s/early 1950s, as determined from dendrogeomorphic analysis of floodplain sediments. The early stages in the construction of FP1 were characterized by the deposition of sediment on top of stabilized active channel surfaces within the previously wide active channel. Lateral accretion of FP1, evidence of which includes ridge and swale topography, indicates that the channel is actively meandering. Horizontal stacked layers of sediment in addition to the vertical growth of levees, features which are evident in the stratigraphy of all three floodplain trenches, indicates that FP1 is actively vertically accreting, a process that in places is reducing the topographic relief between FP1 and FP2. In other places, FP1 has a complex surface expression, which is characterized by crevasse splays and levee-flood channel morphology – these features indicate that FP1 is frequently reworked by overbank floodplain stripping and subject to rearrangement by floods.

FP2 is a vertically accreting unit, where thin layers of sediment have been deposited horizontally on top of Holocene age sediment. Only large magnitude floods are capable of inundating FP2. We deduced that this surface is vertically accreting because we have not seen evidence of catastrophic stripping of this surface i.e., there no erosional contacts. Because large floods are rare in the present hydrologic regime, then the aggradation of FP2 occurs infrequently, such as on a decadal time scale. The height of the FP2 surface above the base flow water surface is greater in the vicinity of Hatt's Ranch

than in the vicinity of Frenchman's Ranch. For example, on Hatt's Ranch, the height of FP 2 varies from 0.5 m to 4 m above the base flow water surface. In contrast, on Frenchman's Ranch, FP2 is 0.5 m to 2.5 m above base flow water surface. We speculate that the greater relief of FP2 in the vicinity of Hatt's Ranch may be related to the channel incising into a wedge of sediment that had been deposited upstream of the Lower MacMillan Ranch dam during the time span between the late 1800s and the 1980s (see Chapter 3).

We suspect, based on observed riparian vegetation composition and topographic relief on aerial photographs and during field excursions, that floodplain assemblages throughout much of the study area are similar to Frenchman's Ranch except for the portion upstream of Hatt's Ranch diversion dam (approximately 16 km) and a portion upstream of the confluence (approximately 2-3 km), where these floodplain assemblages may be similar to the portion of Hatt's Ranch that we mapped. However, additional geomorphic mapping and sedimentologic work is needed to determine if the two styles of floodplain formation that we documented in valley segment three is occurring in the same proportion in other segments in the study area. In addition, further investigations are needed to determine whether valley confinement or other factors control the distribution of floodplain assemblages elsewhere in the study area.

2.7 References Cited

Baker, A.A., 1946. Geology of the Green River Desert-Cataract Canyon region, Emery, Wayne, and Garfield counties, Utah. U.S. Geological Survey Bull. 951, (122 pp.).

Bisson, P.A., Buffington, J.M., Montgomery, D.R., 2006. Valley segments, stream reaches, and channel units. In: Hauer, R., Lamberti, G.A., (Eds.), Methods in Stream Ecology. Elsevier, San Francisco, CA, pp. 23-44.

Bottcher, J.L., 2009. Maintaining population persistence in the face of an extremely altered hydrograph: Implications for three sensitive fishes in a tributary of the Green River, Utah. M.S. Thesis, Utah State University, Logan, UT (61 pp.).

Brierley, G. J., Fryirs, K. A. (2005). Geomorphology and river management: Applications of the River Styles framework. Blackwell Science, Oxford, UK. (398 pp).

Burchard, R W., 1926. Plan and profile of San Rafael River below Castle Dale, Utah, Buckhorn Wash to mile 3. U.S. Geological Survey, Washington, DC, 4 maps.

Church, M., 1992. Channel morphology and typology. In: Calow, P. Petts, G.E. (Eds.), The River's Handbook: Hydrological and Ecological Principles. Blackwell, Oxford, UK, pp. 126-43.

Doelling, H.H., Kuehne, P.A., Willis, G.C., Ehler, J.B., 2014. Geologic map of the San Rafael Desert 30' x 60' quadrangle, Emery and Garfield Counties, Utah. Utah Geological Survey Map 267DM, GIS data, xx p., 2 plates, scale 1:62,500.

Dyer, J., 2008. Soil survey of Hatt's Ranch, Natural Resources Conservation Service, unpublished results.

Frissell, C.A., Liss, W.J., Warren, C.E., Hurley, M.D., 1986. A hierarchical framework for stream habitat classification: viewing streams in a watershed context. Environ. Manage. 10:199–214.

Graf, W.L., 1987. Late Holocene sediment storage in canyons of the Colorado Plateau. Geological Soc. of America Bull. 99, 261-271.

Hereford, R., Thompson, K. S., Burke, K. J., and Fairley, H. C., 1996. Tributary debris fans and the late Holocene alluvial chronology of the Colorado River, eastern Grand Canyon, Arizona, Geological Soc. of America Bull. 108, 3–19.

Hereford, R., Webb, R.H., Graham, S., 2002. Precipitation history of the Colorado Plateau region, 1900–2000, US Geological Survey Fact Sheet 119-02 2002. 4 p.

Montgomery, D. R., Bolton, S.M., 2003. Hydrogeomorphic variability and river restoration. In: Wissmar, R.C., Bisson, P.A. (Eds.), Strategies for Restoring River Ecosystems: Sources of Variability and Uncertainty in Natural and Managed Systems, American Fisheries Society, Bethesda, MD, pp. 39–80.

Pizzuto, J.E., 1994. Channel adjustments to changing discharges, Powder River, Montana. Geological Soc. of America Bull. 106 (11), 1494-1501.

Schumm, S.A., 1963. Sinuosity of Alluvial Rivers on the Great Plains. Bull. the Soc. America 74 (9), 1089-1100.

Sparks, R.E., Bayley, P.B., Kohler, S.L., Osborne, L.L., 1990. Disturbance and recovery of large floodplain rivers. Environ. Manage. 14 (5), 699-709.

Thomson, J., Taylor, M.P., Fryirs, K.A. Brierley, G.J., 2001. A geomorphological framework for river characterization and habitat assessment. Aquatic Conservation: Marine and Freshwater Ecosystems 11, 373-389.

Trimble, L.M., Doelling, H.H., 1978. Geology and Uranium-Vanadium deposits of the San Rafael River mining area, Emery County, Utah. Utah Geological Survey Bull. 113. (122 pp.).

Utah Division of Natural Resources. Division of Wildlife Resources, 2006. Conservation and Management Plan for Three Fish Species in Utah. Publication No. 06-17. Salt Lake City, UT. (80 pp.).

Webb, R.H., Betancourt, J.L., 1990. Climate effects on flood frequency: an example from southern Arizona. In: Betancourt J.L., MacKay, A.M. (Eds.), Proceedings of the Sixth Annual Pacific Climate Workshop, March 5-8, 1989: California Department of Water Resources, Interagency Ecological Studies Program Technical Report 23, pp. 61-66.

Witkind, I.J., 1991. Implications of distinctive fault sets in the San Rafael Swell and adjacent areas, East-central Utah. In: Chidsey, T.C. (Ed.), Geology of East-Central Utah. Utah Geological Association Publication 19, Salt Lake City, UT, pp. 141-148.

Williams, P.L., Hackman, R.J., 1971. Geology of the Salina Quadrangle, Utah. USGS Misc. Investigations Series Map I- 591. 1:250,000.

Woodyer, K.D., Taylor, G., Crook, K.A.W., 1979. Depositional processes along a very low gradient, suspended-load stream: the Barwon River, New South Wales. Sedimentary Geology 22, 97-120.

Table 2.1. Characteristics of the valley, channel and floodplain in 2009. Characteristics are listed for each of the five valley segments in the study area.

Attribute	reef to I-70 (VS 1)	I-70 to Hatt's Ranch (VS 2)	Hatt's Ranch to Dugout Wash (VS 3)	Dugout Wash to SR Desert Road (VS 4)	SR Desert Rd to confluence (VS 5)	sum or averages
valley characteristics						
valley confinement (*sensu* Brierley and Fryirs, 2005)	laterally unconfined to partly confined*	partly confined	laterally unconfined to partly confined*	partly confined	laterally unconfined to partly confined*	
geomorphic process zone - numbers indicate relative importance	(1) accumulation (2) transfer	(1) transfer (2) accumulation	(1) accumulation (2) transfer	(1) transfer (2) accumulation	(1) accumulation (2) transfer	
valley sinuosity	relatively straight	slightly sinuous	relatively straight	sinuous to irregular	relatively straight	
valley slope (m/m)	0.0017	0.0016	0.0017	0.0013	0.0016	**0.0016**
valley length (km)	5.8	7.6	19.6	21.1	2.4	**56.4**
valley area (km^2)	2.6	2.0	13.5	3.5	1.1	**22.7**
reach ave. valley width (m)	446.6	266.5	691.9	165.4	457.4	**405.6**
mainstem alluvium (km^2)	2.2	1.9	10.2	3.2	0.9	**18.5**
bedrock resistance characteristics						
river level geol. formation	Jc, Je	Jms	Js, Jcu, Je, Qe	Jc, JTr	JTr	
mechanical properties of rocks (ie thinly bedded, massive, etc)	Jc: silty, friable sandstone; calcareous mudstone; limestone; thin to thickly bedded gypsum; Je: thin to thick-bedded silty sandstone with massive cross-bedded sandstone beds	Jms: thickly cross-bedded fine to coarse grained lenticular sandstone containing scattered pebbles and thin conglomerate bed; interbeds of variegated sandy mudstone	Jcu: fine to coarse grained thin to thick bedded glauconitic sandstone; siltstone; shale and conglomerate. Je: thin to thick bedded silty sandstone with massive cross-bedded sandstone beds	Jc: fine silty friable sandstone; calcareous mudstone; limestone; thin to thick bedded gypsum; JTr: thickly cross-bedded fine grained calcareous sandstone; few lenses of sandy limestone	JTr: thickly cross-bedded fine grained calcareous sandstone; few lenses of sandy limestone	see Figure 2.8 for correlation of rock formations

(cont.) Attribute	reef to I-70 (VS 1)	I-70 to Hatt's Ranch (VS 2)	Hatt's Ranch to Dugout Wash (VS 3)	Dugout Wash to SR Desert Road (VS 4)	SR Desert Rd to confluence (VS 5)	sum or averages
channel characteristics - 2009						
water surface slope (m/m)	0.0008	0.0011	0.0010	0.0011	0.0012	**0.0010**
channel length (m)	10978.6	11826.0	33361.6	26054.5	4126.0	**86.3**
channel area (m^2)	85003.1	110142.0	312685.0	215968.0	38101.3	**0.76**
reach average channel width (m)	7.7	9.3	9.4	8.3	9.2	**8.8**
valley width : channel width (m/m)	57.7	28.6	73.8	20.0	49.5	**45.9**
planform classification- 2009						
type of meander growth e.g., translation, downstream progression, rotation (*sensu* Brierley & Fryirs, 2005)	all five valley segments contain lateral channel migration patterns: (1) unidirectional bend extension, (2) unidirectional bend translation, and (3) extension and translation, which lead to rotation and meander lobe development, such as compound meanders					
number of avulsions (since 1997)	0	0	0	0	0	**0**
sinuosity	1.9	1.6	1.7	1.2	1.7	**1.6**
type of sinuosity (i.e. sinuous, irregular, regular, tortuous, confined) - *sensu* Schumm (1963) and Church (1992)	irregular & tortuous meanders	irregular & tortuous meanders. One straight	irregular & tortuous meanders. 8 straight reaches	irregular & confined. 4 straight reaches	irregular & tortuous meanders. 2 straight reach	
proportion of straight channel	2.8	21.9	27.4	22.4	34.8	**21.9**
length of secondary channels (m)	0	0	170.6	136.9	61.7	**369.1**
*= The channel is more confined by valley deposits rather than the valley margins. For example, the channel impinges on pleistocene terraces, tributary fans, and aeolian deposits frequently and rarely impinges on the valley margin.						

Table 2.2. Characteristics of the valley, channel, and floodplain in 2009. Characteristics are computed or described for each of the five valley segments delineated in the study area.

Attribute	reef to I-70 (VS 1)	I-70 to Hatt's Ranch (VS 2)	Hatt's Ranch to Dugout Wash (VS 3)	Dugout Wash to SR Desert Road (VS 4)	SR Desert Road to confluence (VS 5)	sum or averages
Geomorphic Map Units	**Hatt's Ranch**					
channel area (km^2)	-	-	0.04	-	-	
floodplain surface 1 (km^2)	-	-	0.58	-	-	
floodplain surface 2 (km^2)	-	-	1.11	-	-	
terrace (km^2)	-	-	0.14	-	-	
aeolian (km^2)	-	-	0.000	-	-	
slopewash (km^2)	-	-	0.12	-	-	
tributary fans (km^2)	-	-	0.15	-	-	
farmland (km^2)	-	-	0.74	-	-	
total area (km^2)	-	-	2.88	-	-	
Geomorphic Map Units	**Frenchman's Ranch**					
channel area (km^2)	-	-	0.05	-	-	
floodplain surface 1 (km^2)	-	-	0.49	-	-	
floodplain surface 2 (km^2)	-	-	0.74	-	-	
terrace (km^2)	-	-	1.16	-	-	
aeolian (km^2)	-	-	0.56	-	-	
slopewash (km^2)	-	-	0.05	-	-	
tributary fans (km^2)	-	-	0.05	-	-	
farmland (km^2)	-	-	0.00	-	-	
total area (km^2)	-	-	3.10	-	-	
Map Units	**entire**					
aeolian (km^2)	-	-	1.56	0.02	-	**1.58**
slopewash (km^2)	0.11	0.03	1.32	0.04	0.15	**1.66**

(cont.) Attribute	reef to I-70	I-70 to Hatt's Ranch	Hatt's Ranch to Dugout Wash	Dugout Wash to SR Desert Road	SR Desert Road to confluence	sum or averages
tributary fans (total area, in km^2)	0.25	0.08	0.49	0.20	0.02	**1.04**
tributary fans (count)	13	21	16	84	3	**137**
non mainstem alluvium (km^2)	0.36	0.11	3.37	0.26	0.18	**4.27**
mainstem alluvium (km^2)	2.24	1.91	10.17	3.23	0.92	**18.47**
alluvial valley (km^2)	2.60	2.01	13.54	3.49	1.10	**22.74**
Length of channel that is confined						
bedrock bank length (m)	558.0	921.5	748.0	4412.6	131.5	**6771.6**
tributary alluvium length (m)	364.9	150.7	975.1	726.9	51.5	**2269.2**
aeolian deposit bank length (m)	-	-	1299.5	193.6	-	**1493.2**
Slopewash bank length (m)	134.3	52.1	372.0	17.6	41.6	**617.5**
hydraulic controls						
beaver dams (count)	1	-	5	1	1	**8**
tributary confluences (count)	5	2	10	11	2	**30**
bedrock bed (count)	1	0	2	0	2	**5**
human controls						
	none	channel straightening, bridge at I-70 crossing	On Hatt's ranch, two meander bends were cutoff; there are two bridges (old Hwy 24 and current Hwy 24), a diversion dam, agriculture and associated ranch roads.	dirt road crossing	bridge at San Rafael Desert Road crossing. Cultivation of valley floor in historic times	

Table 2.3. Characteristics of the valley, channel, and floodplain in 1938. Characteristics are computed or described for each of the five valley segments in the lower river.

Attribute	reef to I-70	I-70 to Hatt's Ranch	Hatt's Ranch to Dugout Wash	Dugout Wash to SR Desert Road	SR Desert Road to confluence	sum or averages
channel characteristics in 1938						
water surface slope in 1925 (m/m)	0.0010	0.0010	0.0010	0.0012	0.0013	**0.0011**
channel length (m)	8558.4	9880.6	31066.2	24583.6	2758.1	**76.8**
channel area (m^2)	419089.0	448320.0	1559750.0	1085950.0	199986.0	**3713.1**
reach average channel width (m)	49.0	45.4	50.2	44.2	72.5	**52.2**
valley width/channel width (m/m)	9.1	5.9	13.8	3.7	6.3	**7.8**
Length of channel that is confined						
bedrock bank length (m)	1345.1	2561.8	1021.6	10939.6	501.2	**16369.3**
tributary alluvium length (m)	330.7	802.0	1492.8	1674.6	220.6	**4520.7**
aeolian deposit bank length (m)	-	-	3298.3	282.8	-	**3581.1**
slope-wash (m)	-	130.0	2736.4	82.8	77.4	**3026.6**
planform classification - 1938						
type of meander growth (e.g., translation, downstream progression, rotation)	Because of the relative inaccuracy of the mapping of the 1925 channel location, it is not possible to interpret the style of meander growth.					
number of avulsions (since 1926)	0	10	10	4	0	**24**
Sinuosity (m/m)	1.5	1.3	1.6	1.2	1.1	**1.3**
type of sinuosity (e.g., sinuous, irregular, regular, tortuous, confined)	irregular. 2 straight reaches	confined. 1 straight reach	irregular & tortuous. 4 straight reaches	confined. 7 straight reaches	irregular. 2 straight reach	**16 straight reaches > .5 km**
length of secondary channels (m)	0	401.4	456.5	0	0	**857.9**

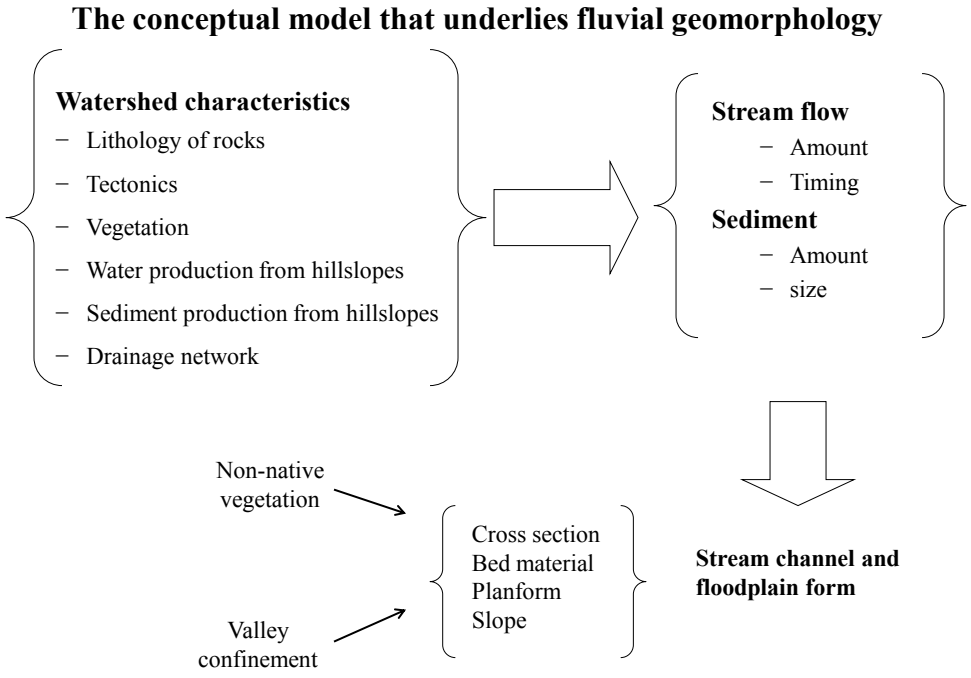

Figure 2.1. Hierarchical framework of factors that control channel/floodplain form. There are four adjustable attributes of channel form, and these are primarily determined by the flux of water and by the typical sediment transported through the channel network.

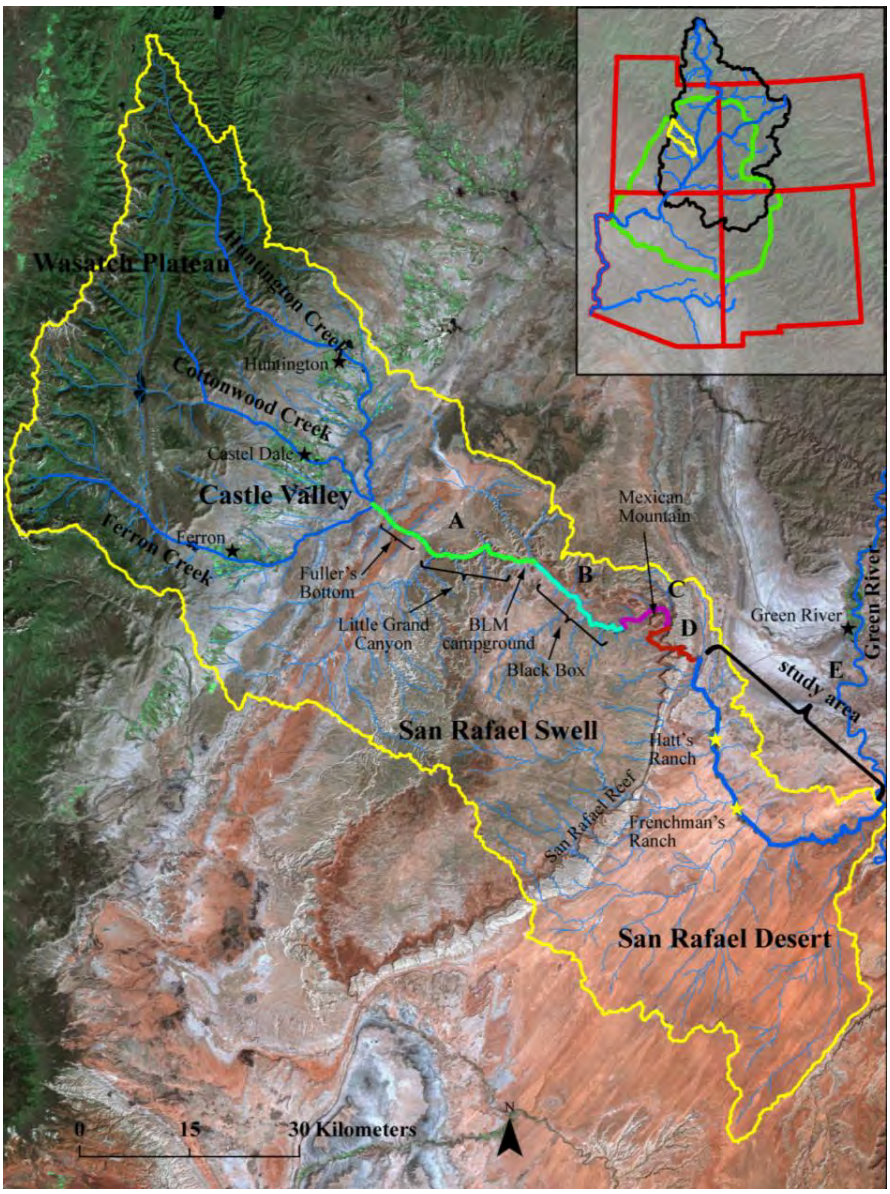

Figure 2.2. Map of the San Rafael River watershed. Valley segments are designated by color: Valley segment A is green, B is cyan, C is indigo, D is red, and E is blue. Valley segment E is the focus are of this study, which begins at the San Rafael Reef and ends at the confluence with the Green River. The background image is a mosaic of Landsat TM imagery courtesy of Intermountain Digital Image Archive Center (http://earth.gis.usu.edu/statemosaic.html). The inset map shows the position of the San Rafael River watershed with respect to the Colorado Plateau (boundary in green), upper Colorado River watershed (black), and the state of Utah (upper left red polygon).

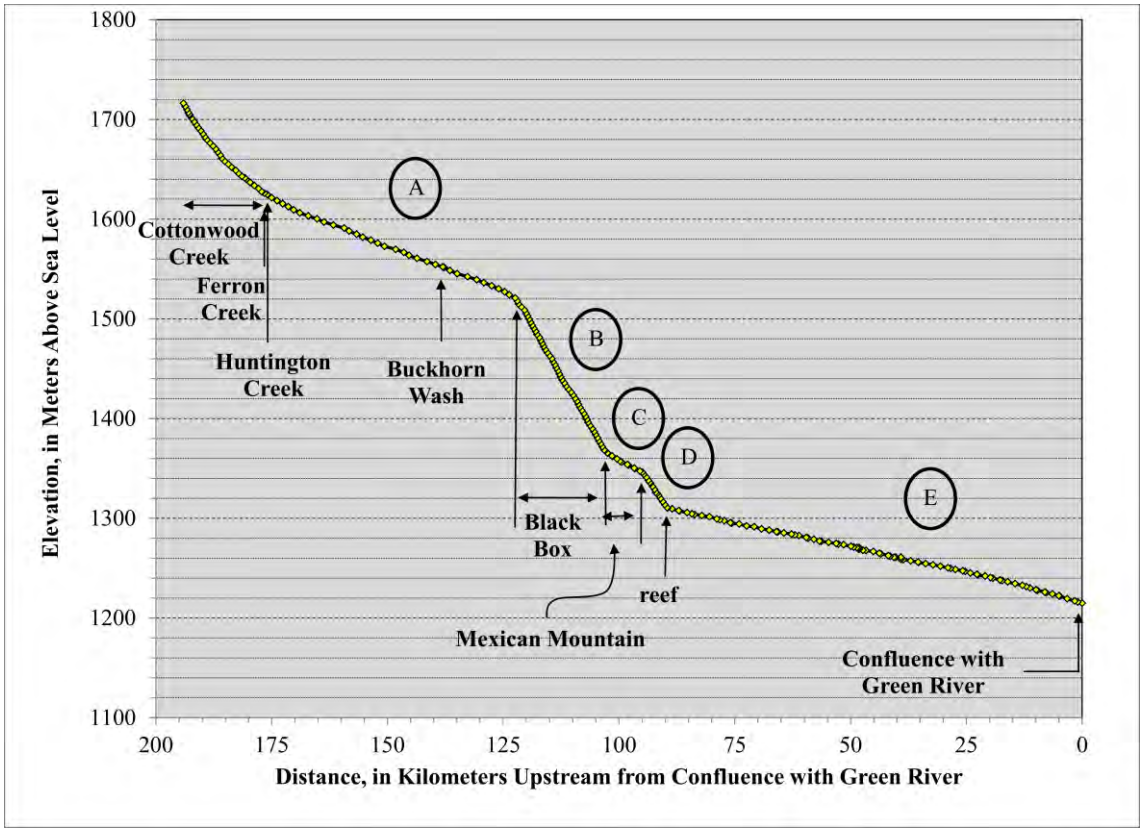

Figure 2.3. Longitudinal profile of the water surface of the entire San Rafael River, as surveyed in 1925 (Burchard, 1926). The profile consists of five valley segments. The focus area of this study is valley segment E, in which the shape of the profile is broadly convex. Convexities that occur in the profile upstream of the study area are located at the upstream ends of two bedrock valleys, where there are transitions in lithology – these convexities define the boundaries of valley segments B and D. See Figure 2 for location of each valley segment.

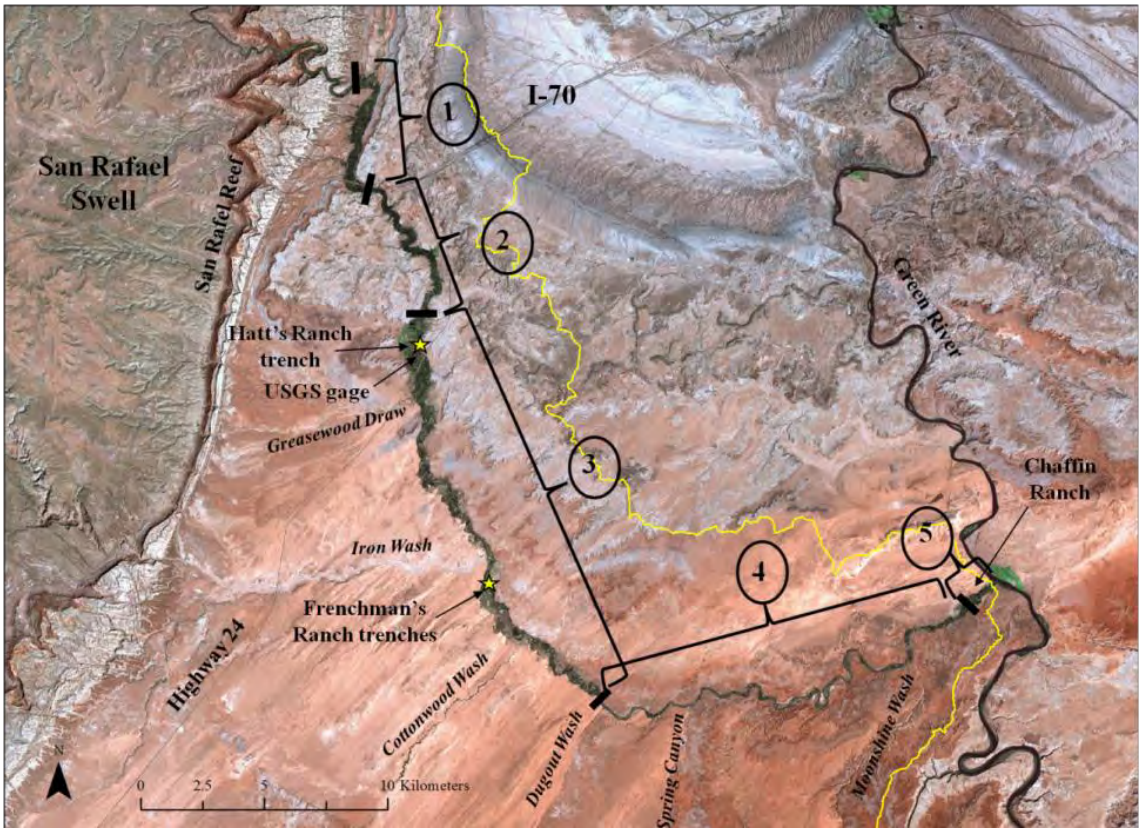

Figure 2.4. Map of the study area. The study area begins at the San Rafael Reef and extends to the confluence with the Green River. Stars designate locations where floodplain trenches were excavated. Background image is a mosaic of Landsat TM imagery courtesy of Intermountain Digital Image Archive Center (http://earth.gis.usu.edu/statemosaic.html).

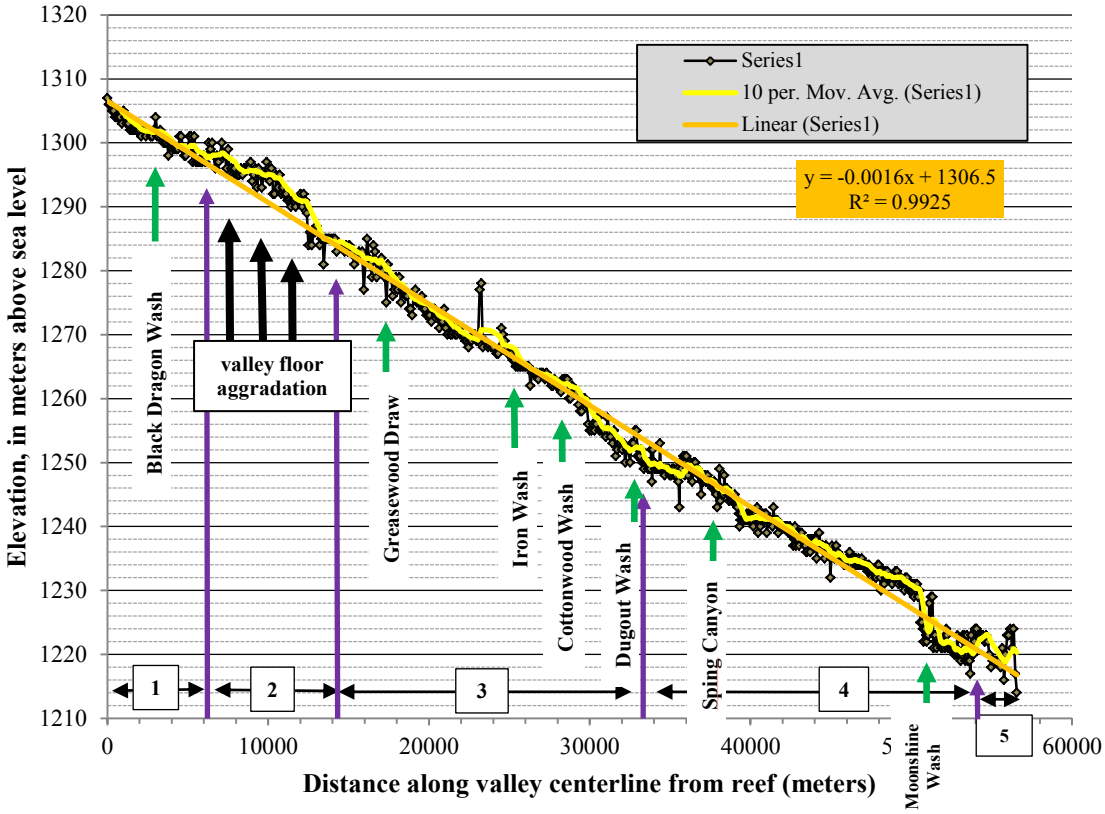

Figure 2.5. Longitudinal profile of the valley in the study area. The elevation data used to create this plot was extracted from an auto-correlated 5 m DEM every 50 to 100 m along the valley centerline. The 5-m DEM was produced from 2006 NAIP imagery and has a 4-m elevation uncertainty.

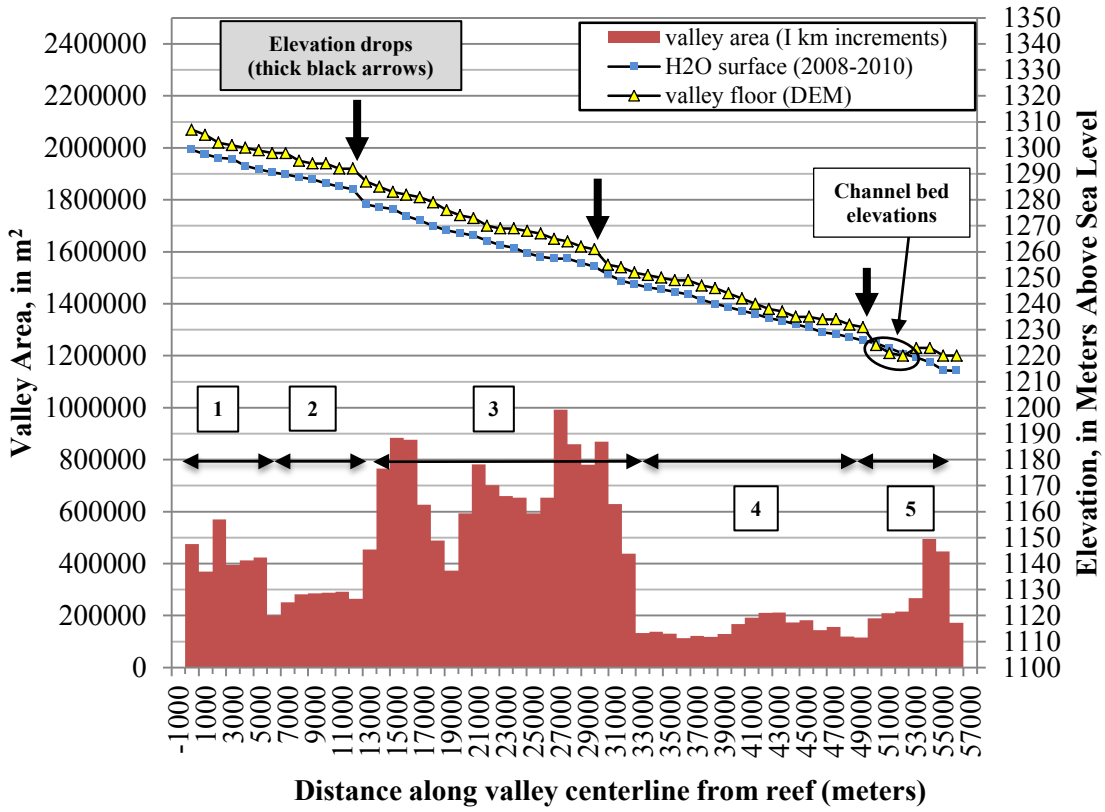

Figure 2.6. Valley area, valley floor elevation, and water surface elevation, plotted at 1-km increments. Elevations were extracted from the 2006 DEM, every 1 km. Aberrant (high or low) data points were adjusted. For a 1-km increment, to convert area (m^2) to average width (m), divide area by 1000.

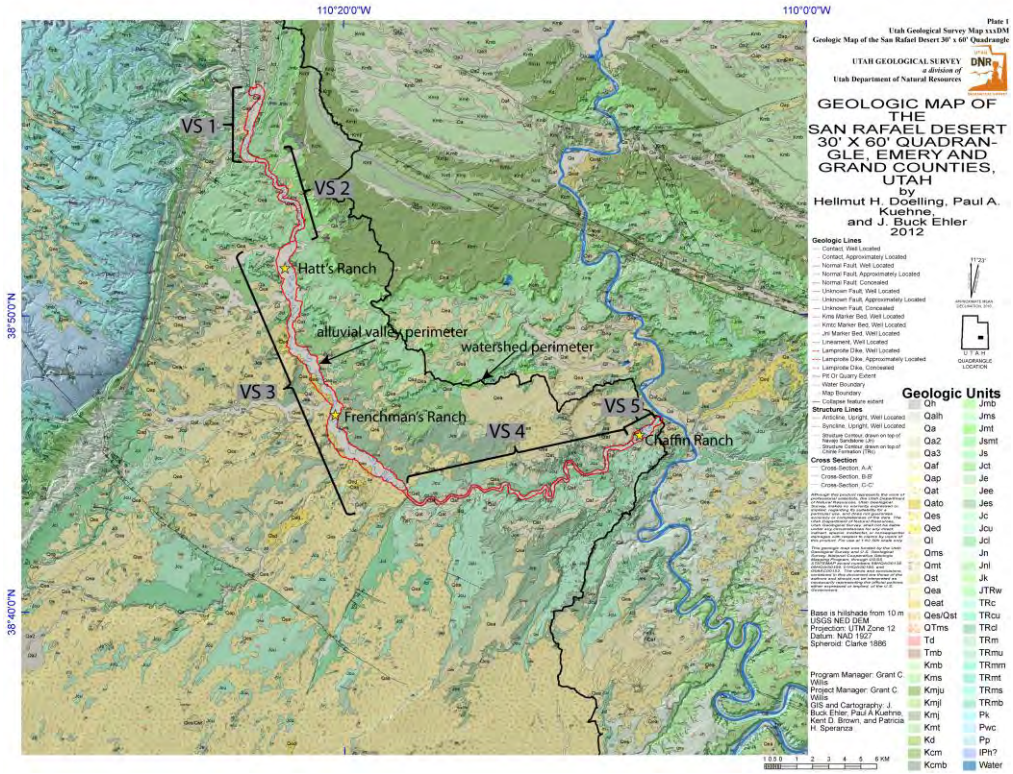

Figure 2.7. Geology of the study area. The map is modified from Doelling et al. (2014). The perimeter of the alluvial valley of the study area is indicated by a red line. The perimeter of the San Rafael River watershed is indicated by a black line. Important places in the study area are indicated by yellow stars. The correlation of map units that are encountered along the study area at valley elevation is shown in Figure 2.8.

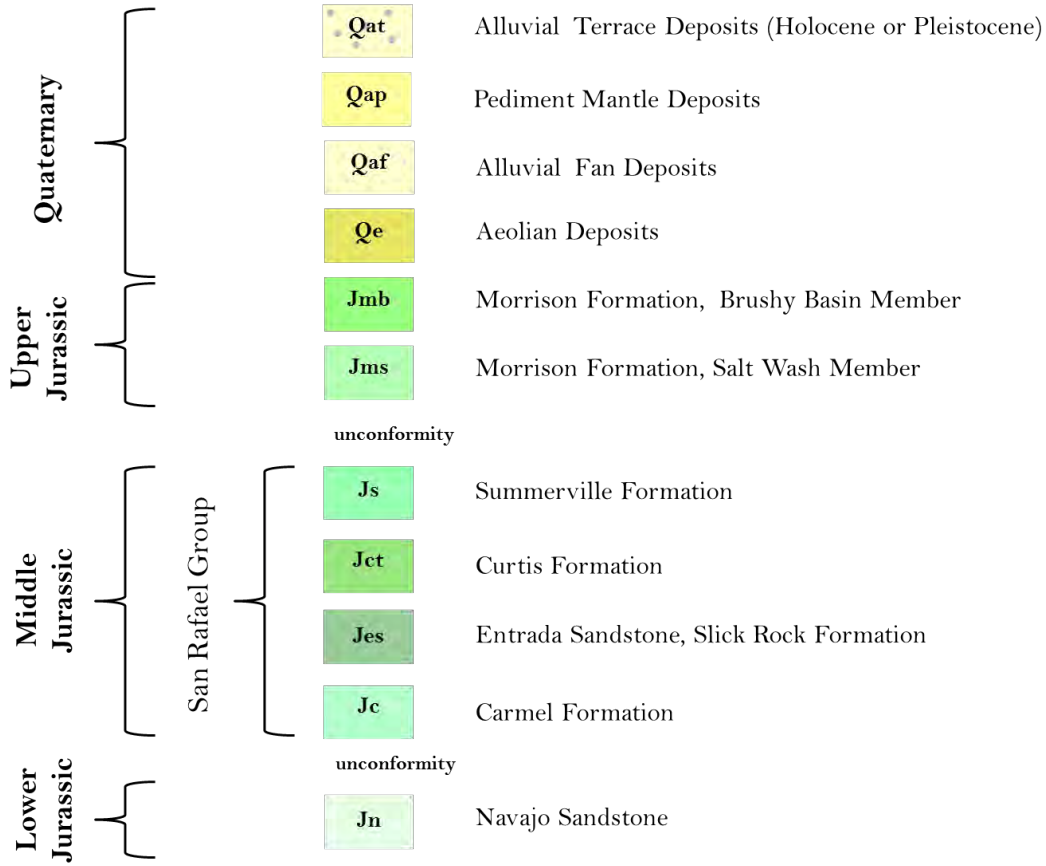

Figure 2.8. Correlation of map units found at valley bottom elevation along the study area

.

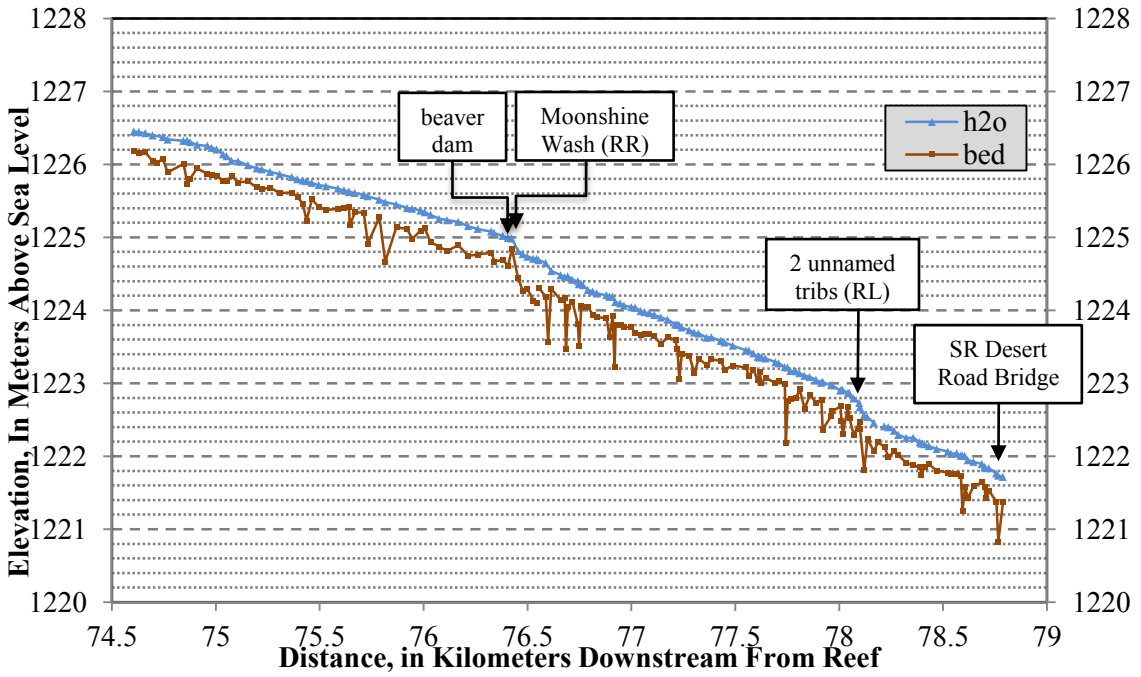

Figure 2.9. Longitudinal profile of a 4-km reach. Reach is located upstream of San Rafael Desert Road bridge. Note the combined hydraulic influence of Moonshine Wash and the beaver dam on the profile, where the slope is gentler upstream of the confluence than it is downstream of the confluence.

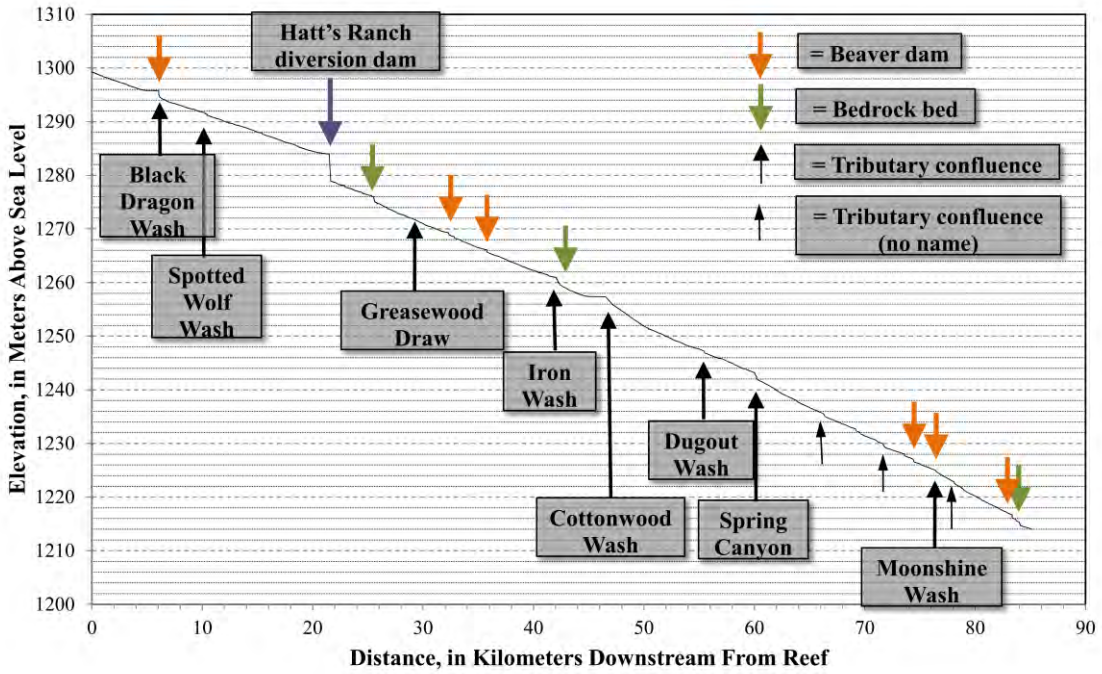

Figure 2.10. Water surface elevation profile in the study area. Data was collected between 2008 and 2010, and has been post processed using orthometric elevations.

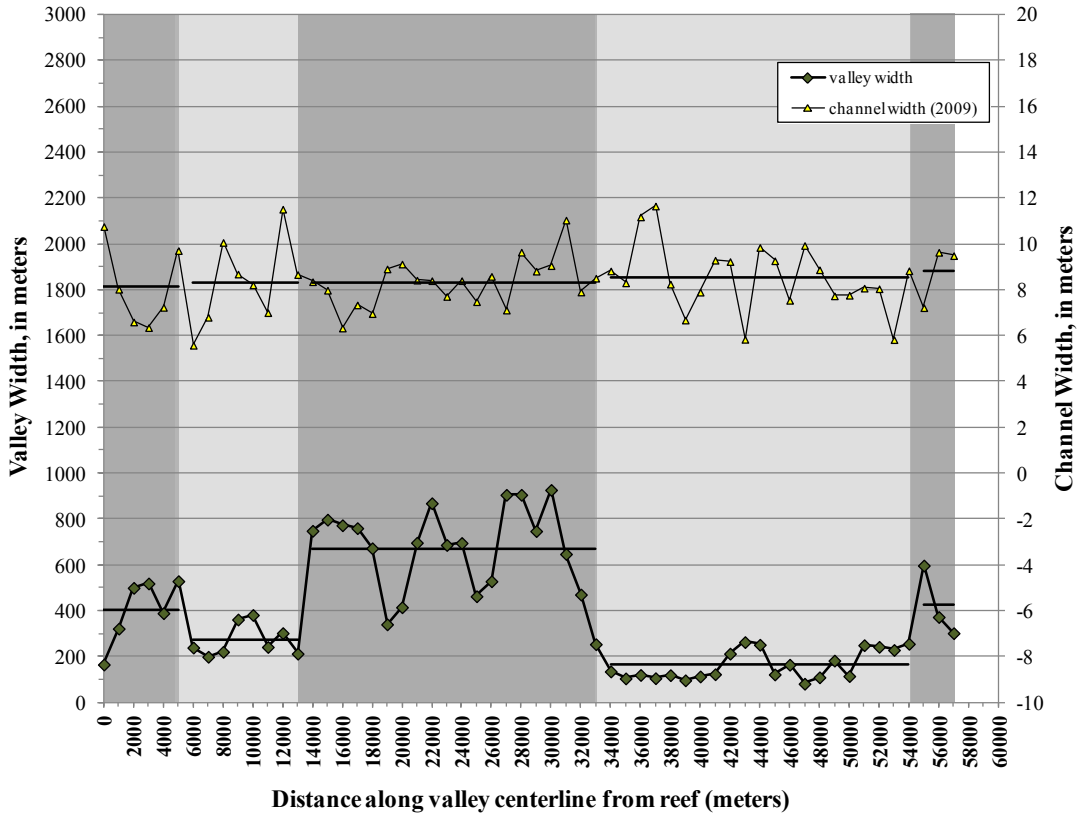

Figure 2.11. Channel width and valley width measured at 1-km valley increments. Also shown is the average channel width and valley width (horizontal lines) for each of the five valley segments in the study area. The average width for each valley segment is the mean of the width values at all 1-km nodes with a segment. Valley segments are denoted by alternating shades of grey.

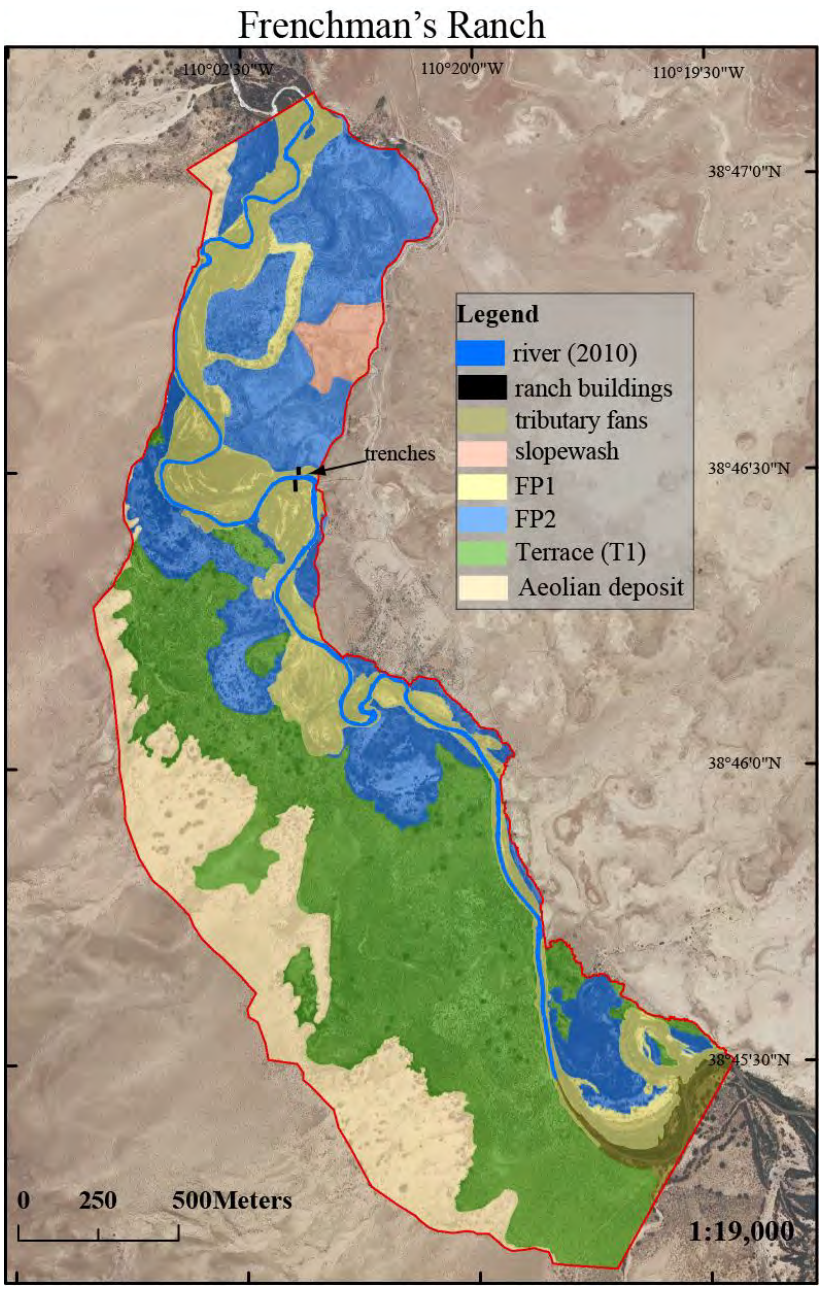

Figure 2.12. Geomorphic map of the alluvial valley in the vicinity of Frenchman's Ranch. The length of the mapped area is 4.0 km. Sites where trenches were excavated in the floodplain are designated by black lines. The background image is the 2009 aerial photograph.

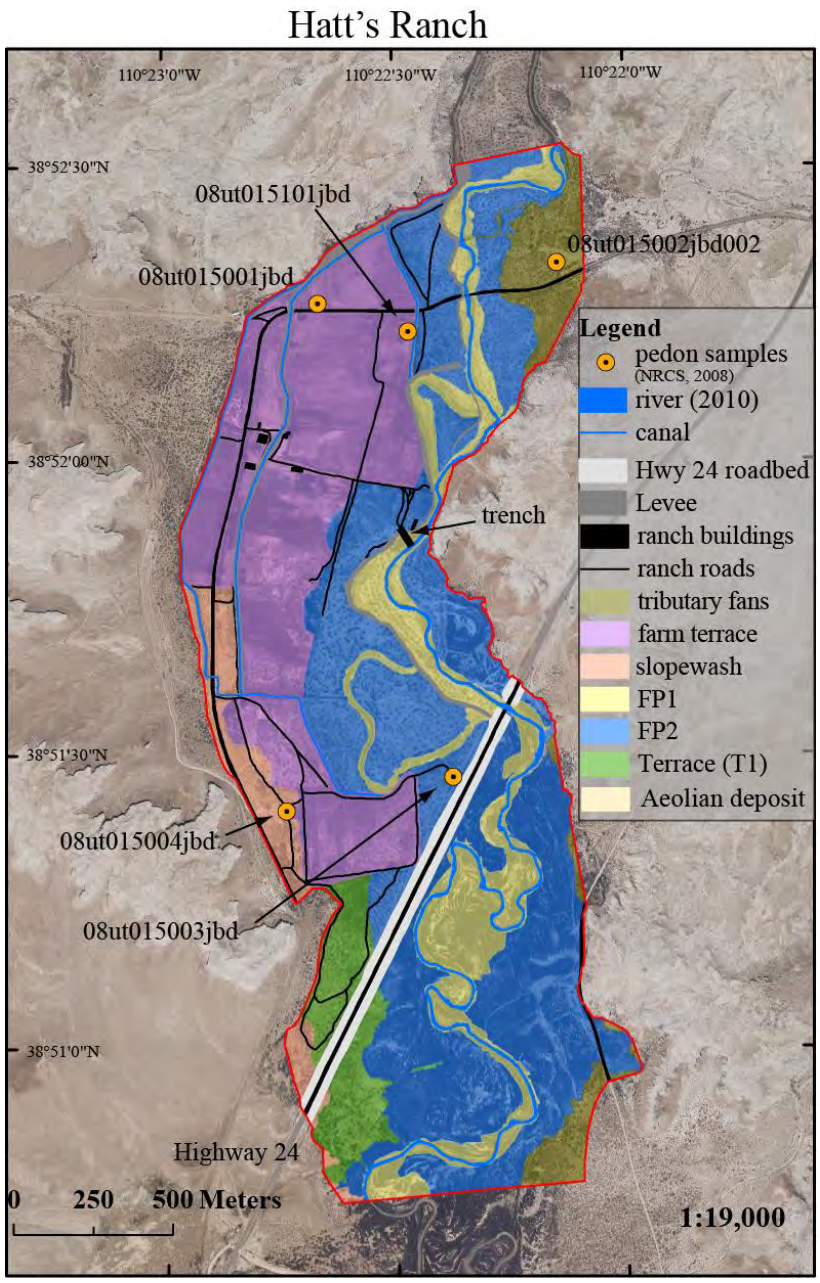

Figure 2.13. Geomorphic map of the alluvial valley in the vicinity of Hatt's Ranch. The length of the segment that was mapped is 3.6 km. Locations of pedon samples are designated by orange bulls-eyes. Sites where a trench was excavated in the floodplain is designated by a black line. The background image is the 2009 aerial photograph

2.8 Appendix A: Description of Geomorphic Map Units Occurring in the Alluvial Valley.

2.8.1 Floodplain Surface #1 (Yellow Unit in Figure 2.12 and Figure 2.13): 0.5 to 4 Meters Above Base Flow Water Surface

Floodplain surface #1 (FP1) is the youngest, and lowest elevation geomorphic surface in the study area. Construction of FP1 began in the late 1940s and early 1950s (see Chapter 3). The elevation above the base flow water surface varies between Hatt's Ranch and Frenchman's Ranch. At Hatt's Ranch, the upper portion of FP1 is approximately 4 m above the base flow water surface. At Frenchman's Ranch, the upper portion is 2.5 m above base flow water surface.

Sand bars are the basal platform of floodplain surface #1. Sand bars are comprised of discontinuous layers of mud, sand, and fine gravel that are centimeters to decimeters thick. Bedding within sand bars may be massive or may have bed forms that include ripple sand, parallel lamination, and dune cross stratification. Overlying the preserved sand bars are layers that contain mud and fine sand, centimeters to decimeters thick. Bed forms in the overlying layers may include planar, or parallel laminated sand, ripple drift cross lamination, climbing ripples, supercritically climbing ripples, or dunes. Little or no pedogenic development is evident in FP1. A typical pedon would be classified as a coarse loamy, mixed, mesic Typic Torrifluvent. Furthermore, FP1 is inundated frequently, at least every few years if not every year. Sediment color within the unit varies and includes grey, red, light brown, and yellow.

The topographic expression of FP1 is complex. Topographic features often include a near channel bench, levees, floodplain troughs, crevasse splays, and abandoned

meander bends. A nearly flat topped bench (Woodyer et al 1979; Pizzuto, 1994), which is located adjacent to the low flow water's edge, occurs nearly everywhere in the study area. Typically, a levee, which occurs onshore of the bench, transitions to a floodplain trough further onshore. In meander bends, several levee/trough sequences may occur, and these sequences may number as great as five or six.

Vegetation varies across FP1 and is roughly correlated to topographic features. Grasses, which include the invasive phragmites (*Phragmites australis*), and sandbar willows (*Salix exigua*) are the dominant vegetation on the "bench" geomorphic surface. *Tamarix spp.* commonly occupies levees and abandoned meanders, however, it also occurs on the other floodplain features. Where tamarisk occurs as dense thickets, often times no other associated vegetation occurs. Cottonwoods galleries (*Populus fremontii*) can be found growing on FP1 in each of the five valley segments in the study area, however, they are most prevalent in valley segments three, four and five. Cottonwood galleries are comprised of trees of varying ages, and some of these trees grow as tall as 12 m. Cottonwood shoots less than 1 m tall are also present, again, mostly in valley segments three, four, and five. Non-native Russian thistle (*Salsola*) has colonized areas where Tamarisk has been mechanically removed. Cheatgrasss (*Bromus tectorum)*, another non native species, is also present on FP1.

FP1 was completely rearranged during the snowmelt flood of 2011(2.3 yr recurrence interval flood). In places, the flood scoured pits up to 2 meters deep. The flood created new floodplain channels and levees, and added new sediment across much of FP1, including the tops of existing levees. The color of the sediment deposited on this

surface during the 2011 snowmelt flood is light tan and is mostly silt and silty sand. However, in flat, low lying areas distal to the channel, such as abandoned meanders, the flood deposited thick layers of mud (> 10 centimeters), which dried and cracked over the course of the summer of 2011. Furthermore, in places, the 2011 flood deposited a fine cap of silt/mud over the FP1.

The portion of the alluvial valley that we mapped as FP1 overlaps portions of three NRCS soil survey map unit series including the Green River-Garley-Glenton series complex (GDA), the Pathead-Tosca complex (115), and the Mussentuchit-Humbug-Sinbad complex (107) (Dyer, 2008). Because each of these three map units is an aggregate of various types of soils, there is variation in the characteristics within each map unit. Nevertheless, map units 115 and 107 are more similar to each other than either of them is to GDA. GDA differs from both 115 and 107 in parent material, soil depth, and available water capacity. For example, the parent material of GDA map unit is alluvium, and the parent material of 115 and 107 map units is colluvium and aeolian sands. Also, the typical soil depth of 115 and 107 is shallower (26 inches to 60 inches) than the typical soil depth in the GDA map unit (60 inches to 75 inches). On the other hand, GDA, 107, and 118 are similar to each other in several ways. All three map units can be found in similar settings i.e., similar air temperature precipitation, and elevation zones. Specifically, these three map units can be found in zones of relatively high elevation, low precipitation, and warm air temperatures. Also, these three soil types have similar drainage properties and particle size distributions. Each map unit is well drained and in general is a loamy soil with low clay content.

2.8.2 Floodplain Surface #2 (Blue Unit in Figure 2.12 and Figure 2.13)**:** *1.5 to 5.5 Meters Above Base Flow Water Surface*

The vertical profile of floodplain surface #2 (FP2) has been described in two places, a pedon located on Hatt's Ranch and a floodplain trench located on Frenchman's Ranch.

At Frenchman's Ranch, the 1.5 m stratigraphic column is comprised of 3 to 90 cm thick horizontal beds of sand and mud with small amounts of gravel. Light brown, medium sand, deposited within an active channel environment (as indicated by dune cross stratification), occurs at the base of exposure. These channel sands contain redoximorphic features, which are evidence of fluctuating water table. A 0.75 m thick package of fine grained, light grey sand overlies the basal unit. Bed forms in the light grey, sandy unit include ripples, dunes, and planar lamination. A 0.5 m-package of indurated, dark brown mud overlies the channel sands. The massive mud has a prismatic structure, and contains crystalized salts and clay films on the inside of pores. Overlying the indurated mud is several horizontally, thinly bedded (2 to 30 cm thick), structureless units of alternating red, silty sand and brown muds.

As part of a NRCS soil survey, Dyer (2008) described a pedon on Hatt's Ranch located within the extent of FP2. The location of the pedon site (ID is "08ut015003jbd") is shown on Figure 2.13. Dyer classified the pedon as a coarse-silty, mixed, superactive, mesic Typic Haplocalcid. The parent material of the profile between 23 cm to 196 cm has been modified by pedogenic processes. For example, a calcic horizon occurs at a depth of 86-114 centimeters. Additionally, B horizons begin at 23 cm below the surface and continue to 196 cm in depth. The soil texture of the top 114 cm of the soil profile is

dominated by silt (proportion of silt ranges from 53%-68%), and below 114 cm, sand dominates the soil texture (34% to 70%). Soil color varies from pinkish gray to light yellowish brown to brown. Pedogenic features include redoximorphic features and carbonate masses. The structure of the soil is predominantly subangular blocky. Horizontal bedding layers are present.

The NRCS map units series that overlap where we mapped FP2 include GDA, 107, 115, 301, 306, and Ab. GDA, 107, and 115 are described in the floodplain unit #1 section above. Here, the differences and similarities among 301, 306, and Ab are described. Map units 301 and 306 were established as part of Dyer's unpublished soil survey of Hatt's Ranch. Information about Map unit 301 was not available at the time we were compiling the research for this thesis, however, there is information about map unit 306. Map unit 306 is comprised of three soil components: a fine-loamy, mixed, superactive, mesic Fluventic Haplocambid (45%); a coarse-silty, mixed, superactive, mesic Typic Haplocalcid (25%); and the Glenton component (25%), which is part of the GDA soil series. A description of the Glenton component can be downloaded from www.websoilsurvey.sc.egov.usda.gov/. The Haplocambid and the Haplocalcid soils are great groups in the Aridosol soil order; they are both well-drained and occur in flat to gentle sloped alluvial terraces.

Much of FP2 is covered with tamarisk (*Tamarix spp.).* Grasses and forbs occupy openings in the tamarisk cover. Non-native Russian thistle (*Salsola*) and new tamarisk shoots have colonized areas where tamarisk has been mechanically removed. Cheatgrasss (*Bromus tectorum)*, another non-native species, is also present on FP2. In the left bank

floodplain at Frenchman's Ranch, dendrochronogy results indicate that tamarisk sprouted at the top of the indurated muds in the early 1950s.

Along the Hatt Ranch segment, FP2 is extensive and in places covers over 50% of the width of the valley. In the present hydrologic regime sediment is deposited on this surface during large overbank floods, (> 5 yr recurrence interval flood). Vertical accretion is the predominant floodplain formative process occurring today. The height of the FP2 surface above the base flow water surface is greater in the vicinity of Hatt's Ranch than in the vicinity of Frenchman's Ranch. For example, on Hatt's Ranch FP 2 ranges in height from 0.5 meters to 4 meters above the base flow water surface. On Frenchman's Ranch, FP2 is 0.5 m to 2.5 m above base flow water surface.

The basal channel sand packages of FP2 may correlate to Late Holocene terraces mapped in other Colorado Plateau streams. The age of the basal unit of the channel sands, determined from an OSL sample taken from the top of the unit, is 970 AD +/- 540 yrs (Figure 3.27 in Chapter 3). The OSL age of the overlying sands is 1470 AD +/- 440 yrs. There is a possibility that the basal unit correlates to the prehistoric alluvium (600-1200 AD) mapped in both the Virgin River (Hereford et al., 1996) and the Paria River (Hereford, 2002). The overlying unit may correlate to the settlement alluvium (1400 to 1880 AD) also mapped in both the Virgin and Paria Rivers (Hereford et al., 1996; Hereford, 2002).

*2.8.3 Terrace (Green Unit in Figure 2.12 and Figure 2.13)***:** *3 m to Approximately 6.5 m Above Base Flow Water Surface*

Stratigraphic and sedimentologic information is not known for the terrace map unit (T1). Characteristics of the map unit that are known are described below and include topography, vegetation community, and distribution.

The height of T1 above the base flow water surface differs between Hatt's Ranch and Frenchman's Ranch. On Hatt's Ranch, T1 is approximately 5.5 m to 6.5 m above the base flow water surface. At Frenchman's Ranch, T1 is approximately 3 m to 5.5 m above the base flow water surface. There is some uncertainty in the elevation of T1 on Frenchman's Ranch because we used the 5-m digital elevation model in GIS to estimate the elevation. On the other hand, on Hatt's Ranch, we have very low uncertainty in the elevation of the T1 surface because we surveyed this area with an RTK GPS.

The vegetation associated with T1 on Frenchman's Ranch is a mixture of shrubs intermingled with an understory of herbaceous plants. Greasewood (*Sarcobatus vermiculatus)* is the predominant shrub on T1, however, other shrub species are also present including Fourwing saltbush (*Atriplex canescens*), Mormon Tea (*Ephedra viridis*), and Blackbrush (*Coleogyne ramosissima*). In the vicinity of Frenchman's Ranch, the "Inter-Mountain Basins Greasewood Flat" class (2004 southwest United States GAP land cover map) and the Blackbrush and Salt Desert Scrub class (1995 Utah GAP land cover map) are located where we mapped T1. On Hatt's Ranch, Utah Department of Wildlife Resources mechanically removed tamarisk from T1. In 2011, Russian thistle in addition to other invasive herbaceous plants and tamarisk occupied T1.

Between Hatt's Ranch and Frenchman's Ranch, there is a large difference in the proportion of the valley that T1 occupies. Specifically, T1 comprises only 5% of the alluvial valley on Hatt's Ranch. On the other hand, T1 is extensive in the vicinity of Frenchman's Ranch, where it comprises 37% of the portion of the valley that we mapped. T1 is present in the 1938 aerial photographs, which indicates that it was formed prior to the historic time period. Most likely, this surface was created during the late Holocene, when climate conditions were favorable for aggradation and the construction of alluvial surfaces. T1might correlate to preserved, late Holocene surfaces in other Colorado Plateau alluvial valleys (Graf, 1987; Hereford, 2002), but further investigation is necessary to determine that there is a correlation.

2.8.4 Farmland (Rose Pink in Figure 2.12 and Figure 2.13): Height Above Base Flow Water Surface is Unknown

The NRCS described two pedons located on the "farmland" surface in the vicinity of Hatt's Ranch (Dyer, 2008). Pedogenic processes are occurring where both pedons were described (site IDs are "08ut015001jbd" *and* "08ut015101jbd").

Soil development characteristics at site "08ut015001jbd" include a moderate prismatic structure in the Apz horizon, weakly cemented masses of carbonate, distinct reticulate noncemented nests of gypsum, noncemented masses of oxidized iron, and gypsum masses. Redox depletions are also apparent. Frequent and long duration flooding occurs in pedon "08ut015001jbd". B horizons are present at a depth of 38 cm down to 208 cm. Silt is the dominant size class (proportions range from 48% to 58%) throughout

the depth of the soil profile, and clay comprises the second largest fraction of grain size distribution (proportions range from 36% to 44%).

Pedon “08ut015101jbd” (Figure 2.13) has two Ap horizons that occur in the top 47 cm of the profile. Below the Ap horizons are six Bw horizons that extend to a depth of 214 cm. The Ap horizons are dark grayish brown (10YR 4/5) with 28- 30% clay. Color in the Bw horizons range from grayish brown (10YR 6/2) to yellowish brown (10YR 5/4) to gray (10YR 6/1). Evidence of soil forming possesses include a subangular blocky structure, and carbonate and gypsum masses that occur between 0.6 m to 2.1 m in depth. Clay proportions range from 18% to 30% throughout the depth of the profile. NRCS soil survey map units (Ab, GDA, 301, 306, and 308) occur where the “farmland” surface was mapped. Map Unit 308 is comprised of two components, the Glenton component (40%) and the Trachute component (55%). The two components are very similar, and have only minor differences between. The Glenton component occurs on drainage ways, while the Trachute component occurs on stream terraces. Alluvium is the parent material of both components, but the parent material of the Trachute component can also be aeolian sands. The Trachute component has a very slightly saline horizon within 30 inches of the soil surface, which is absent in the Glenton component.

The “farmland” surface is no longer cultivated on the Hatt’s Ranch. Presently, grasses and herbs cover the farmland surface on the Hatt’s Ranch. The farmland surface is similar in elevation and character to FP2, however since it has been graded it is difficult to discern if the genetic surface prior to cultivation was either slope-wash or floodplain.

2.8.5 Tributary Alluvium (Dark Umber Unit in Figure 2.12 and Figure 2.13): Height Above Base Flow Water Surface is Unknown

Pedon "08ut015002jbd002" is located on the tributary fan in the northeast corner of Hatt's Ranch where old Hwy 24 traverses. Pedon "08ut015002jbd002" is a coarse, loamy, mixed, superactive, mesic Typic Torrifluvent (Dyer, 2008). The pedon has a calcic horizon. The soil structure is subangular blocky and thin platey. Pedogenic carbonate accumulation is present in two Bk horizons at a depth of 18 cm and down to 65 cm. Sediment color varies from light gray (10YR 7/2) to light brownish gray (10YR 6/2). Silt is the dominant grain size to a depth of 87 cm (proportions range from 44% to 67%). Below 87 cm, sand is the dominant grain size (proportions range from 65% to 80%). Throughout the vertical profile, the proportion of clay varies from 4% to 34%.This pedon occurs in the NRCS soil survey map unit 612.

The vegetation community on established tributary fans is comprised of shrubs, of which Greasewood (*Sarcobatus vermiculatus)* predominates. Fourwing saltbush (*Atriplex canescens*), Mormon Tea (*Ephedra viridis*), and Blackbrush (*Coleogyne ramosissima*) also occur on tributary fans, but to a lesser extent than Greasewood. An understory of herbaceous plants is intermingled among the shrubs. Depending on how recently the tributary alluvium was reworked by floods, vegetation may be absent on the surface.

Tributary alluvium differs between Hatt's Ranch and Frenchman's Ranch. On Hatt's Ranch, tributary alluvium is mapped as established tributary fans that aggraded during millennial time scales. The Holocene-age fan deposits may be inter-fingered with mainstem alluvium and perhaps slope-wash, in places. According to the Dyer's descriptions of pedons on tributary alluvial survaces, soil characteristics widely vary

across the mapped tributary fan located in the northeast portion of Hatt's Ranch. Soil auger bores revealed gravel bar deposits at the surface in places and silt loam textures in other places (Dyer, 2008). On the other hand, the tributary alluvium mapped on Frenchman's Ranch is a recent deposit. A flash flood in 2010 deposited silty sand on top of valley alluvium. The deposit caused backwater conditions for nearly 3 km upstream and forced the river subsurface and across the floodplain for approximately 0.5 km.

2.8.6 Slope-wash (Indigo Unit in Figure 2.12 and Figure 2.13): Height Above Base Flow Water Surface is Unknown

Sedimentology and soil development of the slope-wash unit is unknown, however, the topographic expression, vegetation community, and distribution of the unit is described below.

Slope-wash surfaces slope toward the main axis of the alluvial valley, instead of down-valley like terraces and floodplains. The vegetation community that occupies the slope-wash surface is a desert shrub community dominated by Greasewood (*Sarcobatus vermiculatus)*, but may contain other shrub species including, Mormon tea (*Ephedra spp.),* sagebrush (*Artemesia spp.),* rabbit brush (*Ericameria nauseosa*), and saltbush (*Atriplex spp.*). An understory of herbaceous plants is intermingled among shrubs.

Slope-wash occurs in small proportions in both of the mapped areas. In the vicinity of Hatt's Ranch, it comprises 4% of the alluvial valley. In the vicinity of Frenchman's Ranch, it comprises 1.6% of the mapped valley area. In places, the gradation between slope-wash and mainstem alluvium is difficult to discern. Furthermore, slope-wash may overlie a pediment surface or mainstem alluvium. As a

result, it is difficult to determine if the slope-wash unit, were to restrict the movement of the river channel in places. NRCS soil survey map units 306 and 309 occur where we have mapped slope-wash. Map unit 309 is comprised of two components: The Garley component (25%) and the Glenton component (20%)

2.9 Appendix B: Regional Geology

Regional tectonics exerts an influence on the path of the lower San Rafael River in valley segment E, but less so than in valley segments A, B, C, and D, where the river flows through the San Rafael Swell. The river in valley segment E flows through the San Rafael Desert, which is a "broad, very shallow, northeast plunging syncline." This syncline is also known as the Acerson trough (Trimble and Doelling, 1978). The Acerson trough, which contains scattered faults and gently tilted rocks (Baker, 1946), is influenced by regional tectonics and is bounded on the north by the southern flank of the Uinta Basin; on the south by the Nequoia Arch, a structural ridge that is an extension of the Monument uplift; and on the west by the San Rafael Reef. Upon exiting the San Rafael Reef, the San Rafael River flows directly south where the bedrock strata dip to the east/northeast. Downstream, the dominant rock dip direction in the area of valley segment E is to the north. In valley segment E, the path of the river, which is roughly arcuate and concave to the north/northwest, resembles the orientation of the contact between rock formations to the north. The rock types that occur at valley level along the lower river are listed in Table 2.1.

In addition to tectonics and lithologic controls, Quaternary deposits influence the planform of the river in valley segment E by confining the alluvial valley in certain places. For example, the prevailing southwest wind across the San Rafael Desert forms dunes that comprise portions of the valley perimeter as well as portion of the channel banks along the river between Greasewood Draw and Dugout Wash. Additional Quaternary deposits that occur along the valley perimeter in the study area include terrace gravels and pediment gravels (Trimble and Doelling, 1978).

CHAPTER 3

CHANNEL CHANGE OF THE LOWER 87 KILOMETERS OF THE SAN RAFAEL RIVER, UT

3.1 Introduction

Alluvial valleys on the Colorado Plateau have undergone several cycles of erosion and aggradation during the Holocene (Bryan, 1925; Bailey, 1935; Antevs, 1952; Cooke and Reeves, 1976; Graf, 1983; Webb, 1985; Hereford, 2002; Webb et al., 2007). The most recent episode of erosion occurred between ~1880 and ~1920 and progressed in two stages: lowering of the channel bed followed by widening of the channel (Schumm et al., 1984; Gellis et al., 1991). Researchers have documented a modern period of aggradation that began ~1940 (Emmett, 1974; Love, 1979, 1983: Leopold, 1976; Patton and Schumm, 1981; Hereford, 1984; Hereford, 1986; Hereford, 1987; Graf et al., 1991; Webb and Hereford, 2010). The causes of modern aggradation are unclear, and the mechanisms by which floodplain aggradation and channel narrowing occur have been poorly described. Components of alluvial valley aggradation include floodplain formation and channel narrowing; native and non-native riparian vegetation becomes established within the previously widened channel and plays some role in the aggradation process.

This study describes the 20th century history of channel and floodplain changes in the lower San Rafael River, a tributary to the Green River in Utah. We quantify the rates and magnitude of channel narrowing and floodplain formation and describe the processes responsible for these channel changes. The lower San Rafael River narrowed 83%

between 1938 and 2009. Channel narrowing and inset floodplain construction progressed rapidly, primarily as a result of a reduction in the annual snowmelt flood. Narrowing was exacerbated by the invasion of non-native tamarisk (*Tamarix spp)*. Inset floodplains vertically accreted between 1.0 and 2.5 m.

Quantifying the timing and magnitude as well as describing the mechanisms of channel narrowing and floodplain formation are important for several reasons. Results from this study inform efforts to rehabilitate aquatic habitat for declining populations of three fish species endemic to the Colorado River basin: roundtail chub (*Gila robusta robusta*), bluehead sucker (*Catostomus discobolus*), and flannelmouth sucker (*Catostomus Latipinnis*). Since the distribution of aquatic habitat is dependent on the morphologic characteristics of the channel, then documenting the past and current channel configuration yields insight into the nature of changes to aquatic habitat for these species. Another reason that this study is important is that modern examples of alluvial deposition and erosion are useful in the interpretation of the geologic record. On the Colorado Plateau, documentation of the causes, rates, and style of modern valley alluviation provides insights into the behavior of previous aggradational cycles. Also, quantification of the timing and magnitude of floodplain formation yields insight into the amount of sediment stored in alluvial valleys.

3.2 Background

Reduction in the frequency and/or magnitude of floods on rivers that transport large quantities of suspended sediment induces a shift from a braided to a meandering

planform (Webb et al., 2007; Dean and Schmidt, 2011), increases the sinuosity (Burkham, 1972), decreases the channel width (Burkham, 1972; Dean and Schmidt, 2011), decreases the meander migration rate (Bradley and Smith, 1984), and leads to the deposition of inset floodplains (Dean et al., 2011). Changes in flood regime also cause changes in the structure of riparian vegetation communities, including changing the density of native riparian vegetation or shifting community composition from one dominated by native vegetation to one dominated by non-native vegetation (Johnson, 1997; Friedman and Lee, 2002; Stromberg et al., 2004; Stromberg et al., 2007).

On smaller, regional (*sensu* Graf, 1987) streams of the Colorado Plateau, research has demonstrated that a reduction in flood frequency is responsible for valley alluviation and channel narrowing and is exacerbated by an increase in woody vegetation density (Hereford, 1986; Graf et al., 1991). Research on the lower Green River in Utah illustrates the effects of both an altered sediment supply and tamarisk invasion in causing channel narrowing and inset floodplain formation. Researchers documented changes in both the flow regime and the distribution of riparian vegetation, yet there has not been a consensus on the primary mechanism driving the resultant channel change. Graf (1978) argued that tamarisk colonization was responsible for the largest proportion of the observed channel narrowing. Birken and Cooper (2006) supported Graf's (1978) findings and concluded that channel narrowing has been primarily caused by tamarisk establishment. Alternatively, Everitt (1980), Allred and Schmidt (1999), Grams and Schmidt (2005), and Alexander (2007) argued that reduction in the magnitude and duration of spring snowmelt floods have been the primary causes of channel narrowing. In addition to

reduction in flood frequency and magnitude, other factors attributed to channel narrowing and that are unrelated to vegetation invasion include an increase in sediment supply relative to transport capacity (Everitt, 1993; Grams and Schmidt, 2002) and fine-sediment deposition following channel widening floods (Schumm and Lichty, 1963; Pizzuto, 1994). Some studies have concluded that riparian vegetation establishment is not the fundamental cause of channel narrowing but does accelerate the rate of narrowing (Everitt 1998; Tal et al 2004; Griffin et al., 2005; Tal and Paola, 2007). Researchers have quantified sediment storage in alluvial valleys near the San Rafael River, including the Fremont River (Godfrey et al., 2008), Paria River (Hereford, 1987), Kanab Creek (Graf, 1987), and other streams (Graf, 1987).

Some previous research indicates that the seasonal distribution of floods controls degradation-aggradation processes in Colorado Plateau streams. On the Paria River, Graf et al (1991) found that floodplain formation is caused by summer and fall floods that transport 90% of the annual sediment load. In observations of channel change on the Gila River in Arizona, Burkham (1972) noted that channel widening occurred during periods of large floods that carry little sediment and that channel narrowing occurred during periods of small floods with higher suspended sediment concentrations.

In general, processes responsible for floodplain formation may either be constructive or destructive or be some combination of the two. The paradigm of lateral accretion (Wolman and Leopold, 1957) deemphasizes the importance of vertical accretion and emphasizes the importance of an equilibrium sediment exchange rate between point bars and cut banks. However, in recent decades, researchers have found

that vertical accretion is a significant floodplain formation process – in fact, it is the dominant process of floodplain formation in many suspended load rivers. Furthermore, research has shown that oblique accretion, which is the combination of both lateral and vertical accretion, may be responsible for the majority of the floodplain deposition in suspended load rivers in Australia (Page et al., 2003).

Conceptual models of disequilibrium have been used to explain the vertical accretion of floodplains and subsequent catastrophic stripping by large floods (Nanson, 1986; Dean and Schmidt, 2011). In one example of a system in disequilibrium, Dean and Schmidt (2011) found that low magnitude, short duration floods on the Rio Grande in the Big Bend region of Texas and Chihuahua cause both vertical and horizontal floodplain formation. Furthermore, the absence of large floods allows vegetation to establish on these surfaces. In an examination of the internal architecture of the floodplain, Dean and Schmidt (2011) identified three depositional components: (1) active channel deposits characterized by coarse-grained channel margin bars; (2) floodplain conversion deposits that include sediment deposited within the active channel and sediment deposited by floodplain building processes; and, (3) floodplain deposits characterized by the deposition of suspended sediment which result in vertical accretion of the floodplain and the formation of levees. This particular model of floodplain formation and channel narrowing provides a picture of how a suspended load river in disequilibrium behaves, however, this model does not account for bed elevation changes.

Changes in flood frequency and the types of floods have been linked to bed incision or aggradation. For example, bed elevation may increase during periods of high

flow when sediment flux is high (Friedman et al., 1996), and bed elevation may decrease as a result of a decrease in sediment supply (Burkham, 1972; Topping et al., 2000; Schmidt and Wilcock, 2008).

Bed elevation changes typically occur over decadal time scales and are the cumulative result of inequalities in the magnitude of flood-event or season-scale scour and fill. Bed elevation adjustments during the passage of a flood may be related to a variety of factors. Leopold and Maddock (1953) argued that short-term changes in sediment supply and channel roughness cause changes in flow depth. On the other hand, Colby (1964) argued that the fill-scour sequence during a flood is not dependent on suspended sediment load but rather varies among cross sections within a given reach. A cross section whose bed fills during the rising stages of a flood may be matched by a downstream cross section that scours during the same part of the flood. By documenting bed elevation changes during a single flood and determining patterns of bed fill and scour, it is possible to understand the mechanisms responsible for longer time scale bed elevation change i.e. incision or aggradation.

3.3 Study Area

The San Rafael River drains approximately 6255 km^2 of the northern Colorado Plateau (Figure 3.1). The headwaters of the San Rafael River are on the west side of the Wasatch Plateau where maximum elevations are 3000 to 3400 m. In an average year, the upper elevations receive approximately 1 m of precipitation, mostly in the form of snow between October and April. There is much less precipitation in Castle Valley, where

approximately 250 mm/yr of precipitation falls mostly in the form of rain. Irrigation agriculture, which is the dominant land use in Castle Valley, relies heavily on diverting water from Huntington Creek, Cottonwood Creek, and Ferron Creek, which are the headwater streams that join to form the San Rafael River.

Downstream from Castle Valley, the San Rafael River has carved its course through Mesozoic and Paleozoic sedimentary rocks of the San Rafael Swell, a broad, northeast trending upwarp about 115-km long and 50-km wide (Witkind, 1991). The longitudinal profile of the river across the Swell includes two steep segments and two moderately steep segments (see Chapter 2). The San Rafael River exits the Swell across the San Rafael Reef, a steeply dipping monocline. Thereafter, the river flows for approximately 90 km across the San Rafael Desert before joining the Green River approximately 20 km south from the town of Green River. Average annual precipitation in the San Rafael Desert is approximately 180 mm, the majority of which falls during summer and fall. The portion of the San Rafael River that flows through the San Rafael Desert is the focus area of this study, where both channel slope and valley slope are relatively constant (Figure 2.6 in Chapter 2).

The study area is comprised of five valley segments. Boundaries between valley segments were determined from observed shifts in average valley width. These shifts roughly correlate to changes in lithology of the surrounding bedrock. In general, the alluvial valley alternates between narrow and wide segments (Figure 2.6 in Chapter 2). Valley segment three is the widest valley segment, and Hatt's Ranch and Frenchman's Ranch are located in this segment.

3.4 Methods

This study employs a combination of spatially robust and temporally precise methods to reconstruct the modern history of channel change. We used the temporally precise record of discharge measurements collected at a U.S. Geological Survey (USGS) stream-flow gage to document changes in the cross section during the time span of individual floods and during decades. We also analyzed these records to reconstruct the temporal sequence of long-term changes in bed elevation and channel width. We analyzed the stratigraphy of floodplain deposits in two locations to determine the style, rate, and magnitude of floodplain formation and to corroborate interpretation of the gaging station data.

Analysis of aerial photographs allowed extrapolation of the detailed temporal scale data to the entire study area. We analyzed aerial imagery to quantify changes in channel width, sinuosity, and vegetation establishment. Additionally, we surveyed the longitudinal profile of bed and water surface elevation for the entire study area. The integration of spatially robust and temporally precise methods provides a comprehensive picture of channel transformation during the 20th century.

3.4.1 Floodplain Stratigraphy

We excavated three trenches in the floodplain. These trenches were excavated adjacent, and perpendicular, to the channel. On the Hatt's Ranch, we excavated a 35-m long trench that was 2 to 3 m deep. The Hatt's Ranch trench was located approximately 700 m upstream from the current highway 24 bridge (Figure 3.3). We excavated two

trenches on the Frenchman's Ranch, which is located approximately 20 km downstream from the Hatt's Ranch. The Frenchman's Ranch trenches were excavated on both banks of the river, directly across from each other (Figure 3.4). The left bank trench was 18.5-m long and 1 to 2 m deep. The right bank trench was 21-m long and 1 to 2 m deep.

In each trench, we analyzed the sedimentology and dendrogeomorphology of floodplain deposits. We surveyed the trench using a Real Time Kinematic Global Positioning System (RTK GPS). We identified depositional layers based on observed contacts that were determined from observed changes in the color of the sediment, sedimentary structures, and grain size of depositional layers. We collected sediment samples in vertical profiles spaced at increments along the length of the trench to characterize both vertical and horizontal grain size trends. Additionally, we located the contacts between the stratigraphic layers on buried individual tamarisk shrubs. We noted the depth of the root crown and removed the root stock of each plant for analysis at the USGS Dendrochronology Laboratory in Fort Collins, CO. We collected a total of 20 plants: 7 from the Hatt's Ranch trench, 8 from the left bank of Frenchman's Ranch trench, and 5 from the right bank.

Our interpretation of the dendrogeomorphology of floodplain sediments included determining the rate and style of channel narrowing and floodplain formation by employing Freidman et al's (2005) method of dating floodplain sediment. When a tamarisk shrub is buried, the annual rings become narrower, vessels within the rings become larger, and annual transitions become less distinct (Friedman et al., 2005). Based on these observations, it is possible to interpret the anatomical changes to determine the

precise year(s) when layers of sediment were deposited by floods. By cross correlating among plants excavated in a single trench, it is possible to validate the interpretation of burial signals, thus providing a robust method for dating recent floodplain deposits.

3.4.2 Repeat Photography: Aerial Imagery and Ground Photographs

We acquired eight series of aerial photographs that span a 72-yr period (Table 3.1). Six of the eight photo series cover the entire study area. The photos taken in 1952, 1962, and 1974, however, provide only partial coverage of the study area. To align the historic aerial photographs with the more recent orthorectified aerial photographs, we georectified the historic aerial photographs in Erdas IMAGINE 10. Each photo was resampled using the cubic convolution method, and geo-corrected with a nonlinear transformation, which was in most cases a 3rd order polynomial transformation. Table 3.2 displays the number of photographs that were georectified, the number of control points used to georectify each photograph, and the Root Mean Square Error (RMSE) of the output georectified images. RMSE tolerances for each series of images varied, based on the spatial resolution and quality of the input image. The largest average RMSE was 3 m for the 1938 photographs and the smallest RMSE was 1.2 m for the 1962 photographs.

In ArcMAP 10, we delineated the active channel for each series of aerial photographs. We defined the active channel based on several criteria: (1) break in slope as observed in stereoscopic analyses; (2) relative absence of vegetative cover; and (3) change in sediment color. In photo series where large floods occurred in the year or two prior to the photograph date, unvegetated (bare) surfaces occurred at multiple elevations. In these instances, we included the lower elevation surfaces that we determined would be

inundated by common floods. We divided the area of the active channel calculated for each photo series by the length of the channel centerline to determine the Reach Average Active Channel Width (RAACW).

Results from channel width analyses are reported for three spatial scales in the study area. We report results for the entire study area, for a 32-km segment, and for individual valley segments. The length of the study area varies from 76.8 km to 86.3 km in channel length, depending on the year of the photograph. Four series of aerial photographs cover the entire study area. At a smaller scale, we present results for a 32-km segment between Tidwell Bottom and Frenchman's Ranch (hereafter called TbFr), because three of the photo series only overlap in this area. By reporting results for this segment, we are able to compare all seven series of aerial photographs. The TbFr segment incorporates part of valley segment one, all of valley segment two, and part of valley segment three. At a smaller spatial scale, we report results for each valley segment. Valley segments lengths vary from 2.4 km to 21.1 km.

We quantified change in erosion and deposition between successive aerial photographs. These changes were reported for the TbFr segment. By overlaying the active channel polygons delineated in ArcGIS and performing a spatial union analysis, we determined the area converted from floodplain to active channel (erosion), and the area converted from active channel to floodplain (deposition) between each photo series.

Additionally, we matched four historic ground photographs of the river, two located near the BLM campground in the Swell, one at the wood and steel bridge on

Hatt's Ranch, and one at the former San Rafael Desert Road crossing near the confluence with the Green River (see Figure 3.1 for locations).

3.4.3 USGS Gage Data

We analyzed the record of stream flow and the data associated with the discharge measurements at USGS gage 09328500 (San Rafael near Green River). The USGS began operation of the gage on October 1, 1909, temporarily halted operations on September 30, 1918, and resumed operation of the gage on October 1, 1945. We also analyzed the record of suspended sediment measurements at the gage. Except for a few missing records, the USGS measured daily suspended sediment concentrations for 8 years, in 1949 and 1951 to 1958.

The USGS moved gage 09328500 6 times within a 1.5-km length of river (Figure 3.3). Between 1909 and 1976, the gage was located within 10 m of the wood and steel bridge on Hatt's Ranch (the former Highway 24 bridge), except for two years between 1945 and 1947 when the gage was located approximately 200 m downstream. In 1976, the USGS moved the gage approximately 1.5 km downstream from the wood and steel bridge where the gage has remained to this day. The current location is approximately 120 m upstream from the current Highway 24 bridge. Presently, the USGS measures flood discharges from the wood and steel bridge where the gage used to be located. Unfortunately, of the four datum that were established at the various gage locations, no two of them are linked. Neither the datum of 1909-1920 nor the datum of 1945-1947 is related to the datum of 1947-1976. Likewise, the 1947-1976 datum is not related to the present day datum. Because the datum prior to 1947 and subsequent to 1976 are not tied

together, it is only possible to compare reconstructed cross sections for the period 1947-1976. Furthermore, we were not able to compare cross sections between 1976 and 2009, because the USGS has measured flood discharge at numerous places including both bridges on Hatt's Ranch, the current gage location, and a nearby bedrock riffle located approximately 300 m downstream from the current gage location.

Flood discharges have always been measured at a bridge or a cableway, except when they were measured at the bedrock riffle. Between 1909 and 1920, the USGS measured flood discharge at either the upstream cableway or the old highway 24 bridge that was located approximately 20 m upstream from the wood and steel bridge. Between 1947 and 1976, the USGS measured flood discharges at the cableway located 150 m downstream from the wood and steel bridge. Between 1976 and 1995, the USGS measured flood discharge mainly at the current highway 24 bridge. From 1996 to 2005, flood measurements were made at the bedrock riffle downstream of the current highway 24 bridge. Since 2006, the USGS has measured flood discharge at the wood and steel bridge.

We followed the methods described by Smelser and Schmidt (1998) when analyzing gage data. In total, we analyzed 1450 discharge measurements that span the time period that the gage has been in operation. It was necessary to account for all datum shifts and rectify the data to the appropriate common datum(s). In our analyses, we rectified data to two common datum, the datum of 2010 for the period between 1976-2010, and the datum of 1976 for the period between 1947-1976. We analyzed changes in

cross section, temporal sequence of thalweg elevations, temporal sequence of width and width-to-depth, hydraulic geometry, and rating relations.

In order to reduce error and avoid misrepresentation of channel change, we applied filters to the various gage data analyses. First, in our reconstruction of cross sections, we excluded discharge measurements outside the range of 22.4 m^3/s and 64.6 m^3/s (1.1-yr to 2.6-yr recurrence floods), which was a range of discharge that likely filled the channel but did not spill over the banks. Second, to avoid any differences in channel geometry that could be attributed to different locations (there were many), we analyzed cross sections that were measured at one only location, the abandoned cableway, which is located approximately 150 m downstream from the old highway 24 bridge (Figure 3.3). Between 1947 and 1976, the USGS measured discharge at many locations, ranging from 3.2 km upstream from the gage (Interstate highway 70) to 3.2 km downstream from the gage, but commonly measurements were made within approximately 300 m of the gage. Third, in the construction of rating relations and bed elevation time series, we ignored all measurements affected by ice, since backwater caused by ice creates an anomalous stage. Fourth, in the construction of the temporal sequence of width-to-depth and width, we excluded both low flows that did not fill the active channel (less than 7 m^3/s), and large floods that possibly spilled over the banks of the active channel (greater than 28.3 m^3/s). We did not filter the width and width-to-depth time series by measurement location, but included all measurement locations including those taken at either bridge, cableways, the bedrock riffle located approximately 400 m downstream from the current gage, and various other locations. Fifth, in the construction of at-a-station hydraulic geometry

relations, we filtered for measurement location and excluded measurements affected by ice. We removed all of the measurements taken at both bridges, since a bridge unnaturally constricts the width of the channel especially at high stream flows, and measurements taken at the bedrock riffle.

3.4.4 Longitudinal Profile

A USGS crew led by Roland W. Burchard surveyed the topography and water surface elevation of the entire length of the San Rafael River in 1925 (Burchard, 1926). It is likely that Burchard followed the same protocol that was used to survey the Grand Canyon in 1923 (Birdseye, 1928). Therefore, it is likely that the crew collected continuous elevations with a theodolite and stadia rod. The results of the survey are compiled in 4 maps, 2 plan view maps of the topography, and 2 longitudinal profile elevation plots. The profile was plotted in feet above mean sea level. The survey elevations were likely based on the North American Datum, which was the basis for the NGVD29 datum. Diversion dams and bridges and other structures such as houses are located on the maps.

The Natural Resources Conservation Service (NRCS) surveyed the water surface of the Hatt's Ranch portion of the river in 2008. In 2009 and 2010, we surveyed the remaining portion of the river. Both the NRCS and our survey measured precise elevations using a RTK GPS. We measured the water surface elevation and bed elevation approximately every 30 m at a predefined horizontal precision of 15 mm and a vertical precision of 30 mm. Both of the recent survey efforts were conducted during low flow

discharge (0.31 m^3/s to 0.96 m^3/s). The 2008-2010 survey data was post processed with orthometric elevations.

In order to compare the water surface elevation profiles surveyed in 1925 and 2008-2010, first we georectified the 1925 plan view maps in ArcMap 10.0 using a 1st order polynomial transformation. A total of 75 control points distributed across the study area were used in the georeferencing procedure. Initially, we tried using the Public Land Survey System (PLSS) section corners as control points. This strategy, however, resulted in a large offset in the valley perimeter between the 1925 maps and the 2009 orthorectified imagery, which led to several findings. First, in some places the 1925 section lines do not align to the recent PLSS section lines. Second, we noticed places where the valley perimeter in relation to the 1925 section lines does not match the 2009 valley perimeter in relation to the recent section lines (either the Emery DRG 24K topographic map *or* the PLSS sections available from Utah AGRC). Therefore, in order to accurately match the valley position in 1925 to the valley position in 2009, we used valley perimeter locations as control points. Locations where the topography from 1925 best matched the topography from 2009 were used as control points and included where tributaries enter the main valley, and steep hill slopes. Irreconcilable errors in the georectified 1925 map are due likely to errors in the extrapolation of the 1925 topography between surveyed section lines.

Second, we compared the 2 water surface elevation profiles at distances along the 1925 channel. This was necessary, because the channel in 2008-2010 is longer than the channel was in 1925, 86.3 km and 79.3 km, respectively. Distances on the 1925 profile

are reported as miles upstream from the confluence with the Green River. At each of the river mile locations identified on the 1925 maps (48 points), we extracted water surface elevations from the 2008-2010 survey data. Where the position of the 2 river channels did not align, we compared the elevation of the 2 profiles at the same valley cross-section.

3.4.5 Suspended Sediment Transport

The USGS measured suspended sediment transport at gage 09328500 daily during water years 1949 and 1951-1958. Collection of the transport data was part of a large effort in the 1950s to predict the rate of sedimentation that would occur in Lake Powell reservoir following completion of Glen Canyon Dam (Andrews, 1990). During the eight year time span that transport was measured, there were 212 missing records, which is 0.8% of the total number of days.

For this study, we developed transport relations for each of the four types of floods that occur in the San Rafael River. Short duration, warm season floods were distinguished between monsoon floods and floods that occur as a result of tropical cyclones and/or cut off low pressure storms. We determined the beginning and end of a flood based on the increase in discharge above base flow and subsequent return to base flow following the flood. In general, snowmelt floods occur in spring, monsoon floods occur in summer, tropical cyclone/cut off low-pressure floods occur in fall, and floods produced from frontal storms occur in winter and early spring. However, some floods overlapped seasons. Additionally, we calculated the unit load per volume of water and unit load per day for each of the four types of floods. We summed the load for all the

days that we distinguished as a particular flood type, then divided the load by both the volume of water and the number of days for each flood type to determine unit loads.

We calculated effective discharge using the suspended sediment data and stream flow data collected in 1949, 1951-1957 at USGS gage 09328500. The effective discharge, which is the discharge that transports the most sediment, is the mode of a sediment load histogram. The creation of a histogram involved four steps. First we sorted the discharge data, then we discretized the discharge data into 26 bins that ranged in size from 1 m^3/s to 20 m^3/s. Second, we calculated the average sediment load for each discharge bin. Third, we found the average exceedance probability of daily discharge for each bin. Fourth for each discharge bin, we multiplied the average load by the average percentage of time that each discharge bin was equaled or exceeded.

3.4.6 Cadastral Survey Notes

Cadastral survey field notes contain some of the earliest records of the measurement and description of the channel and alluvial valley in the study area. The General Land Survey Office began surveying the study area in 1882. Subsequent surveys in the study area took place in 1885, 1908 and 1915. In a search of the surveyor's field notes, we found mention of channel measurements in seven places. Originally, land surveyors used chains for measuring distances. We assumed that the type of chain used to survey the study area was a Gunter's or surveyors chain, which was approximately 66 ft long and was comprised of 100 links. The length of each link was approximately 201.2 mm. We converted measurements reported in either links or chains to meters. Also found

within the cadastral survey field notes are descriptions of the vegetation community in the riparian zone and alluvial valley.

3.5 Results

3.5.1 Land Use (1880s to the Present)

Presently, there are no year round residents in the study area, but in the past there was a small population of homesteaders and ranchers. Homesteading in the study area began in the mid-1800s. Tom Tidwell established one of the first ranches, just downstream from the exit from the San Rafael Reef (Bauman, 1987). In an area that came to be known as Tidwell Bottoms, Tom and his sons Frank, Keep, and Roland raised horses and cattle. In the mid-1880s, downstream from Tidwell Bottoms, the Halverson brothers homesteaded a portion of the valley that is now Hatt's Ranch (Kelsey, 1992). In 1885, as seen on general land office survey plats (1884), there were 14 cabins in the study area including both the Halverson' Ranch and the Tidwell's Ranch. By 1925 according to a series of topographic maps, there were only 10 structures located in the study area. In the 1930s, Baker (1946) estimated that approximately 25 people lived in the San Rafael Desert, a broad region encompassing the study area. Since the 1930s, population further declined, and presently no one lives in the study area year round; however, 2 ranches are still operational. The Hatts operate an upland game bird hatchery and hunting grounds, and the Frenchman's Ranch is used seasonally for cattle operations.

Ranching and farming have occurred in the study area since the late 1800s. The earliest evidence of land use appears on the 1885 plat maps, which show an irrigation

ditch and 2 cultivated areas of the valley, one in the vicinity of the Frenchman's Ranch and the other approximately 1.6 km upstream from the Dugout Wash confluence. In the 1930s, four ranches in the study area had cattle operations: Hatt's Ranch, Gillis' Ranch, Moore's Ranch (now called Frenchman's Ranch), and Chaffin's Ranch. Together, these 4 ranches owned between 1900 and 2400 head of cattle that grazed the study area (Hatt interview, 2011). Grazing pressure in the study area has since declined. Currently, approximately 1000 cattle graze the valley bottom and adjacent desert between October and March. Sheep also grazed the study area. From the late 1800s through the 1940s, sheep crossed the San Rafael River when migrating between winter grazing grounds in the San Rafael Desert and summer grazing in the higher elevations located in the Swell. R.L. Hatt recalls that in the early 20th century, at most, 12,000 to 18,000 sheep used to graze the San Rafael Desert between the San Rafael River and the Dirty Devil River.

Diversion dams were common in the early 20th century. Diversion dams in the study area were constructed with cottonwoods that were tied together with cable and stacked on top of each other (Hatt interview, 2011). In 1925, there were two diversion dams, one on the Gillis Ranch directly across from the Iron Wash confluence and one located approximately 3 km downstream from the confluence with Greasewood Draw on the former McMillan Lower Ranch. The elevation drop at the Gillis' Ranch dam was 2.1 m and the drop at the McMillan Lower Ranch dam was 1.8 m (Figure 3.5). By 1938, 2 additional dams were constructed, one located on Hatt's Ranch approximately 1.5 km upstream from the current wood and steel bridge and one on Chaffin's Ranch in the place where the current San Rafael Desert Road bridge is located. In the late 1930s and 1940s,

frequent floods washed away the dam on Hatt's Ranch, but the Hatts reconstructed the dam after each failure (Hatt interview with author, April 18, 2011). After the dam failure during the 1952 snowmelt flood, the Hatt's moved the dam to its current location by forcing the river to a boulder area where the river loses approximately 5.8 m of elevation over a distance of 170 m.

Of the four dams in the study area, the Hatt's Ranch diversion dam is the only remaining active dam. The dam near Iron Wash confluence washed out sometime between 1952 and 1974, and the dam on Chaffin's Ranch washed out sometime between 1938 and 1985. The dam on the McMillan Lower Ranch remained until the 1983 snowmelt flood carved a new path around the dam (Hatt interview, 2011; Figure 3.5), thereby bypassing the dam.

Homesteaders and ranchers controlled the river in portions of the study area through the construction of levees. On Hatt's Ranch, levees were constructed in the 1950s, 1960s, and 1970s to prevent the river from meandering and destroying farm land (Figure 3.6 and Figure 3.7). In addition, the Hatt's straightened the channel upstream from the wood and steel bridge in the winter of 1952/1953, and again downstream from the wood and steel bridge between November 30, 1961 and May 15, 1962 (Figure 3.6, Figure 3.7, and USGS station analysis report, 1962). Both channel straightening events involved cutting off large meander bends.

The natural migration of the San Rafael River has been restricted by bridges. There are four bridges in the study area: the Interstate-70 bridge, the wood and steel bridge on the Hatt's Ranch (formerly Highway 24 bridge), the current Highway 24

bridge, and the San Rafael Desert Road bridge (Figure 3.2). There has been a bridge over the San Rafael River on the Hatt's Ranch for 130 years (since the 1880s). The first bridge that was built was a wagon bridge. In 1910, a suspension bridge replaced the wagon bridge. In the early 1940s, the current wood and steel bridge was built, which replaced the suspension bridge. In 1971, Highway 24 was rerouted to its current location and the current highway 24 bridge was built. The I-70 bridge was completed in 1970.

3.5.2 Hydrology

Three types of floods occur in the San Rafael River. Snowmelt floods, which historically were the longest duration, typically occur in May or June. The second type, flash floods, occurs in the summer and fall and is of short duration – this type of flood may last only a few hours or up to a week. Three types of weather patterns are responsible for these short duration flash floods: the North American monsoon, cut-off low-pressure cells, and dissipating tropical cyclones (Hereford and Webb, 1992). Floods produced by dissipating tropical cyclones and by cut-off low-pressure cells typically last a few days to one week. The third type of flood occurs in winter – these rare floods are produced by low intensity frontal storms.

Collectively, reservoirs, diversions, and decadal scale climate variation (Webb and Betancourt, 1992; Hereford et al 2002) have decreased the mean annual flow and the magnitude and duration of the annual snowmelt flood, as well as the magnitude of the magnitude of warm season floods.

Many dams and diversions have been constructed on the Wasatch Plateau, where the snowmelt flood originates. Construction of diversions and dams began in the late

1880s (Geary, 1996). Today, eight major reservoirs contain a total usable capacity of 142 hm^3 (Mundorff and Thompson, 1980). The first three significant dams that were built include a dam on Ferron Creek (built in 1890), the dam that created Cleveland Reservoir on Huntington Creek (built in 1905), and the dam that created Rolfson Reservoir (completed in 1935). In the 1960s and 1970s, five additional storage projects were completed. Two of these storage projects - Joe's Valley Reservoir, which is impounded by a dam on Cottonwood Creek (78 hm^3), and Huntington North Reservoir, which is an off-stream impoundment (7 hm^3) - were completed in 1966 as components of the Emery County Project. The Emery County Project was part of the Colorado River Storage Project Act of 1956. In the 1970s, two additional dams were constructed, Mill Site Dam (23 hm^3) and Electric Lake Dam (39 hm^3).

In the headwaters, water is diverted in many places for both agricultural and industrial purposes (Figure 3.8). Between 1961 and 1990, approximately 60% of the average annual unregulated runoff (287 hm^3/yr) was diverted for municipal, industrial, and agricultural purposes (UBWR, 2000). Fourteen percent of the total unregulated annual runoff was diverted for agriculture, and an additional 46% was diverted for municipal and industrial purposes (UBWR, 2000). Because of the numerous diversions and significant capacity for water storage in the Wasatch Plateau and Castle Valley, spring snowmelt floods pass through the San Rafael Swell only in years of abundant snowfall and rapid snowmelt.

The magnitude and duration of the annual snowmelt flood has declined considerably in the 20th century. Between 1910 and 1918, the median spring snowmelt

flood contributed 67% of the total annual runoff, and the duration and peak of the snowmelt flood was approximately 70 days and 37.4 m^3/s, respectively (Figure 3.9). In contrast, the annual snowmelt flood for the time period 2000-2008 lasted only approximately 23 days, and the magnitude of the peak flow was 9.8 m^3/s, a 67% and 93% reduction from the early 1900s, respectively. Furthermore, between 2000 and 2008, the median annual snowmelt flood comprised only 25% of the total annual runoff, a 62% decrease from 1910-1918.

The notable decline in the magnitude and duration of the snowmelt flood is manifested in the mean annual flow as well. Mean annual flow was the greatest for the period 1910-1918 (Figure 3.10 and Table 3.3), and declined for each subsequent period, except between 1980 and 1986 when mean annual flow was nearly as large as in the beginning of the 20^{th} century.

Changes in total stream flow are also reflected in changes in the duration of those flows (Figure 3.11). Between 1987 and 2010, there was virtually no stream flow in the study area 5 % of the time (18 days per year). In contrast, flows were extremely low for only about 1 % of the time between 1910 and 1918.

Although snowmelt floods have the longest durations and greatest flood discharge, they do not produce the largest instantaneous peak discharges. The five largest measured peak flows occurred in summer or fall (Table 3.4 and Figure 3.12). These notable floods occurred on September 2, 1909 (339.8 m^3/s), October 8, 1916 (325.6 m^3/s), November 4, 1957 (273.5 m^3/s), August 22, 1947 (244.6 m^3/s), and September 10, 1961 (134.2 m^3/s) (Table 3.4, Figure 3.12, Figure 3.13). It is also evident in Figure 3.12

that the years with the largest total annual runoff - 1984, 1983, 1952, and 1914 - were years with the largest snowmelt floods. The largest snowmelt flood recorded at USGS gage 09328500 reached its peak on June 4, 1952 (126.8 m^3/s). Not only has the magnitude of snowmelt floods declined, but the magnitude of warm season floods has also declined over the 20^{th} century. In fact, when comparing the partial duration flood frequency for each flood type split into two time periods, the decline in the warm season flood magnitude for specific recurrence intervals is more pronounced than that of snowmelt floods (Figure 3.14 and Figure 3.15). For example, at the 25-year recurrence interval, the snowmelt flood decreased 38%, whereas the warm season flood decreased 64%. The spread of the two LPIII curves for warm season floods is undoubtedly affected by the anomalously large magnitude warm season floods in 1909, 1916, 1947, and 1957; whereas, the large snowmelt floods in 1983 and 1984 may contribute to the lack of spread between the two time periods for the snowmelt flood population. Differences in the σ_{logx} parameter of the LPIII distribution between the two flood types as well as the two time periods within a population provides further evidence of the decrease in flood variability, i.e. the ratio of large to small floods (Table 3.5).

Coincident with a decrease in flood variability, there has been a shift from a flood dominated regime to a drought dominated regime with fewer floods overall. For example, a snowmelt flood exceeded 26 m^3/s nearly every year between 1909 and 1920 and between 1945 and 1958. However, between 1959 and 2008, snowmelt floods greater than 26 m^3/s occurred, on average, only once every 3 years. There is a similar decline in the frequency of the warm season floods. For example, on average, between 1909 and 1958,

warm season floods greater than 26 m^3/s occurred 3 times every 2 years, and from 1959 to 2008 a warm season flood occurred four times every five years.

3.5.3 Suspended Sediment Transport

More suspended sediment is transported during the monsoon season than is transported during the snowmelt season. Over a wide range of flows, the suspended sediment load transported by monsoon floods is an order of magnitude more than during the snowmelt season (Figure 3.16, Table 3.6). Monsoon floods also have greater concentrations of suspended sediment than both winter frontal storms and autumn flash floods. These observations are based on sediment transport measurements made in 1949 and between 1951 and 1958.

According to the sediment load histogram, small to moderate sized floods transport the greatest amount of suspended sediment per unit discharge. The two largest modes of the sediment load histogram are of similar magnitudes (Figure 3.17). The mode with the highest sediment load is 30-35 m^3/s, which is a 1.2 -1.3 recurrence interval flood (Figure 3.13), and the subordinate mode is 20-25 m^3/s, which is a 1.1 yr recurrence flood. At Frenchman's Ranch, the two largest modal values of the effective discharge curve inundates not only the near channel bench but also the near channel levee of FP#1 At Hatt's Ranch the largest mode of the effective discharge curve inundates just the near channel bench portion of FP#1. The difference in the elevation and extent of inundation for the same discharge at each trench site may be explained by the difference of incision history at the two sites.

3.5.4 Channel Change

3.5.4.1 1871 to 1908: Large Floods, High Water Table, No Tamarisk

There is little information about the stream flow regime of the late 1800s and the earliest 1900s. Floods of this period maintained a channel that was between 10 and 40 m wide (Table 3.7). One of the earliest accounts of the San Rafael River was Dellenbaugh's description of the river mouth in July 1871 during the second J.W. Powell expedition (Dellenbaugh, 1908). Dellenbaugh estimated the dimension of the San Rafael River near the confluence with the Green River to be approximately 7.6 m wide and 0.25 m deep, likely a measurement of wetted width. A few days later, Dellenbaugh reported a "booming flood" that was presumably caused by a monsoon storm. Some of the monsoon floods at the turn of the 20th century were exceptional enough to be reported in newspapers. For example, monsoon floods that occurred on September 12, 1897, and July 30, 1899, were noted in local newspapers (Table 3.4). Further upstream, just east of the San Rafael Swell in July 1876, a discharge of 47.5 m^3/s was measured (Powell, 1879). Powell stated that this measurement was made at "high water, though not when the streams were at their flood."

Channel width estimates contained in cadastral survey field notes range from 10 to 40 m (Table 3.7). These data, however, cannot be compared to active or bankfull channel widths of the 20th century, because the 1880s estimates were imprecise, the discharge at the time of measurement is not known, and the reported measurements may have been of only the wetted portion of the active channel. Surveyors reported that the

channel was approximately 10-m wide in 1881, and 40-m wide on November 24, 1885 when the river was probably in flood.

3.5.4.2 1909 to 1952: Maintenance of a Laterally Unstable Channel by Large Floods

There was more stream flow in the San Rafael River in the first part of the 20th century than at any subsequent time. Mean annual flows were greater, and floods were larger. The mean annual flood for the period between 1909 and 1958 was 115.6 m^3/s (Table 3.3). Floods were especially large between 1910 and 1918 when the average flood was 138.9 m^3/s. The largest of these floods occurred in the summer and fall. The flood of record on the San Rafael occurred on September 2, 1909, and was 339.8 m^3/s. The second largest flood of record occurred on October 8, 1916, and was 325.6 m^3/s. The August 22, 1947, flood of 244.6 m^3/s was the fourth largest flood of record. Although there is a gap in the stream-flow record between 1918 and 1946, various sources including newspapers documented floods during this time period (Table 3.4). This period ended with the very large snowmelt flood of May and June 1952. During the 1952 snowmelt flood, daily stream flow exceeded 30 m^3/s from May 3 to June 27, and exceeded 50 m^3/s between May 28 and June 16. The peak stream flow occurred on June 4 and was 126.8 m^3/s.

Between 1909 and the 1930s, riparian vegetation was similar to the descriptions made by explorers and surveyors in the late 1800s. Cottonwoods, willows, and grasses were dominant. Accounts of the San Rafael River valley describe abundant grass, sedges, and wetlands that suggest that the water table was near the surface in much of the valley. As seen in an oblique aerial photograph taken in 1929 (Figure 3.18), cottonwood stands

were scant in the San Rafael Swell but were prevalent in the study area (Baker, 1946, Figure 3.19). R.L. Hatt recalled the abundance of sedge (locally known as bullsod), which cattle liked to graze (Hatt interview, 2011). Dunham (interview, 1999) stated that thousands of cattle died in bogholes in the study area, which implies that wetlands were abundant. Then in the 1930s and 1940s, tamarisk began to establish. R.L. Hatt remembered a few scattered clumps of tamarisk when he first moved to the San Rafael River valley in 1934 (Hatt interview, 2011). In the late 1940s and 1950s, dense stands of tamarisk up to 2.1 to 2.4 m tall covered the floodplain at USGS gage 09328500 (Figure 3.44 in Appendix 2 and Figure 3.45 in Appendix 2).

The channel depicted in the 1938 aerial photographs was braided and comprised of numerous bars. The typical point bar was comprised of surfaces at multiple elevations that were sparsely covered with vegetation (Figure 3.20). Other in-stream geomorphic units present in 1938 were lateral bars, mid-channel bars, and unvegetated benches. There were multiple low flow channels within the wide active channel. The main thread of the low-flow channel was much more sinuous than the sinuosity of the active channel. At a channel filling flow, the river was a single-threaded, meandering stream with short secondary channels.

The channel shifted course frequently during the first half of the 20th century. R.L Hatt recalls the sand and mud bedded channel of the San Rafael River being laterally unstable. Floods overtopped the banks frequently, and water spread as much as 800 m across the valley in the vicinity of Hatt's Ranch (Hatt interview with author, April 18, 2011). The recollections of lateral instability are confirmed by comparing the channel

course depicted in 1925 topographic maps and aerial photographs taken in 1938. We identified twenty-four cut off meander bends; most of these occurred in valley segments two and three (see Table 2.3 in Chapter 2). There were fewer avulsions between 1938 and 1952; only 6 meander bends in the study area were cut off. Meander bends that were not abandoned grew by translation, extension, and rotation. Although meanders actively migrated, the average channel sinuosity over the length of the TbFr segment did not increase (Table 3.8).

Meander migration caused nearly equal amounts of floodplain construction and bank erosion. Results from a spatial union of active channel polygons mapped in the 1938 and 1952 aerial photographs indicate that there was approximately 0.64 km^2 of bank erosion and approximately 0.67 km^2 of floodplain construction in the TbFr segment (Figure 3.21 and Table 3.9).

During this period, the channel expanded and contracted, yet there was a lack of net change in channel width. The lack of net change in channel width is evident in analyses conducted over the large spatial extent of the 32-km long TbFr segment, as well as at the site of USGS gage 09328500. Between 1909 and 1920, the average width of the active channel at the gage was 30.9 m (Table 3.10), and the average width-to-depth ratio was 66 (Table 3.11). Between 1945 and 1953, the average channel width was 34.4 m. The width of the channel at USGS gage 09328500 is likely narrower than most of the rest of the river, however, because of the constriction of the channel by the bridge. For example, the reach active channel width delineated on 1938 aerial photographs, at both

the TbFr segment (48.9 m) and for entire study area (48.3 m), was 30% wider than the width measured at USGS 09328500 (Table 3.8 and Table 3.12).

Between 1909 and 1920, the stream bed scoured during each snowmelt flood and filled to the preflood elevation over the course of the months following the flood (Figure 3.22). However, during the snowmelt flood of 1952 the bed scoured 0.75 m, and following recession of the 1952 flood, the bed did not fill to the pre-flood elevation.

3.5.4.3 1953 to 1958: channel narrowing, incision, floodplain formation, channel reset

During the short period between 1953 and 1958, streamflow was highly variable and there was considerable channel change. Following four years of low stream flow (1953-1956), three successive floods occurred in a 14-month period. A significant snowmelt flood in 1957 was followed by an extremely large flash flood, which was followed by a significant snowmelt flood in 1958. The November 4, 1957, flash flood was the third largest instantaneous peak discharge (273.5 m^3/s) ever measured, exceeded only by the floods of 1909 and 1917 (Table 3.4 and Figure 3.10). Because the flood was of short duration – it lasted only approximately 3 days, and the peak discharge lasted only a few hours – the peak mean daily discharge of 117.8 m^3/s was half of the magnitude of the instantaneous peak. The snowmelt flood of 1958, which was bigger and longer than the 1957 snowmelt flood, had a peak mean daily discharge of 63.4 m^3/s and lasted approximately 86 days.

At USGS gage 09328500, the channel narrowed by 24% in the 4 years between the recession of the 1952 snowmelt flood and the onset of the 1958 snowmelt flood (Figure 3.23 and Table 3.10). The 1958 snowmelt flood re-widened the channel at the

gage. Tamarisk established on and stabilized the in-channel 1952 flood deposits, as seen at both floodplain trench sites, which in turn facilitated channel narrowing. The combination of narrowing and incision caused a decrease in the width-to-depth ratio from 88.7 to 45.7 between the periods 1945-1953 and 1953-1958, respectively (Figure 3.23 and Table 3.11).

Incision, which began during the recession of the 1952 snowmelt flood continued throughout this time period at a rate of approximately 0.2 m/yr, for a total bed elevation decrease of 1.5 m (Figure 3.24). The evidence of bed lowering in a comparison of photographs taken on August 21, 1951 and again on November 22, 1957 at USGS gage 09328500 validates the record of bed lowering in the minimum stream bed elevation time series measured at the USGS gage 09328500 (Figure 3.45 in Appendix).

3.5.4.4 1959 to 1979: Channel Narrowing, Bed Level Changes, and Floodplain Formation During Expansion of Tamarisk and Decreases in Stream Flow

During this 20-year period, the channel narrowed significantly throughout the study area, channel capacity decreased, and the bed incised in the vicinity of Hatt's Ranch. Ultimately, the channel's shape changed from wide and shallow to narrow and deep.

The largest floods of this period occurred during the monsoon season, and there were no significant snowmelt floods. The biggest flood of this period occurred on September 9-11, 1961 (instantaneous peak = 134.2 m^3/s). In general, flood magnitudes were small; the mean annual flood magnitude between 1959 and 1979 was 44.4 m^3/s (Table 3.3).

During this period, the river narrowed by 50%. At the gage, narrowing was caused primarily by deposition of an inset floodplain on the left bank that vertically accreted approximately 1 m (Figure 3.25). Further downstream at the trench location, the lateral accretion (13 m) of an inset floodplain along the right bank accounted for nearly all of the channel narrowing in the 1960's and 1970s (Figure 3.26).

Tamarisk facilitated the growth of the inset floodplain at the trench location, and presumably at the USGS gage site as well as throughout the study area. We excavated five tamarisk trees that germinated on near channel floodplain surfaces (a near channel bench and a levee) that had been deposited in the 1960s and 1970s. At the larger spatial scale of the TbFr segment, the channel narrowed 58% between 1952 and 1974. However, the rate of narrowing was greater between 1952 and 1962 (1.78 m/yr) than between 1962 and 1974 (0.65 m/yr), presumably because the accommodation space, or width of the active channel, in 1952 was greater than in 1962 at which time the channel had narrowed considerably (Table 3.8).

In addition to lateral accretion, the inset floodplain vertically accreted during this time period. At the Hatt's Ranch trench site, the floodplain vertically accreted approximately 2 m. At the Frenchman's Ranch trench site, we don't know the magnitude of the vertical accretion of the floodplain, because little to no floodplain that had formed during this time period is preserved (Figure 3.27). Nevertheless, tamarisk stabilized lower elevation point bar deposits that had formed during this period and consequently these deposits are preserved in the floodplain depositional record. Specifically, we excavated two tamarisk trees that germinated in 1965 and 1976 on point bar surfaces.

Coincident with channel narrowing, the channel bed in the vicinity of Hatt's Ranch continued to incise, however, the rate of incision was slower than the previous period 1952-1958. Between 1958 and 1965, the elevation of the bed lowered at a rate of approximately 0.05 m/yr for a total decrease of 0.3 m in bed elevation. The 1965 snowmelt flood halted incision, and a period of aggradation continued until 1976. During this period, the bed slowly filled at a rate of 0.03 m/yr for a total bed increase of approximately 0.5 m.

These changes in channel width and bed elevation caused the channel to accommodate discharge differently than in the past. Increasing discharge can be accommodated by either increases in cross-section area or increases in velocity, and the rate at which width, depth, and velocity increase with increasing discharge is a fundamental channel attribute called hydraulic geometry (Leopold and Maddock, 1953). Between 1965 and 1976, the channel was typically deeper than it was in the first half of the 20^{th} century (Figure 3.28). Mean section velocity in the narrower channel was typically faster in 1958-1976 than early in the 20^{th} century (Figure 3.28).

Although floodplain construction outpaced bank erosion, moderate sized floods in the 1960s and 1970s eroded banks and parts of the floodplain (Figure 3.21 and Table 3.9). In the TbFr segment during the period 1962-1974, 0.43 km^2 of active channel was converted to floodplain, and 0.21 km^2 of floodplain was eroded and converted to active channel. In addition to inset floodplain formation, vertical accretion in abandoned meanders also reduced the complexity of aquatic habitat.

A decrease in channel capacity as a result of channel narrowing resulted in the ability of small floods to reach higher stages. For example, the flood on June 15, 1965, with a peak magnitude of 51.8 m^3/s, achieved a similar stage (1260.1 m asl) as did a slightly larger flood of 56.4 m^3/s that occurred 7 years earlier on May 27, 1958 (Figure 3.29). In another example of the effect of decreasing channel capacity, a flood of 28.5 m^3/s on June 5, 1970, achieved a slightly higher stage than a flood of 34.6 m^3/s on May 20, 1958 (Figure 3.29). Despite the overall decrease in stream flow, these small and moderate floods inundated and increased the elevation of the recently aggraded floodplain. Floodplain inundation by floods in the 1950s, 1960s, and 1970s was the likely mechanism by which tamarisk became widespread in the San Rafael valley. R.L. Hatt recalled that tamarisk were widespread in the valley by the 1950s.

3.5.4.5 1980 to 1987: Incision, Vertical Accretion, and Channel Widening Followed by Narrowing

The snowmelt floods of 1983 and 1984 re-initiated bed incision in the vicinity of Hatt's Ranch, widened the channel by bank erosion, caused avulsions and chute cut offs, formed new inset floodplains, and vertically accreted existing floodplains. Between 1974 and 1985, the average width of the channel in the TbFr segment (Table 3.8) increased by 58% from 22.4 to 35.5 m. Multiple channels were created. Sinuosity increased in some places, while avulsions straightened the river elsewhere.

The 1983 and 1984 floods eroded banks and the surfaces of existing floodplains, while depositing sediment elsewhere. In planform, more floodplain was converted to active channel than was constructed; the ratio of areas of erosion to areas of deposition

was 3.15 (Figure 3.21 and Table 3.9). These powerful floods eroded and subsequently deposited fresh sediment on to floodplain surfaces. For example, the wavy unconformable contact at the base of the 1983 flood deposit in the Hatt's Ranch trench indicates that the 1983 flood stripped some of the upper portion of the floodplain surface before depositing new sediment (Figure 3.26). The 1980s floods added between 0.5 m and 0.75 m of fine to very fine sand at Hatt's Ranch trench and approximately 1 m of very fine sand in the right bank trench at Frenchman's Ranch (Figure 3.26 and Figure 3.27).

The channel bed in the vicinity of the Hatt's Ranch incised approximately 0.75 m during the 1983 snowmelt flood (Figure 3.30). During and following the recession of the snowmelt flood, the bed failed to fill to the elevation prior to the 1983 flood. Between the recession of the 1983 snowmelt flood and 1987, bed elevation was maintained.

3.5.4.6 1988 to Present: Channel Narrowing, Incision, and Vertical Accretion

Further narrowing and vertical accretion of the floodplain throughout the study area, and incision of the bed in the vicinity of Hatt's Ranch occurred in the last two decades, during this period of declining stream flow. Since 1988, the channel bed in the vicinity of Hatt's Ranch incised approximately 0.4 m. In combination with the 0.75 m of scour during the 1983 flood, the bed in the vicinity of Hatt's Ranch is now approximately 1.2 m lower than it was immediately preceding the 1983 flood (Figure 3.30).

Over the entire study area between 1985 and 1997, the channel narrowed 65% at a rate of 1.7 m/yr (Table 3.12). Reach average channel width was 31.9 m in 1985 and 11.2 m in 1997. The rate of narrowing decreased between 1997 and 2009 to 0.2 m/yr. Today,

there is little variation in channel width throughout the study area (Figure 3.31 and Table 3.13).

There occurred significant variation in the magnitude of channel narrowing among sites during this time period. For example, at the Hatt's Ranch trench site, the channel narrowed less than 10 m since the 1980s; nearly all of this narrowing was accomplished by the construction of an inset floodplain along the right bank (Figure 3.26). In contrast, the channel at the Frenchman's Ranch trench site narrowed twice as much (approximately 20 m) in the same time period as a result of the construction of inset floodplains along each bank. In each bank at Frenchman's Ranch, the inset floodplain is comprised of the same sequence of topographic features: a near channel bench that climbs upward and onshore to a levee which descends to a floodplain trough.

At both trench sites during this time period, tamarisk stabilized both active channel surfaces and nascent inset floodplains. In total, we excavated 8 tamarisk shrubs that germinated in the 1990s, one at Hatt's Ranch, and seven at Frenchman's Ranch. At Frenchman's Ranch, the excavated tamarisk shrubs germinated on active channel surfaces including a point bar as well as on channel banks including the offshore side of a levee. At Frenchman's Ranch, stratigraphic evidence reveals tamarisk promoted sediment deposition which facilitated the growth of levees and near channel benches.

Since the 1980s, inset floodplains vertically accreted. At Frenchman's Ranch, newly created inset floodplains vertically accreted 1.0 to 1.5 m. The uppermost layers of sediment on this floodplain (FP#1) were deposited during monsoon floods that occurred in 1999 and 2006. At Hatt's Ranch, floods during this time period failed to inundate the

older, onshore floodplain surfaces (FP#2 – see Chapter 2). However, the inset floodplain that had formed during this period at Hatt's Ranch vertically accreted approximately 2 m (Figure 3.26).

As channel capacity continued to decrease, the stage of floods in the most recent two decades has increased. Increasing flood stage has occurred despite a decrease in bed elevation in the vicinity of Hatt's Ranch. For example, a flood on October 7, 2006, with a peak discharge of 40.5 m^3/s, reached a stage of 1258.8 m (Figure 3.32); a smaller flood on October 7, 2010, with a peak discharge of 27.4 m^3/s, reached a higher stage of 1259.5 m. At Frenchman's Ranch, the October 2010 flood inundated and deposited a veneer of mud across the "lower" of the 2 floodplain surfaces (labeled floodplain surface #1 in Chapter 2).

3.5.5 Changes in the Longitudinal Profile

The overall shape and elevation of the longitudinal profile has not changed significantly since 1925, but large changes have occurred locally. There are five segments where bed aggradation has occurred and one segment where incision is evident (Figure 3.33). The most downstream reach of aggradation extends from the San Rafael Desert Road bridge upstream into the downstream half of valley segment four. The second aggradational reach is located in the upstream portion of valley segment four, and it extends for approximately 5 km upstream of Spring Canyon and ends at Dugout Wash. The third aggradational reach is located at the confluence of Cottonwood Wash and was impacted by a monsoon flood in 2010 in Cottonwood Wash. Fine sediment deposited from the 2010 flood blocked the flow of the San Rafael River causing backwater

conditions approximately 5 km upstream. A fourth aggradational reach is located upstream of Iron Wash and extends for approximately 7 km upstream. The fifth aggradational reach is located upstream of the Hatt's Ranch diversion dam and extends approximately 18 km upstream to the San Rafael Reef. Of the five aggradational segments, the most upstream aggradational segment is the longest and exhibits the greatest magnitude of aggradation. Of the four downstream aggradational segments, average aggradation was approximately 1 m, and the greatest magnitude of aggradation was 3 m, which occurred in the short segment upstream from Cottonwood Wash.

A short, incised segment is located in valley segment three. The incised segment begins at the former Lower MacMillan Ranch diversion dam and extends upstream for approximately 6 km. The greatest magnitude of incision noted in the profile comparison is approximately 2 m. Additionally, bedrock is currently exposed in the bed of the river in three places (Figure 3.33). In these three places, the bed of the river in 1925 was nearly the same elevation or slightly higher (<0.5m). Thus, the bed of the river was likely to either have been on bedrock or close to bedrock in 1925 in these three places.

3.5.6 Processes That Cause Channel Change

3.5.6.1 Unequal Amounts of Scour and Fill

There have been two periods of incision in the vicinity of Hatt's Ranch. The first period occurred from 1952 to 1965, and the second period occurred from 1983 to 2009. Both periods of incision began during a large snowmelt flood (1952 and 1983) when the magnitude of scour exceeded the magnitude of fill during the flood. Additional bed

incision occurred during subsequent snowmelt and warm season floods as well as during periods of low flow. Thus, bed incision cannot be uniquely linked to either snowmelt floods or warm season floods. Furthermore, bed lowering occurred during periods of both relatively small floods, e.g. 1952-1956, and during periods of large floods, e.g.1957 and 1958. Thus, bed lowering cannot be linked to a period of time characterized by either small or large flood magnitudes.

The sequence of scour and fill during the passage of a snowmelt flood varies from place to place on the Hatt's Ranch. The general pattern of scour during rising stages and fill during falling stages is apparent at four locations on the Hatt's Ranch where the USGS has measured stream flow: (1) the cableway upstream of the wood and steel bridge, (2) the wood and steel bridge, (3) the current location of the USGS gage, (4) and the current Highway 24 bridge (Figure 3.3). Conversely, the bed fills during rising stages and scours during falling stages at two locations, the abandoned cableway downstream from the wood and steel bridge, and the bedrock riffle (Figure 3.3). Different patterns of scour and fill is consistent with observations made in other streams (Colby, 1964; Topping et al., 2000).

The pattern of scour and fill was relatively similar at each cross section during the time period each cross-section was used to measure discharge, however, there were a few exceptions to the general trends of scour and fill. For example, at the abandoned cableway where the USGS measured discharge from 1947 to 1976, there were a few floods where the sequence of scour and fill differed from the general pattern of fill during rising stages and scour during falling stages (Figure 3.34). For example, during the 1952

snowmelt flood, the bed filled during the rising limb, scoured at the peak then filled during the falling limb. Also, during the 1953 snowmelt flood, the bed scoured during the rising limb and peak, then filled during the falling limb. Also, during the 1957 snowmelt flood, the bed scoured during the rising limb and peak, then filled during the falling limb, then scoured during the secondary peak and continued scouring during the final falling limb. Additionally, at the current gage location, the fill/scour sequence during two snowmelt floods differed from the usual pattern observed here (Figure 3.35). During the measurement of the relatively small snowmelt flood in 1978, 30 m from the current gage location, the bed filled during the rising stage and scoured during the falling stage. Also, during the discharge measurement of the 1980 snowmelt flood at the current Highway 24 bridge, the bed filled during the rising stage, yet failed to scour or fill during the falling stages. Since the hydraulic controls did not change at these cross sections, then it is likely that a change in sediment supply was responsible for the anomalous scour and fill pattern during these floods.

The sequence of scour and fill can be determined for only a few flash floods. Because of the typical long duration of a snowmelt flood, discharge is measured several times during the duration of a snowmelt flood. On the other hand, because of the short duration and unpredictable nature of warm season floods, discharge measurements during these floods are uncommon. Consequently, the precise timing of bed elevation change during flash floods is rarely available. For example, between 1947 and 1976, there were only three flash floods where bed elevation changes could be discerned: 1950, 1951, and 1960 (Figure 3.34). During these instances, the bed filled during the rising limb and

scoured during the falling limb, which is the same pattern that was observed during snowmelt floods during this same time period at the abandoned cableway. More recently, between 1976 and 2008, the scour and fill sequence could only be determined for four floods other than snowmelt floods, including a winter flood (1979), and three warm season flash floods: 1980, 1982, and 2006. During these four floods, the bed responded in the same pattern as occurred during snowmelt floods, which was scour during rising stages and fill during falling stages. (The flood discharges of 1979, 1980, and 1982 were measured at the current highway 24 bridge, and the flood discharge of 2006 was measured at the wood and steel bridge.)

3.5.6.2 Inset floodplain formation

In the following section of the results, we present sedimentologic and dendrogeomorphic data from each of the three trenches that we excavated in floodplains of the study area. We use sedimentologic evidence of floodplain deposits to determine how inset floodplains formed. Then, we correlate dendrogeomorphic data to the hydrologic record to determine the timing of inset floodplain formation. In general, we found that the incipient stages of inset floodplain formation are characterized by the preservation of in-channel sand bars during sequential years of low peak flood and low mean annual flow. Subsequently, moderate and large floods deposited fine grained sediment, both obliquely and vertically, on top of the sand bars, which both narrowed the channel and increased the height of the floodplain.

The sedimentology of a sand bar is diverse. Typically, sediment layers within a sand bar are discontinuous and the contacts between the layers are often indiscernible

(Figure 3.36 and Figure 3.37). Mud layers are often massive, which indicate that portions of sand bars were deposited in a low velocity environment where silt and clay could settle (Dean and Schmidt, 2011). Sedimentary structures within a sand bar include rippled sand, parallel lamination, or dune cross-stratified sand. There may also be lenses of gravel within a sand bar. The vertical profile may contain either fining upward sequences, or coarsening upward sequences, or no clear grain size gradation. The top of a buried sand bar may be flat or slightly convex. Sand bar packages exposed at the base of each of the three trenches are obliquely accreted onto adjacent sand bar deposits or may be inset against the channel bank. The inclined layers, similar to Thomas and other's (1987) inclined heterolithic stratification, usually thin and fine onshore and may transition to horizontal layers that conformably overlie higher floodplain surfaces. Vegetation induced sedimentary structures (Rygel et al., 2004; Dean et al., 2011) are present in sand bars and include upturned and downturned beds, root casts, and mud filled voids created by decayed vegetation.

Sand bar sedimentary structures are preserved at the base of each floodplain trench. In the Hatt's Ranch trench, there are ten sand bar packages, which are layers of sediment that were deposited within the active channel and preserved in the sedimentary record. The Hatt's Ranch sand bar packages located furthest onshore are higher in elevation than those located closer to the present day channel. At the base of the right bank trench at Frenchman's Ranch, there is a sequence of five sand bar packages. In contrast to the Hatt's Ranch trench, the bar platforms at Frenchman's Ranch are primarily comprised of horizontal bedding, but may also include minor oblique components, where

sediment layers conformably drape over older sand bars. Furthermore, the sequence of bars in the right bank at Frenchman's Ranch are positioned at relatively the same elevation, the oldest are located furthest onshore and progressively get younger toward the channel. The trench at the right bank at Frenchman's Ranch is located on the inside of a meander bend. Thus, the exposed sequence of bars records a record of channel narrowing through the deposition and stabilization of point bars. In the left bank at Frenchman's Ranch, only the top of one preserved sand bar is exposed at the base of the trench.

The vertical accretion of inset floodplains is accomplished by the construction of levees and/or benches on top of sand bars. A bench is constructed by the oblique and vertical accretion of mud and fine sand. Layers within a bench may be continuous in both the offshore and onshore directions (Figure 3.38). The contacts between the layers may either be conformable or erosional. There is no clear trend of fining upward from the bottom of a bench to the top of a bench. A preserved thin layer of duff accumulation may occur at the top of a bench.

A levee is constructed of obliquely and vertically accreted layers of fine sediment that overlie either sand bars or benches (Figure 3.39). Levees are mostly comprised of very fine to fine sand and contain climbing ripples, ripple drift cross stratification, and wavy and planar parallel laminae. Layers of sediment within a levee may be continuous in both the onshore and offshore direction. In the onshore direction, continuous layers thin and fine, and typically conformably drape over an onshore trough and/or additional levees, thus contributing to the vertical accretion of the floodplain. A thin layer of duff

may occur at the top of a buried levee. There is no clear grain size trend from the bottom to the top of a levee deposit. However, within a levee, there may be preserved a cyclothem, which is a sequence of coarsening upward sediment that then transitions to a fining upward sequence. A cyclothem is the complete record of sediment deposition during both the rise and fall of a flood. Furthermore, bioturbation occurs within both bench and levee deposits, and includes vegetation induced sedimentary structures such as upturned and downturned beds, root casts, and mud filled voids created by decayed vegetation.

The stabilization and vertical accretion of channel sand bars occurred during consecutive years of low magnitude floods and low mean annual flow. The oldest modern sand bars exposed in the stratigraphic record of the excavated trenches were deposited in the early 1950s. Following the 1952 flood, tamarisk germinated in and stabilized sand bars that were deposited during four consecutive years of low magnitude floods and low mean annual flow, from 1953 to 1957. Subsequent to the 1950s, floodplain formation occurred rapidly during a period of low mean annual flow and low peak floods of the 1960s and 1970s, when tamarisk continued to stabilize sand bars and overlying benches. Not only did tamarisk shrubs effectively stabilize recently deposited bars, but the shrubs also actively promoted sedimentation, as shown by the upturned and downturned beds surrounding buried tamarisk shrubs (Figure 3.40). Following the stabilization of sand bars and growth of benches, moderate sized floods deposited additional layers of sediment, thereby forming levees and adding to floodplain troughs between levees. Levee construction, in addition to the deposition of horizontal layers in floodplain troughs, has

vertically accreted the inset floodplain at Hatt's Ranch approximately 1.5 m to 2.5 m since 1952 (Figure 3.26), and approximately 1.5 m to 1.75 m at Frenchman's Ranch (Figure 3.27).

Floods of both types, snowmelt and warm season, have contributed to the development and growth of inset floodplains. The 1952 snowmelt flood widened the channel as shown on both aerial photographs and in the stratigraphic record of the floodplain (erosional truncation of older floodplain and channel deposits). However, the 1952 snowmelt flood also deposited sediment within the channel, which then was stabilized by vegetation during a 4-year period of low magnitude floods. Furthermore, the large sequential snowmelt floods that occurred in 1983 and 1984 both widened the channel as shown in a comparison of the 1974 and 1985 aerial photographs, and stripped sediment from parts of the floodplain as shown by the truncation of underlying deposits. They also increased the height of the floodplain by depositing very fine to fine rippled and dune cross-stratified sand (Figure 3.26 and Figure 3.27). Additionally, monsoon floods have also contributed to the growth of levees, and thus the vertical accretion of the floodplain. For example, the monsoon flood of October 2006 deposited sediment on top of near channel benches in trenches at both locations. Also, the flood of October 2006 built the levee that is currently the near channel levee, exposed in the trenches at both Hatt's Ranch and Frenchman's Ranch.

3.6 Discussion

3.6.1 Geomorphic Response to Direct Human Modifications of the Channel and Floodplain

The geomorphology of the San Rafael River has responded rapidly to both natural and anthropogenic perturbations. Natural perturbations have included the invasion of tamarisk and the reduction in the magnitude of monsoon floods. Anthropogenic perturbations include water development and the direct human modification of the channel and floodplain. Both natural and anthropogenic perturbations have resulted in rapid geomorphic changes. In particular, the construction of dikes and levees as well as the abandonment and failure of irrigation dams during floods have produced local scale changes in the bed elevation.

Since 1952, two discrete episodes of incision have occurred in the vicinity of Hatt's Ranch. The first episode of incision, from 1952 to 1965, is a response to two channel straightening events. The first straightening event occurred in the winter of 1952/1953 (shortly after aerial photographs were taken in November 1952) upstream of USGS gage 09328500, where the Hatt's cut off two meander bends and at the same time relocated a diversion dam (Hatt interview with author, April 18, 2011). Prior to the relocation of the dam, the Hatt's frequently rebuilt washed-out dams that were constructed out of cottonwood trees and cable. It is suspected that the two large floods in 1952 inspired the Hatt's to relocate the diversion dam to it's current location in order to avoid having to repair future wash-outs. In contrast to other case studies, where researchers have found that channel straightening causes incision upstream and bed

aggradation downstream (Winkley, 1977; Galay, 1983; Simon, 1989), the bed aggraded upstream of the dam relocation and incised downstream of the channel straightening. The second channel straightening event, which took place between 1960 and 1962, occurred between the wood and steel bridge and the current Highway 24 bridge, where the Hatt's cut off two meander bends, again. The response to the second channel straightening event was similar to what researchers reported in previous studies; the bed lowered upstream of the channel straightening. The bed response to the downstream channel straightening, though, is not discernible from the incision that had been occurring since 1952. Bed aggradation ended the first episode of incision, and was likely the response of a head cut that formed during the 1960-1962 channel straightening as it propagated upstream and evacuated sediment, which was then deposited further downstream at the wood and steel bridge.

The second episode of incision, initiated in 1983, was a response to a drop in the downstream base level control. During the 1983 snowmelt flood, the river abandoned the large meander bend where the MacMillan Lower Ranch dam was located (Figure 3.5). Subsequently, during the falling limb of the 1983 snowmelt flood, the channel bed upstream of the avulsion at USGS gage 09328500 failed to fill to the elevation recorded prior to the onset of the 1983 snowmelt flood. The magnitude of the second episode of incision was less than the first episode, but the duration was longer. Since 1983, the bed has lowered 0.5 m.

Processes that were occurring simultaneous with human modifications of the stream channel must also have contributed to bed lowering. We assert that the

construction of inset floodplains, which have been stabilized by tamarisk, concentrated stream flow into a narrowed channel, thus increasing the shear stress on the bed. In conjunction with local base control lowering and gradient changes, the increased shear stress facilitated the evacuation of sediment from the bed.

In a comparison of two longitudinal profiles surveyed in the San Rafael River approximately 85 years apart, bed incision is evident in only one short river segment, a 6-km segment between rkm 48 and rkm 54 (in 1925 distances upstream from the confluence). There is no evidence of incision in the remaining portion of the study area, where either there were no bed elevation changes or there was aggradation. For example, since 1925 there has been no bed elevation change at Frenchman's Ranch, an observation seen in both the longitudinal profile comparison and the floodplain stratigraphy. In the right bank deposits at Frenchman's Ranch, the elevation of the historic active channel bar deposits do not change, whereas at Hatt's Ranch the elevation of the active channel deposits progressively decrease toward the present day channel. It is perplexing, however, that bed incision is not apparent in the profile comparison between rkm 54 to rkm 58 on the Hatt's Ranch, where there is evidence of incision in both the bed elevation time series at USGS gage 09328500 as well as the floodplain deposits found in the Hatt's Ranch trench.

Very small differences in bed elevation on the longitudinal profile comparison between rkm 54 and rkm 58 may not indicate no change. Instead, there may have been changes, but these changes may have cancelled each other. We propose that the magnitude of the post-1952 incision was the same as the magnitude of aggradation that

occurred between 1925 and 1952. For this explanation to be true, then an aggradational wedge (Mackin, 1948; Smith, 1973) must have formed upstream of the MacMillan Lower Ranch dam, into which the river began incising in 1952. Indeed, in the 1925 profile, a depositional wedge of sediment is apparent upstream of the MacMillan Lower Ranch dam. Other explanations for the lack of incision may be (1) the spatially course nature of the profile comparison – elevation data is compared at 1-km increments, or (2) errors in the georectification of the 1925 maps.

A correlation of bed incision with the hydrologic record supports our theory that bed incision was a local process initiated by changes in gradient. Incision since 1952 occurred during periods of low flow as well as during both snowmelt and monsoon floods; in other words, incision was not caused by particular types of floods, nor was it caused by shifts in the flood regime. If floods were responsible for incision, then most likely incision would have occurred throughout the entire study area. Furthermore, we believe that the observed bed elevation adjustments were not caused by changes in bed material grain size, though we do not have empirical evidence to support this assertion.

3.6.2 Spatial Variation of Channel Adjustments

In addition to bed elevation adjustments, other geomorphic characteristics have varied spatially throughout the study area. Among valley segments, there is variation in the distribution of floodplain assemblages (see Chapter 2), the distribution of tamarisk, sinuosity, and the potential for channel widening. Historically, channel width varied among valley segments, but today because of widespread channel narrowing the width of the channel is consistent throughout the study area.

Channel widening does not occur consistently across all valley segments. For example in valley segment two, the reach average channel width did not increase between 1974 and 1985 (Table 3.13). In contrast in the TbFr segment, reach average channel width increased by 58% (Table 3.8), which implies that if the width of the channel in valley segment two did not increase then all of the 58% increase occurred in valley segments one and three. Potential reasons for a lack of average segment scale channel widening in valley segment two during the snowmelt floods of the 1980s may include the high floodplain height relative to the channel bed, the relative gentle gradient of the channel due to the downstream base level control at Hatt's Ranch diversion dam, and the high degree of bank cohesion and stability caused by tamarisk and other vegetation.

Unlike the potential for channel widening, which varies among valley segments, inset floodplain formation during successive years of low stream flow has resulted in a relatively uniform channel width throughout the study area. This finding is different from the style of channel change that occurred in the Paria River during the 20th century (Topping, 1997).

In the Paria River, Topping (1997) found evidence that contradicted the findings of Graf et al. (1991), and concluded that there have been only local changes in the reach average channel geometry. It is relevant to compare the San Rafael River and the Paria River, because they both drain similar geologic landscapes, they both have been invaded by tamarisk, and historically both rivers have had similar hydrologic regimes. During the course of the 20th century, however, the hydrologic regimes of the two systems have diverged. Stream flow in the San Rafael River has been drastically reduced as a result of

water development in the headwaters, whereas, because of the lack of extensive water withdrawal, there have been no statistically significant hydrologic changes between 1923 and 1996 in the Paria River (except for a decrease in mean instantaneous streamflow and decrease in peak annual discharge, but only when including the three largest floods in 1909, 1925, and 1940). As a result of the hydrologic differences, geomorphic responses in the two rivers have differed. The lower 90 km of the San Rafael River narrowed 83% between 1952 and 2009, but the reach averaged cross section in most of the Paria River has not changed since the late 1800s/early 1900s (Topping, 1997). In the reach near the confluence with the Colorado River (Lee's Ferry reach), however, Topping (1997) reported that the channel narrowed by 30% between 1972 and 1992. Both rivers have experienced local changes in bed elevation during the period of modern alluviation.

Tamarisk has established throughout the entire study area, however, the proportion of the valley covered by tamarisk differs among valley segments. For example, most of valley segments one and two are covered from valley wall to valley wall with tamarisk (Figure 3.46 in Appendix) and have very few cottonwoods. On the other hand, there are portions of the downstream half of valley segment three and valley segment four that contain only patches of tamarisk and contain healthy mixed-aged stands of cottonwoods (Figure 3.47 in Appendix C). It is possible that both historical and present local base level controls e.g., diversion dams and the confluence with the Green River, have resulted in varying depositional histories throughout the study area, and that this variation has resulted in variation in the distribution of floodplain assemblages, which in turn has governed the distribution and type of vegetation communities among

valley segments. This logic, however, needs to be tested by further examination of the sedimentology, dendrogeomoprhology, and depositional history of floodplain sediments.

3.6.3 Timing of Channel Adjustments

Modern alluviation of the San Rafael River valley began in 1952, about a decade later than several other Colorado Plateau rivers that experienced similar periods of modern aggradation. For example, valley alluviation began in 1940 in the Fremont River (Godfrey et al., 2008), and in 1937 in the Little Colorado River (Hereford, 1984). In the Paria River, the timing and extent of channel narrowing and valley alluviation has been debated. Graf et al (1991) found that channel narrowing and valley alluviation began in 1939, however, Topping (1997) reported that in the upstream reaches of the Paria River the channel cross section geometry did not change and the only reach average narrowing occurred in the Lee's Ferry reach which did not begin until 1972.

Following the 1952 snowmelt flood, the process of channel narrowing replaced the behaviors of lateral instability and maintenance of a wide channel that formerly governed channel morphology. Following the 1952 flood during a four-year period of low stream flow, tamarisk along with grasses and willows, colonized in-channel surfaces and promoted sediment deposition. Inset floodplains developed as the vegetated, in-channel surfaces grew both vertically and laterally. Following a sequence of three large floods in 1957 and 1958, another 4-year period of low stream flow allowed vegetation to establish on active channel surfaces which in turn facilitated further inset floodplain development. This reoccurring sequence of events – (1) flood, (2) period of low flow, (3) the establishment of vegetation on in-channel surface, (4) inset floodplain formation − is

the mechanism by which the San Rafael River has narrowed throughout the study area. This concatenation, or sequence of causal events, is similar to the mechanism by which the Rio Grande River in Big Bend Nation Park has narrowed rapidly (Dean and Schmidt, 2011). Additional studies documented a similar mechanism of narrowing where vegetation encroachment occurred during periods of low flow (Johnson, 1994; Miller and Friedman, 2009).

In the San Rafael River, a positive feedback mechanism has accelerated channel narrowing. We found similar evidence of a feedback mechanism that Dean and Schmidt (2011) discovered in the Rio Grande. We found upturned sediment layers around buried tamarisk in floodplain deposits, which indicates that tamarisk actively promoted sediment deposition. We found evidence of a reduction in channel capacity leading to continued overbank flooding. We found that the large floods in the 1980s failed to widen the channel in portions of the study area, especially in valley segment two where reach average channel width did not increase between 1974 and 1985. That said, without the invasion of tamarisk, it is likely that the San Rafael River still would have narrowed during the last 60 years considering the magnitude of hydrologic changes. However, one might speculate: had there not been an invasion of tamarisk, the floods in the 1980s may have reset channel width to that of the first half of the 20th century.

3.6.4 Geomorphic Effectiveness of Floods

On the San Rafael River, it is floods that primarily control the rates and magnitude of channel expansion, and periods of low flow that result in the contraction of the channel. More specifically, the characteristics of a flood including the suspended

sediment concentration, duration, and magnitude determine the magnitude of channel widening. The results presented in this study agree with results from previous research on suspended load systems on the Colorado Plateau and elsewhere that have attributed floodplain formation and channel widening to certain types of flood. Researchers have shown that long duration floods with low suspended concentrations are erosional forces (Burkham, 1972) and short duration, high suspended sediment concentration floods are depositional agents (Burkham, 1972; Graf et al., 1991; Dean and Schmidt, 2011). In addition to these findings we have found that long duration, relatively low sediment concentration floods can also contribute to floodplain formation.

Inset floodplains on the San Rafael River have been constructed by both snowmelt and warm season floods. Some notable snowmelt floods responsible for floodplain construction include the floods of 1984, 1995, 2005, and 2006. For example, the 1984 snowmelt flood deposit constitutes approximately 50% of the vertical accretion of two onshore levees in the right bank trench at Frenchman's Ranch. The 1995 snowmelt flood converted a former near-channel bench into a levee along the left bank at Frenchman's Ranch. The 2005 snowmelt flood deposit comprises 0.5 - 1 m of the near channel levee on each bank. Notable warm season flood deposits include the July 1999 flood and the October 2006 flood; specifically, these floods constructed levees. Snowmelt floods and monsoon floods are characterized by different sediment concentrations, hence we conclude that inset floodplains in the study area have been built by floods of varying sediment concentrations.

A range of flood magnitudes (24 m^3/s to 273 m^3/s) have been responsible for constructing inset floodplains. The 1957 flood deposit is the largest flood preserved in the analyzed record of floodplain deposits (instantaneous peak = 273 m^3/s). In contrast, an extremely small flood in 2000 (instantaneous peak = 24.4 m^3/s) deposited sediment on the offshore side of the right bank levee at Frenchman's Ranch. In the recent two decades, all of the floods that have contributed to floodplain accretion have had either small or moderate peak magnitudes; some of these floods include the flood of: 1990 (26.1 m^3/s), 1999 (76.1 m^3/s), 2002 (41.0 m^3/s), 2005 (67.7 m^3/s and 50.4 m^3/s), 2006 (77 m^3/s), and 2008 (30.0 m^3/s).

Moderate magnitude floods continue to contribute to the vertical accretion of existing floodplain surfaces. Despite increases in floodplain height over the past 40 to 60 years, these moderate magnitude floods are able to overtop banks and deposit sediment on the floodplain because a reduction in channel capacity causes higher stages. For example, the 2006 flood, which had a peak magnitude of 77 m^3/s deposited a 50-100 mm layer of sediment across much of the floodplain surface exposed along the right bank at Frenchman's Ranch.

Currently, reach scale channel widening occurs only during large magnitude, long duration floods, which have decreased in frequency over the course of the 20^{th} century. In the last 50 years, catastrophic widening was achieved only once, by a succession of snowmelt floods in the mid 1980s. Bank erosion from these floods caused a net increase in channel width of 60% over the entire study area. The largest of these floods occurred in 1983 and 1984 and had peak magnitudes of 101.9 m^3/s and 110.7 m^3/s, respectively.

These flood magnitudes used to occur more frequently. In a frequency analysis using a partial duration flood series (PDFS) of snowmelt floods that occurred prior to 1959, these flood magnitudes were 3.9 yr and 6.3 yr recurrence interval events. Now, these flood magnitudes are 8.5 yrs and 17 yrs recurrence interval events (PDFS frequency analysis since 1959). More important, perhaps, than the magnitude of the peak in causing bank erosion are the long duration and relatively low suspended sediment concentration characteristics of a snowmelt flood.

Prior to the mid-1950s, when channel narrowing began, large snowmelt floods including the 1952 snowmelt flood maintained a wide and laterally unstable channel. For example, the channel was already wide prior to the 1952 snowmelt flood, thus there was little to no reach scale widening during this flood.

3.6.5 Future Trajectory of Channel Adjustments

Although the lower floodplain surface (FP#1) at Frenchman's Ranch and Hatt's Ranch are genetically the same, between sites there is a difference in the height of the floodplain relative to the channel bed. Thus, different flood magnitudes are required to inundate FP#1 at each site. For example at Frenchman's Ranch, small to moderate floods are capable of inundating and vertically accreting FP#1. In contrast at Hatt's Ranch, because the surface of FP#1 is 3 - 4 m taller than the channel bed, inundation and vertical accretion of FP#1 can only be achieved during moderate to large floods.

Our discovery of continued floodplain aggradation as the channel narrows and the floodplain height increases diverges from the model of floodplain formation proposed by Brakenridge (1988). In an attempt to correlate flood regimes to floodplain deposits,

Brakenridge (1988) proposed that when the height of a floodplain increases, then a channel's flow capacity increases, which in turn requires larger floods to overtop the channel banks. This model, however, does not account for channel narrowing. Nevertheless, if this model did incorporate channel narrowing, and the current flood regime of the San Rafael River was in a steady state, then we would conclude that the floodplain has not reached equilibrium yet, because accumulation of the "top stratum" of sediment is still occurring.

Tamarisk establishment, which began in the 1930s, is currently limiting the erosional effectiveness of floods. It is likely that the "ratchet effect" of tamarisk, described by Tal et al (2004) and Dean and Schmidt (2011), will continue to limit the erosion potential of future snowmelt floods, especially where local channel gradients are gentle.

3.7 Conclusion

During the 20th century, the morphology of the San Rafael River underwent a fundamental shift, from a wide and shallow channel to the narrow, deep channel of today. The character of the river was once highly variable, and today it is homogenous. The shift in channel morphology was induced by a hydrologic shift from a flood-dominated regime with high flood variability, to a regime characterized by low mean annual flow and low flood variability. The hydrologic shift was primarily caused by progressive development of surface water in the headwaters, however decadal scale climate fluctuations likely also contributed - for example, the lack of large warm season floods since 1962 is likely an

artifact of climate change. Consequently, the current processes governing channel morphology, that is channel narrowing and floodplain aggradation, have replaced the historic processes of bank erosion, lateral migration, and avulsions that once maintained an unstable channel with high width-to-depth ratio.

In modern times, channel narrowing occurred during two time periods, 1952 to 1979 and 1987 to the present. Both periods are characterized by low mean annual stream flow and low magnitude floods. Snowmelt floods and monsoon floods, as well as floods of various magnitudes, sediment concentration, and duration have contributed to channel narrowing. In general, our results indicate that channel narrowing is a direct result of the river's inability to transport the abundant supply of fine sediment. In other words, the river is transport limited. The reduction in transport capacity coupled with the establishment of tamarisk has resulted in rapid channel narrowing and vertical accretion of the floodplain.

Tamarisk is a dual agent of geomorphic change. First, the establishment of tamarisk in the previously wide active channel and along channel banks has promoted sediment deposition and facilitated inset floodplain formation. Furthermore, we identified a positive feedback loop in which tamarisk plays an important role in accelerating channel narrowing. Second, the stabilization of floodplains by tamarisk has reduced the erosion potential of snowmelt floods. In particular in recent decades, low to moderate magnitude snowmelt floods have had minimal success in causing reach average channel widening. Furthermore, only the two largest snowmelt floods in the last 50 years have been capable of widespread channel widening. The successive snowmelt floods of 1983

and 1984 were effective at widening the channel, not only because of their long duration and large magnitude, but also because they occurred in successive years. These floods, however, failed to cause reach average channel widening in valley segment two where the channel gradient is gentle and cohesive floodplains are tall relative to the channel bed.

Local bed elevation changes have accompanied channel narrowing and floodplain aggradation. Local bed incisions is caused by unequal amounts of scour and fill and took place in two discrete episodes, from 1952-1965 and from 1983 to the present. Both episodes of incision were caused by local changes in channel gradient due to either channel modification or lowering of the local base control. Bed aggradation upstream of tributaries is a result of a reduction in the capacity of the mainstem river to transport tributary sediment, and bed aggradation upstream of the Hatt's Ranch diversion dam is a result of an increase in the local base control elevation resulting in a decrease in upstream local channel gradient.

Future efforts to improve aquatic habitat for declining populations of endemic fish species that currently reside in the study area must consider the implications of the results presented in this study. A successful rehabilitation plan must account for the magnitude and types of changes that have occurred during the last 100 years. Furthermore, a rehabilitation plan will need to either address the mechanisms of channel change or recognize that these mechanisms will likely continue to govern channel morphology in the future unless driving forces are altered. More specifically, restoring stream flow may be the most effective but most politically challenging option for creating greater channel

complexity and restoring channel processes. Finally, local bed elevation changes and the implications of these changes must be considered in any effort to improve aquatic habitat.

3.8 References Cited

Alexander, J.S., 2007. The Timing and magnitude of channel adjustments in the upper Green River below Flaming Gorge Dam in Browns Park and Lodore Canyon, Colorado: an analysis of the pre- and post-dam river using high resolution dendrogeomorphology and repeat topographic surveys. unpublished M.S. Thesis. Utah State University, Logan, UT (362 pp.).

Allred, T.M., Schmidt, J.C., 1999. Channel narrowing by vertical accretion along the Green River near Green River, Utah. Geol. Soc. Amer. Bull. 111 (12), 1757–1772.

Andrews, E. D. 1991. Sediment transport in the Colorado River basin. In: Colorado River Ecology and Dam Management, Proceedings of a Symposium May 24 -25, 1990, National Academy Press, Santa Fe, NM (pp. 54 –74).

Washington, D.C., USA. Antevs, E. 1952. Arroyo cutting and filling. Journal of Geology, 60, 375-385.

Bailey, R.W., 1935, Epicycles of erosion in the valleys of the Colorado Plateau province. Journal of Geology 43, 337–355.

Baker, A.A., 1946. Geology of the Green River Desert-Cataract Canyon region, Emery, Wayne, and Garfield counties, Utah. U.S Geological Survey Bulletin 951, (122 pp.).

Bauman Jr., J.M., 1987, Stone house lands: The San Rafael Reef. Bonneville Books University of Utah Press, Salt Lake City, UT (225 pp.).

Birdseye, C. H., 1928. Topographic instruction of the United States Geological Survey, U.S. Geological Survey Bulletin 788. (432 pp.).

Birken, A.S., Cooper, D.J., 2006. Processes of tamarix invasion and floodplain development along the lower green river, Utah. Ecological Applications 16 (3), 1103–1120.

Brakenridge, G.R., 1988. River flood regime and floodplain stratigraphy. In: Baker, V.R., Kochel, C.R., Patton, P.C. (Eds.), Flood Geomorphology, John Wiley and Sons, New York, pp 139-156.

Bradley, C., Smith, D.G., 1984. Meandering channel response to altered flow regime: Milk River, Alberta and Montana. Water Resources Research, 20 (12), 1913-1920.

Bryan, K., 1925. Date of channel trenching (arroyo cutting) in the arid southwest. Science 62, 338–344.

Burchard, R W., 1926. Plan and profile of San Rafael River below Castle Dale, Utah, Buckhorn Wash to mile 3. U.S. Geological Survey, Washington, DC, 4 maps.

Burkham, D.E., 1972. Channel changes of the Gila River in Safford Valley, Arizona 1846- 1970. U.S. Geological Survey Professional Paper 655-G. (24 pp.).

Cooke, R.U., Reeves, R.W., 1976. Arroyos and Environmental Change. Clarendon Press, Oxford, UK (213 pp.).

Colby, B.R., 1964. Scour and fill in sand-bed streams, U.S. Geol. Surv. Prof. Pap. 462-D. (37 pp.).

Dean, D.J., Schmidt, J.C., 2011. The role of feedback mechanisms in historic channel changes of the lower Rio Grande in the Big Bend region, Geomorphology 126 (3-4), 333-349.

Dean, D.J., Scott, M.L., Shafroth, P.B., Schmidt, J.C., 2011. Stratigraphic, sedimentologic, and dendrogeomorphic analyses of rapid floodplain formation along the Rio Grande in Big Bend National Park, Texas. Geol. Soc. Amer. Bull. 123(9-10), 1908-1925.

Dellenbaugh, F.S., 1908. A canyon voyage: the narrative of the second Powell expedition down the Green-Colorado River from Wyoming, and the explorations on land, in the years 1871 and 1872, G.P. Putnam's Sons, New York (277 pp.).

Dunham, G., 1999. Interview with Steve Allen. Green River, UT. December 6, 1999. Transcribed by Ellen Meehan. Print available at Green River Archives, Green River, UT.

Emmett, W.W., 1974. Channel aggradation in western United States as indicated by observations at Vigil Network sites: Zeitschrift fur Geomorphologie, Supplement Band 21, v. 2, 52-62.

Everitt, B.L., 1980. Ecology of saltcedar: a plea for research. Environmental Geology 3, 77-84.

Everitt, B.L., 1993. Channel responses to declining flow on the Rio Grande between Ft. Quitman and Presidio, Texas. Geomorphology 6 (3), 225-242.

Everitt, B.L., 1998. Chronology of the spread of tamarisk in the central Rio Grande. Wetlands 18 (4), 658–668.

Friedman J.M., Lee V.J., 2002. Extreme floods, channel change, and riparian forests along ephemeral streams. Ecological Monographs 72, 409-425.

Friedman, J.M., Osterkamp, W.R., Lewis, W.M., 1996, The role of vegetation and bed-level fluctuations in the process of channel narrowing: Geomorphology, v. 14, no. 4, p. 341–351.

Friedman, J.M., Vincent, K.R., Shafroth, P.B., 2005. Dating floodplain sediments using tree-ring response to burial. Earth Surface Processes and Landforms 30 (9), 1077–1091.

Galay, V.J., 1983. Causes of river bed degradation. Water Resour. Res., 19 (5), 1057-1090.

Geary, E. A, 1996. A History of Emery County. Utah Centennial County History Series. Utah State Historical Society, Salt Lake City, UT (448 pp.).

Godfrey, A.E., Everitt, B.L., Martin Duque, J.F., 2008. Episodic sediment delivery and landscape connectivity in the Mancos Shale badlands and Fremont River system, Utah, USA, Geomorphology, 102, 242-251. doi:10.1016/j.geomorph.2008.05.002.

Graf, J.B., Webb, R.H., and Hereford, R., 1991. Relation of sediment load and flood-plain formation to climatic variability, Paria River drainage basin, Utah and Arizona. Geol. Soc. Amer. Bull. 103, 1405-1415.

Graf, W.L., 1978. Fluvial adjustments to the spread of tamarisk (*Tamarix chinensis*) in the Colorado Plateau region Green River, channel restrictions, erosion control. Geol. Soc. Amer. Bull., 89, 1491-1501.

Graf, W.L., 1983, The arroyo problem-Paleohydrology and paleohydraulics in the short term, In: Gregory, K.J. (Ed.), Background to Paleohydrology. John Wiley and Sons, New York, pp. 279-302.

Graf, W.L., 1987. Late Holocene sediment storage in canyons of the Colorado Plateau. Geol. Soc. Amer. Bull. 99, 261-271.

Grams, P.E., Schmidt, J.C., 2002. Stream-flow regulation and multi-level flood plain formation: channel narrowing on the aggrading Green River in the eastern Uinta Mountains, Colorado and Utah. Geomorphology 44 (3–4), 337-360.

Grams, P.E., Schmidt, J.C., 2005. Equilibrium or indeterminate? Where sediment budgets fail: Sediment mass balance and adjustment of channel form, Green River

downstream from Flaming Gorge Dam, Utah and Colorado. Geomorphology, 71 (1–2), 156–181.

Griffin, E.R., Kean, J.W., Vincent, K.R., Smith, J.D., Friedman, J.M., 2005. Modeling effects of bank friction and woody bank vegetation on channel flow and boundary shear stress in the Rio Puerco, New Mexico. J. Geophysical Res. 110, F04023.

Gellis, A., Hereford, R., Schumm, S.A., Hayes, B.R., 1991. Channel evolution and hydrologic variations in the Colorado River basin: factors influencing sediment and salt loads. J. Hydrol., 124:317 344.

Hereford, Richard, 1984. Climate and ephemeral-stream processes: Twentieth-century geomorphology and alluvial stratigraphy of the Little Colorado River, Arizona. Geol. Soc. Amer. Bull., 95, p. 654-668.

Hereford, R., 1986. Modern alluvial history of the Paria River drainage basin. Quaternary Res. 25, 293-311.

Hereford, R., 1987. The short term: fluvial processes since 1940, In: Graf, W.L., (Ed.), Geomorphic Systems of North America. Geological Society of America Centennial Special Paper, 2, 276-288.

Hereford, R., 2002. Valley-fill alluviation during the Little Ice Age (Ca A.D. 1400-1880), Paria River basin and southern Colorado Plateau, United States. Geol. Soc. Amer. Bull. 114, 1550-1563.

Hereford, R., Webb, R.H., 1992. Historic variation of warm-season rainfall, southern Colorado Plateau, Southwestern U.S.A. Climatic Change, 22, 239-256.

Hereford, R., Webb, R.H., Graham, S., 2002. Precipitation history of the Colorado Plateau region, 1900–2000, US Geological Survey Fact Sheet 119-02 2002. (4 pp.).

Johnson, W.C., 1994. Woodland expansion in the Platte River, Nebraska: patterns and causes. Ecological Monographs, 64 (1), pp. 45-84.

Johnson, W.C., 1997. Equilibrium response of riparian vegetation to flow regulation in the Platte River, Nebraska. Regulated Rivers: Res. & Manage. 13, 403-415.

Kelsey, M.R., Hiking, Biking and Exploring Canyonlands National Park and vicinity. Kelsey publishing, Provo, UT (320 pp.).

Leopold, L.B., 1976. Reversal of erosion cycle and climatic change. Quaternary Res. 6, 557-562.

Leopold, L.B., Maddock Jr., T., 1953. Relation of suspended sediment concentration to channel scour and fill. Proceeding of the Fifth Hydraulics Conference (Iowa Institute of Hydraulic Research), Studies in Engineering, Bull. 34, 159-178.

Love, D.W., 1983, Quaternary facies in Chaco Canyon and their implications for geomorphic-sedimentologic models. In: Wells, S.G., Love, D.W., Gardner, T.W., (Eds.), Chaco Canyon Country, Albuquerque, New Mexico: Field Trip Guidebook, 1983 Conference, American Geomorphological Field Group, pp. 195-206.

Love. D. W., 1979. Quaternary fluvial geomorphic adjustments in Chaco Canyon, New Mexico. In: Rhodes D. D. Williams, G.P. (Eds.), Adjustments of the Fluvial System. Kendall/Hunt, Dubuque, IA, pp. 277-308.

Mackin, J.H., 1948. Concept of the graded river. Bull. of the Geological Society of America 59, 463-512

Miller, J.R., Friedman, J.M., 2009. Influence of flow variability on flood-plain formation and destruction, Little Missouri River, North Dakota. Geol. Soc. Amer. Bull. 121:752-759.

Mundorff, J.C., Thompson, K.R., 1980. Reconnaissance fo the quality of surface water in the San Rafael River Basin, Utah. U.S. Geological Survey Open File Report 80-574. (104 pp.). http://digitalcommons.usu.edu/govdocs/100

Nanson, G.C., 1986. Episodes of vertical accretion and catastrophic stripping—A model of disequilibrium floodplain development: Geol. Soc. Amer. Bull. 97, 12, 1467–1475.

Page, K.J., Nanson, G.C., Frazier, P.S., 2003. Floodplain formation and sediment stratigraphy resulting from oblique accretion on the Murrumbidgee River, Australia: Journal of Sedimentary Research, v. 73, no. 1, 5–14.

Patton, P.C., Schumm, S.A., 1981. Ephemeral-stream processes: implications for studies of Quaternary valley fills. Quaternary Res. 15, 24-43.

Pizzuto, J.E., 1994. Channel adjustments to changing discharges, Powder River, Montana. Geol. Soc. Amer. Bull. 106 (11), 1494-1501.

Powell, J.W., 1879. Report on the lands of the arid region of the United States with a more detailed account of the lands of Utah. Government printing Office, Washington, DC. (195 pp.).

Richards, K., 1982. Rivers, Form and Process in Alluvial Channels. Meuthen, London, UK (358 pp.).

Rygel, M.C., Gibling, M.R., and Calder, J.H., 2004. Vegetation-induced sedimentary structures from fossil forests in the Pennsylvanian Joggins Formation, Nova Scotia: Sedimentology, v. 51, p. 531–552, doi:10.1111/ j.1365-3091.2004.00635.x.

Schmidt, J.C., and Wilcock, P.R., 2008. Metrics for assessing the downstream effects of dams, Water Resour. Res. 44, W04404.

Schumm, S.A., Lichty, R.W., 1963. Channel widening and flood-plain construction along the Cimarron River in Southwestern Kansas. U.S. Geological Survey Professional Paper 352-D (88 pp.).

Schumm, S.A., Harvey, M.D., Watson, C.C., 1984. Incised channels: morphology, dynamics, and control. Water Resources Publications, Littleton, CO (200 pp.).

Simon, A., 1989. The discharge of sediment in channelized alluvial streams. Water Resour. Bull. 25 (6), 1177-1188.

Smelser, M.G., and Schmidt, J.C., 1998. An assessment methodology for determining historical change in mountain streams. RMRS-GTR-6, U.S. Department of Agriculture, Forest Service, Rocky Mountain Research Station, Fort Collins, CO (29 pp.).

Smith, D.G., 1973. Aggradation of the Alexandra-North Saskatchewan River, Banff Park, Alberta. In: Morisawa, M. (Ed.), Fluvial Geomorphology. Proceedings of 4th Annual Geomorphology Symposium., SUNY-Binghamton, New York, NY, pp. 201–219.

Stromberg, J., Briggs, M., Gourley, C., Scott, M., Shafroth, P., Stevens, L., 2004. Human alterations of riparian ecosystems. In: Baker Jr., M., Ffolliott, P., DeBano, L., Neary, D.G. (Eds.), Riparian Areas of the Southwestern United States: Hydrology, Ecology, and Management. Lewis Publishers, Boca Raton, FL, pp. 101-126.

Stromberg, J.C., Beauchamp ,V.B., Dixon, M.D., Lite, S.J., Paradzick, C., 2007. Importance of low-flow and high-flow characteristics to restoration of riparian vegetation along rivers in arid southwestern United States. Freshwater Biology 52, 651-679.

Tal, M., Gran, K., Murray, A.B., Paola, C., Hicks, D.M., 2004. Riparian vegetation as a primary control on channel characteristics in multi-thread rivers. In: Bennett, S.J., Simon, A. (Eds.), Riparian Vegetation and Fluvial Geomorphology: Hydraulic: Hydrologic, and Geotechnical Interaction. American Geophysical Union, Washington, DC, pp. 43–58.

Tal, M., Paola, C., 2007. Dynamic single-thread channels maintained by the interaction of flow and vegetation. Geology 35 (4), 347–350.

Thomas, R.G., Smith, D.G., Wood, J.M., Visser, J., Calverley-Range, E.A., Koster, E.H., 1987. Inclined heterolithic stratification - terminology, description, interpretation and significance. Sedimentary Geology 53, 123–179.

Topping, D. J., Rubin D. M., and Vierra Jr., L. E., 2000. Colorado River sediment transport: 1. Natural sediment supply limitation and the influence of Glen Canyon Dam, Water Resour. Res., 36, 515–542.

Topping,D . J., 1997. Physics of flow, sediment transport hydraulic geometry, and channel geomorphic adjustment during flash floods in an ephemeral river, the Paria River, Utah and Arizona, (Ph.D. Thesis), University of Washington, Seattle (406 pp.).

Utah Board of Water Resources, 2000. State Water Plan, West Colorado River Basin Salt Lake City, UT (277 pp.).

U.S. Geological Survey, 1962. USGS gage (09328500) San Rafael Near Green River, UT Gage Station Analysis Report.

Webb, R. H., Leake, S.A., Turner, R.M., 2007. The ribbon of green: change in riparian vegetation in the southwestern United States. University of Arizona Press, Tucson, AZ (462 pp.).

Webb, R.H., 1985. Late Holocene flooding on the Escalante River, south-central Utah. (Ph.D. Thesis). Tucson, University of Arizona (204 pp.).

Webb, R.H., and Betancourt, J.L., 1992. Climatic variability and flood frequency of the Santa Cruz River, Pima County, AZ. US Geological Survey Water-Supply Paper 2379 1992 (40 pp.).

Webb, R.H., Hereford, R., 2010. Historical arroyo formation: documentation of magnitude and timing of historical changes using repeat photography. In: Webb, R.H., Boyer, D.E., Turner, R.M., (Eds.), Repeat Photography: Methods and Applications in the Natural Sciences, Island Press, Washington D.C., USA. pp. 89-104.

Winkley, B.R.,1977. Man-made cutoffs on the lower Mississippi River: conception, construction, and river response. Potamology Investigations, Report 300-2, US Army Corps of Engineers, Vicksburg, MS (219 pp.).

Witkind I.J., 1991. Implications of distinctive fault sets in the San Rafael Swell and adjacent areas, East-central Utah. In: Chidsey, T.C. (Ed.), Geology of East-

Central Utah. Utah Geological Association Publication 19, Salt Lake City, UT, pp. 141-148.

Wolman, M.G., Leopold, L.B., 1957. River flood plains: some observations on their formation, U.S. Geological Survey Professional Paper 282-C (20 pp.).

Table 3.1. Relevant information for the 8 series of aerial photographs analyzed in this study. Five of the 8 photo series provide entire coverage of the study area. "NARA" is acronym for U.S. National Archives and Records Administration. "USDA APFO" is the acronym for U.S. Department of Agriculture Aerial Photography Field Office. "USGS EROS" is the acronym for USGS Earth Resources Observation and Science Center. The AGRC (Automated Geographic Reference Center) website is the state of Utah's GIS web portal.

Year	Type	Flight date	Scale or Resolution	Photo Size	Source	Stream-flow (m^3/s)	Coverage	Length (km)
1938	B&W prints	July 6 & 20	1:31680	9 x 9 in	NARA	unknown	entire study area	76.8
1952	B&W prints	Nov 17	1:20000	9 x 9 in	USGS EROS website	2.2	partial coverage	49.9
1962	B&W prints	June 16	1:20000	15 x 15 in	USDA APFO	22.4	partial coverage	59.7
1974	B&W prints	Sept 26	1:40000	12 x 12 in	USDA APFO	1.0	partial coverage	40.6
1985	B&W prints	Aug 15	1:60000	17 x 17 in	USDA APFO	2.2	entire study area	80.9
1997	B&W DOQ	July 4 & 14	1 meter	11.00 x 13.97 km	AGRC website	2.0 & 1.5	entire study area	84.6
2009	CIR DOQ	June 30	1 meter	6.12 x 7.61 km	AGRC website	3.7	entire study area	86.3
2010	natural color	Aug 25	~.12 meter	NA	BOR	0.3	entire study area	86.3

Table 3.2. Error associated with georectifying historic aerial imagery. Error is reported as the Root Mean Square Error (RMSE) in meters for each photo series. The RMSE reported here is the average RMSE of all output georectified images for each photo series. The number of photographs that were georectified for each photo series varies and is listed here. Also included is the maximum, minimum, and average number of control points used to georectify each photograph.

year	number of photos	RMSE (m)			control points		
		maximum	minimum	average	maximum	minimum	average
1938	21	5.26	0.80	2.98	100	15	40
1952	21	3.65	0.56	1.66	93	21	51
1962	14	2.46	0.53	1.23	236	16	86
1974	13	2.40	0.74	1.38	151	27	69
1985	30	3.48	0.80	1.34	277	18	73

Table 3.3. Stream-flow statistics measured at USGS gage 09328500. Statistics are reported for the period of record as well as the record divided into time periods. Notice the decline in flood magnitude for specific recurrence intervals over the course of the 20th century, except for the period of the 1980s when exceptional flooding occurred. The annual peak discharge series was used to calculate flood frequencies shown in this table. Those recurrence interval discharges that were calculated from the Log Pearson Type III distribution are designated with an asterisk (*). All other recurrence interval discharges that are listed were calculated from the Weibull plotting position method.

	1910-2010	**1910-1918**	**1946-1958**	**1959-1979**	**1980-1986**	**1987-2010**	**1909-1958**	**1959-2010**
recurrence interval	**Q, in m^3/s**	**Q, in m^3/s**	**Q, in m^3/s**	**Q, in m^3/s**	**Q, in m^3/s**	**Q, in m^3/s**	**Q, in m^3/s**	**Q, in m^3/s**
1.01		*25.7	*9.3	*3.8	*17.1	*8.4	*10.3	*5.5
1.25	26.1	84.6	31.0	26.6	40.0	22.9	35.4	25.4
2	51.0	104.8	73.1	39.5	65.1	35.3	90.6	41.2
5	98.2	266.2	143.7	56.2	107.1	69.1	118.1	67.0
10	109.7	337.2	257.0	66.3	*128.7	74.8	265.7	79.1
25	276.4	*358.0	*298.3	*94.3	*156.6	*91.1	*305.8	111.2
50	330.9	*439.2	*373.3	*101.4	*176.5	*105.1	*380.5	*107.6
100	350.3	*528.4	*455.0	*106.8	*195.6	*119.0	*461.2	*114.7
mean annual flood	69.0	138.9	97.7	44.4	74.7	41.0	115.6	47.2
mean annual flow	3.7	7.7	4.1	2.6	7.2	1.9	5.6	2.9

Table 3.4. Table of notable floods since 1871. Only the instantaneous flood magnitudes reported in this table are those reported at USGS gage 09328500 that exceeded 100 m^3/s. Floods that were not measured are also reported in this table. For these floods, the peak discharge is listed as "NA", which means not available.

Date	Peak discharge, in cubic meters per second	Source
Sept 6, 1871	NA	Dellenbaugh, 1908
Nov 24, 1884	NA	cadastral survey, 1884
9/12/1897	NA	Webb, 1985
7/30/1899	NA	Webb, 1985
1900	NA	Geary, 1996
August 26, 1905	NA	Webb, 1985
1907	NA	Geary, 1996
September 2, 1909	339.8	USGS gage 09328500
June 5, 1912	103.6	USGS gage 09328500
September 9, 1913	107.6	USGS gage 09328500
June 2, 1914	106.4	USGS gage 09328500
August 6, 1916	106.2	USGS gage 09328500
October 8, 1916	325.6	USGS gage 09328500
July 17, 1921	NA	Webb, 1985
August 3, 1929	NA	Webb, 1985
April 13, 1905	NA	Geary, 1996
1932	NA	Geary, 1996
July 12, 1933	NA	Webb, 1985
September 4, 1935	NA	Webb, 1985
1937	NA	Geary, 1996
August 22, 1947	244.6	USGS gage 09328500
August 4, 1951	105.9	USGS gage 09328500
June 4, 1952	126.8	USGS gage 09328500
November 4, 1957	273.5	USGS gage 09328500
September 10, 1961	134.2	USGS gage 09328500
September 11, 1980	105.9	USGS gage 09328500
June 21, 1983	101.9	USGS gage 09328500
June 8, 1984	110.7	USGS gage 09328500

Table 3.5. Magnitude of specific recurrence interval floods for two flood populations. Also shown are the values of the parameter σlogx for the log Pearson's Type III distribution. Flood magnitude decreased for all but one recurrence interval. 25-year recurrence interval warm season floods exhibited the largest decline.

Recurrence interval	**Snowmelt 1909-1958**	**Snowmelt 1959-2008**	**Percent decrease**	**Warm season 1909-1958**	**Warm season 1959-2008**	**Percent decrease**
σ_{logx}	0.2	0.1		0.3	0.2	
25.00	140.2	87.6	38%	252.2	90.5	64%
10.00	110.7	76.0	31%	173.1	71.5	59%
5.00	88.7	66.5	25%	123.2	58.3	53%
2.00	57.8	51.4	11%	66.8	39.9	40%
1.25	37.6	39.7	-6%	37.9	30.1	21%

Table 3.6. Suspended sediment load and suspended sediment concentration for each type of flood. Suspended sediment transport data used in these computations was measured at USGS gage 09328500. To demonstrate the magnitude of influence of the 1952 snowmelt flood on unit loads, the unit calculations were computed for the record, both including and excluding the 1952 calendar year.

flood type (season)	floods (1951,1953-1957)			floods (1951-1957)		
	# of days	Suspended sediment concentration (Mg/hm^3)	Sediment load (Mg/day)	# of days	Suspended sediment concentration (Mg/hm^3)	Sediment load (Mg/day)
frontal (winter)	141	25.0	895.5	207.0	33.1	2311.5
snowmelt (spring)	270	21.4	5940.0	366.0	22.8	13381.5
monsoon (summer)	172	260.5	16399.3	209.0	188.6	13948.3
trop. cyclones (fall)	106	173.7	8873.7	118.0	151.9	7996.6

Table 3.7. Channel width measurements extracted from cadastral survey notes.

cadastral notes file name	Page #	Township	Range	Date/year	Surveyor	chain location	excerpts related to the channel or alluvial valley	channel width (m)
R0184-0387	171	22 South	15 East	1882	A.D. Ferron	46.4	"Bank 12 feet high of San Rafael River, 100 links wide. 2 ft deep. runs SW 10 chains then SE"	20.1
R0184-0387	196	24 South	15 & 16 East	1882	A.D. Ferron	20.5	"Point of triangulation top of ledge, 75 feet high. San Rafael River 1.00 chains wide beneath."	20.1
R0184-0387	251	24 South	14 East	1882	A.D. Ferron	36.5	"Enter bottom "?" NW & SE & heavy undergrowth. Bank of San Rafael River. 20 inches deep, 83 links" wide"	16.7
R0184-0387	270			11/2/1881	A.D. Ferron	56.75	"San Rafael River, 50 links wide, 20 ins deep, runs East"	10.1
R0184-0387	291	24 South	16 East	10/31/1881	A.D. Ferron	52.3	"San Rafael River 1.25 chains wide, 18 inches deep, runs NE"	25.2
R207-0439	439	24 South	15 & 16 East	9/6/1884	Stewart M. Pancake		"San Rafael River 100 links wide, 2 feet deep, runs East"	20.1
R207-0511	519	24 South	15 East	11/24/1885	Stewart M. Pancake		"San Rafael River runs East. 2 chains wide, 2 feet deep."	40.2
							average	**21.8**

Table 3.8. Historic changes in active channel width and sinuosity in a 32-km segment between Tidwell Bottom and Frenchman's Ranch. Channel width values displayed here were digitized on aerial photographs. Channel width progressively declines between subsequent photo series with the exception of the 1985 photo series. The highest rate of narrowing occurred between 1952 and 1962 and between 1985 and 1997.

Year	Segment	Centerline length (km)	Area (km^2)	RAACW (m)	Sinuosity	Rate of narrowing (m/yr)
1938	Tidwell Bottom to Frenchman's Ranch	31.9	1.56	48.9	1.49	
1952	Tidwell Bottom to Frenchman's Ranch	31.9	1.53	48.0	1.50	0.07
1962	Tidwell Bottom to Frenchman's Ranch	32.1	0.97	30.2	1.50	1.78
1974	Tidwell Bottom to Frenchman's Ranch	33.8	0.76	22.4	1.58	0.65
1985	Tidwell Bottom to Frenchman's Ranch	32.9	1.17	35.5	1.54	-1.19
1997	Tidwell Bottom to Frenchman's Ranch	35.1	0.40	11.4	1.64	2.01
2009	Tidwell Bottom to Frenchman's Ranch	35.9	0.32	8.8	1.68	0.22
valley	Tidwell Bottom to Frenchman's Ranch	21.4	10.45	489.5		

Table 3.9. Tabular results from spatial union analysis performed in GIS.

years	segment	erosion (km^2)	deposition (km^2)	no change (km^2)	net change (km^2)	Erosion/ deposition	floodplain construction/ year (km^2/yr)	floodplain construction/ year/river km (m^2/yr-km)
1938 to 1952	Tidwell Bottom to Frenchman's Ranch	0.64	0.67	0.89	0.03	0.96	0.0019	61
1952 to 1962	Tidwell Bottom to Frenchman's Ranch	0.24	0.80	0.73	0.56	0.30	0.0562	1750
1962 to 1974	Tidwell Bottom to Frenchman's Ranch	0.21	0.43	0.54	0.21	0.50	0.0177	523
1974 to 1985	Tidwell Bottom to Frenchman's Ranch	0.60	0.19	0.57	-0.41	3.15	-0.0373	-1134
1985 to 1997	Tidwell Bottom to Frenchman's Ranch	0.08	0.85	0.32	0.77	0.09	0.0640	1823
1997 to 2009	Tidwell Bottom to Frenchman's Ranch	0.07	0.16	0.25	0.09	0.45	0.0071	197

Table 3.10. Active channel width statistics computed for six time periods of adjustment. Units are in meters.

statistic	Width ('09 to '20)	Width ('45 to '52)	Width ('53 to '58)	Width ('59 to '79)	Width ('80 to '86)	Width ('87 to '10)
Minimum	23.2	23.8	20.7	12.2	16.5	11.0
Maximum	39.0	36.6	35.7	25.6	27.4	16.2
Points	8	49	18	44	14	12
Mean	30.9	32.8	26.6	15.5	19.2	13.7
Median	30.9	34.4	24.4	14.9	18.0	13.9
Std Deviation	4.5	3.5	5.5	2.4	3.1	1.3
Variance	20.0	12.2	29.8	5.7	9.7	1.6

Table 3.11. Width-to-depth ratio statistics computed for four time periods of adjustment. Values are unitless (m/m).

statistic	Width/Depth ('09 to '20)	Width/Depth ('45 to '52)	Width/Depth ('53 to '58)	Width/Depth ('59 to '10)
Minimum	13.9	54.3	26.0	6.0
Maximum	106.2	131.6	83.5	47.7
Points	8	49	18	70
Mean	66.0	88.7	45.7	22.4
Median	70.0	86.5	41.2	20.4
Std Deviation	27.5	18.4	16.3	6.9
Variance	757.3	337.5	267.2	48.3

Table 3.12. Historic changes in active channel width and sinuosity for the entire study area. Channel widths displayed here were digitized on aerial photographs. Note that since aerial photographs taken in 1952, 1962, and 1974 provide only partial coverage of the study area then they are excluded from this table.

Year	Reach	Centerline length (km)	Area (km^2)	RAACW (m)	Sinuosity	Rate of narrowing (m/yr)
1938	entire lower river	76.8	3.71	48.3	1.36	
1985	entire lower river	80.9	2.58	31.9	1.43	0.3
1997	entire lower river	84.6	1.35	11.2	1.50	1.7
2009	entire lower river	86.3	1.08	8.8	1.53	0.2
valley	entire lower river	56.7	24.15	425.8		

Table 3.13. Historic changes in active channel width and sinuosity for each of the five valley segments delineated in the study area. Channel width data displayed here were digitized on aerial photographs. The width data shown here is displayed graphically in Figure 32. "RAACW" is short for "reach average active channel width". The rate of narrowing was computed for the time period between successive aerial photographs.

Year	valley segment	Centerline length (km)	Area (km^2)	RAACW (m)	Sinuosity	Rate of narrowing (m/yr)
1938	1	8.6	0.42	49.0	1.47	
	2	9.9	0.45	45.4	1.31	
	3	31.1	1.56	50.2	1.59	
	4	24.6	1.09	44.2	1.16	
	5	2.8	0.20	72.5	1.15	
1952	1	9.1	0.46	51.0	1.56	-0.15
	2	10.1	0.43	42.8	1.34	0.18
	3	30.7	1.73	56.5	1.57	-0.45
1962	2	10.2	0.27	26.9	1.35	1.60
1974	2	10.6	0.22	20.5	1.40	0.54
1985	1	10.2	0.26	25.5	1.75	0.78
	2	11.0	0.22	20.3	1.45	0.00
	3	30.7	1.35	44.1	1.57	-0.01
	4	25.3	0.61	24.0	1.20	0.43
	5	3.8	0.14	36.2	1.57	0.77
1997	1	10.8	0.12	11.1	1.85	1.19
	3	32.4	0.40	12.3	1.66	2.65
	4	25.8	0.25	9.8	1.22	1.19
	5	4.0	0.05	12.0	1.66	2.01
2009	1	11.0	0.09	7.7	1.89	0.28
	3	33.4	0.31	9.4	1.70	0.24
	5	4.1	0.04	9.2	1.72	0.23
	2	7.6	2.01	266.1		
	3	19.6	13.53	691.6		
	4	21.1	3.45	163.7		
	5	2.4	1.09	455.3		

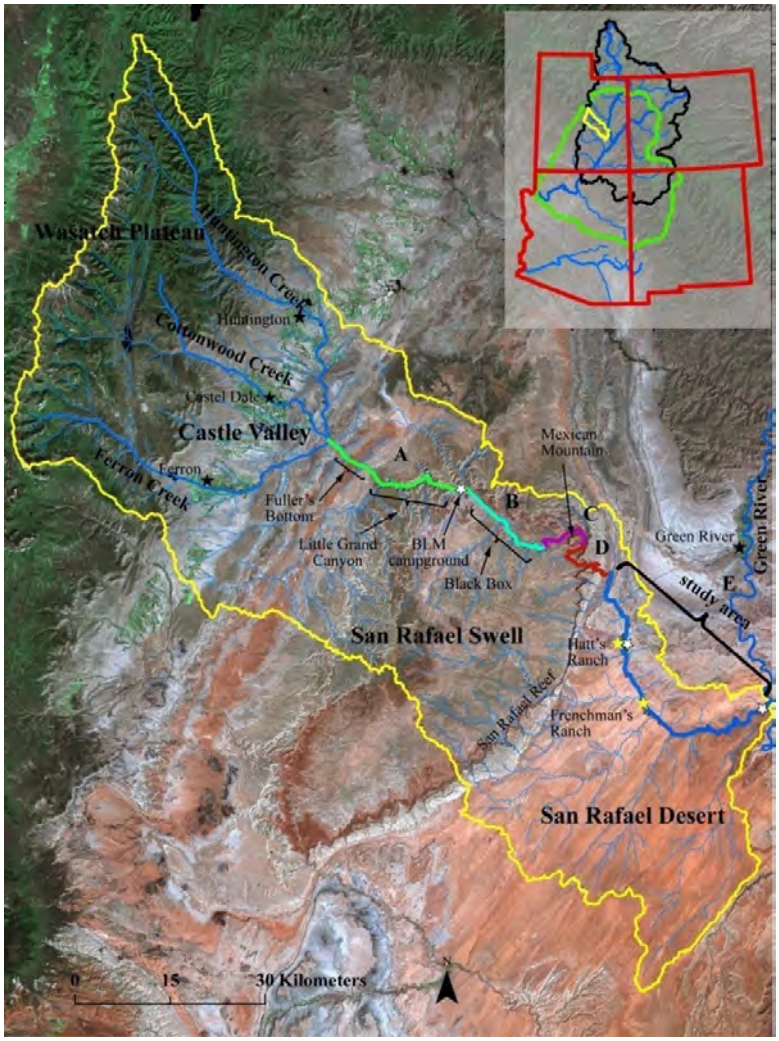

Figure 3.1. Map of the San Rafael River watershed. The location of the watershed within the (1) Upper Colorado River watershed (black) and the (2) Colorado Plateau (green) are shown in the inset map. The headwaters of the San Rafael River are in the Wasatch Plateau. The San Rafael Swell and the San Rafael Desert are underlain by erodible sedimentary rocks. Prevailing southwest winds have covered much of the San Rafael Desert with fine sand, which has a metallic, orangish-brown color on the landsat image. The study area is located between the San Rafael Reef and the confluence with the Green River. Locations of floodplain trench excavations are indicated by yellow stars. Locations of matched historic photos are indicated by white stars. Background image is a mosaic of Landsat TM imagery courtesy of Intermountain Digital Image Archive Center (http://earth.gis.usu.edu/statemosaic.html).

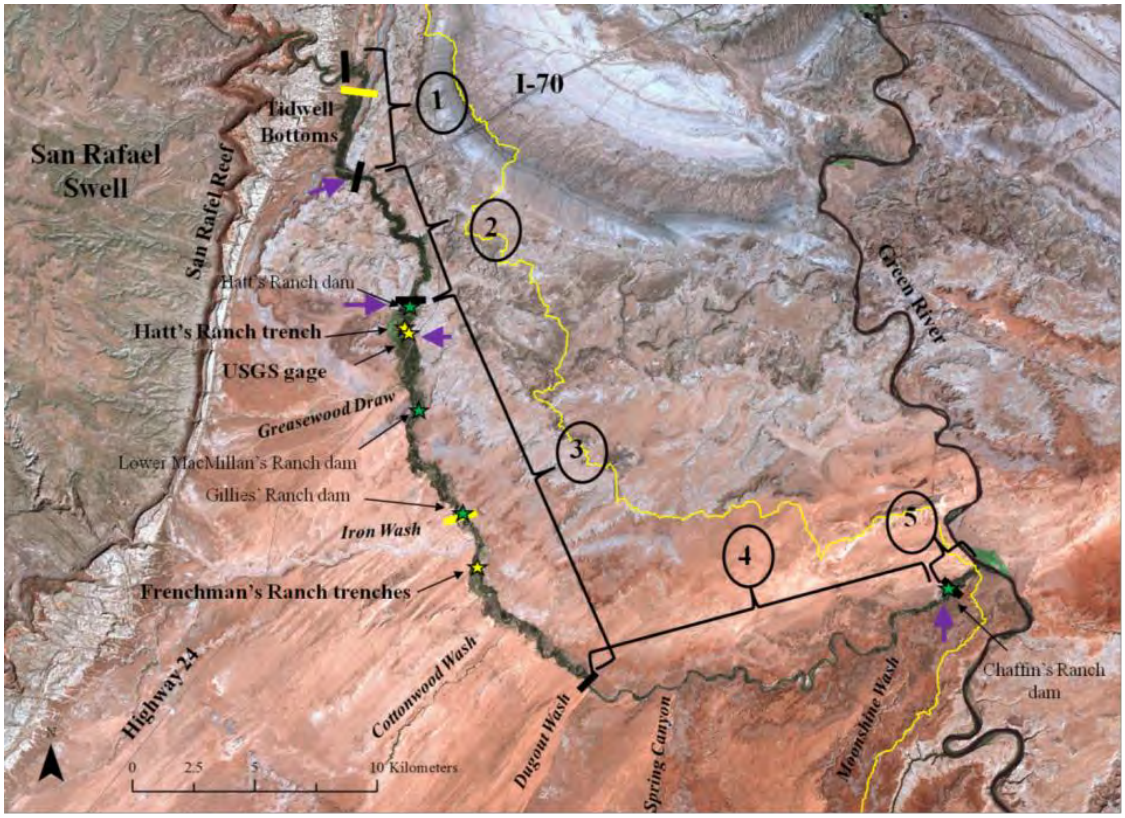

Figure 3.2. Map of the study area, which includes the San Rafael River from the San Rafael Reef to the confluence with the Green River, a distance of approximately 87 km. The study area is comprised of five valley segments. Boundaries between segments are shown by thick black lines. The characteristics of each segment are described in detail in Chapter 2. The thin yellow line is the watershed boundary. Sites where floodplain trenches were excavated, as well as the location of USGS gage 09328500, are denoted with yellow stars. Green stars denote the locations of past and current diversion dams. Short, thick yellow lines denote the upstream and downstream extent of the Tidwell Bottom to Frenchman's Ranch (TbFr) segment. Purple arrows indicate the location of bridges. The town of Green River is located just off the top of the map. The basemap is a mosaic of Landsat TM imagery courtesy of Intermountain Digital Image Archive Center (http://earth.gis.usu.edu/statemosaic.html).

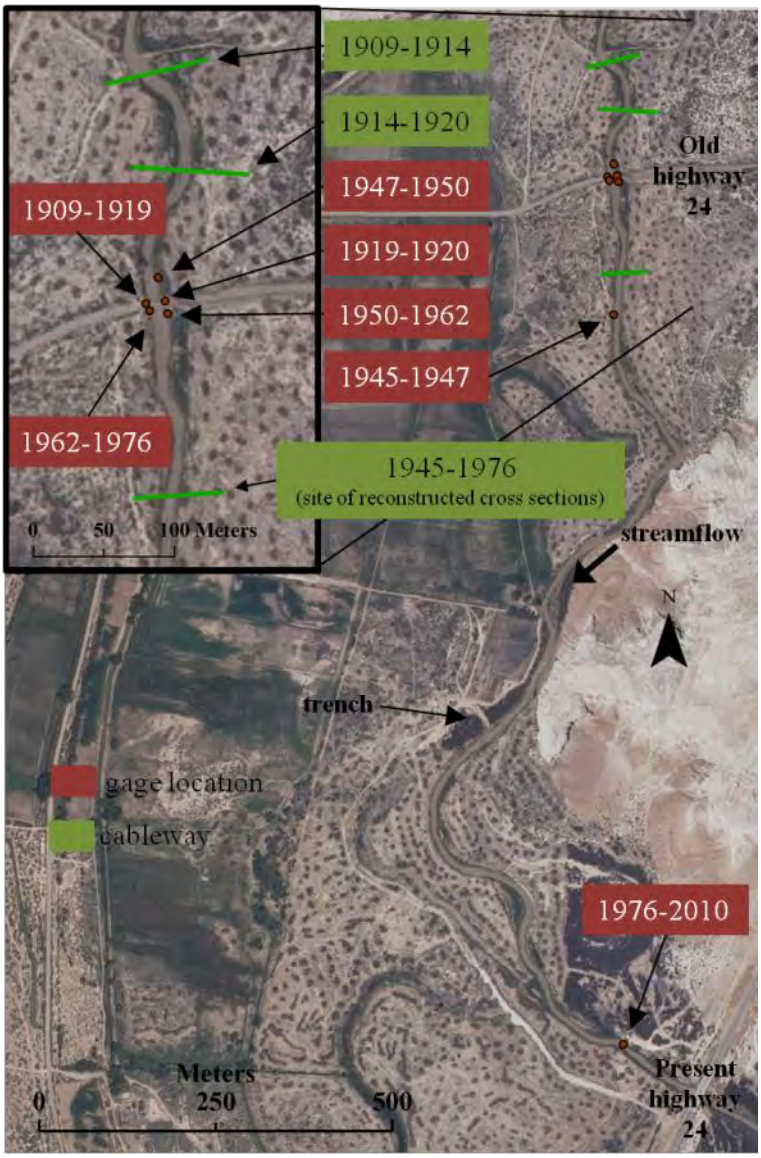

Figure 3.3. Locations of USGS gage 09328500 on Hatt's Ranch. On this 2009 aerial photograph are identified the location of cableways used to measure high stream flow, and each of 7 gage locations. The USGS moved the gage 5 times between 1909 and 1976, and again in 1976. Since 1976, the gage has been in the same location, approximately 150 m upstream from the current Highway 24 bridge. At present, flood discharge is measured from a wood and steel bridge on the Hatt's Ranch (the former Highway 24 bridge). Stream flow is from top to bottom. Dark spots seen in portions of the photo are piles of mechanically removed tamarisk. Upper left inset is a magnification of the reach near the wood and steel bridge.

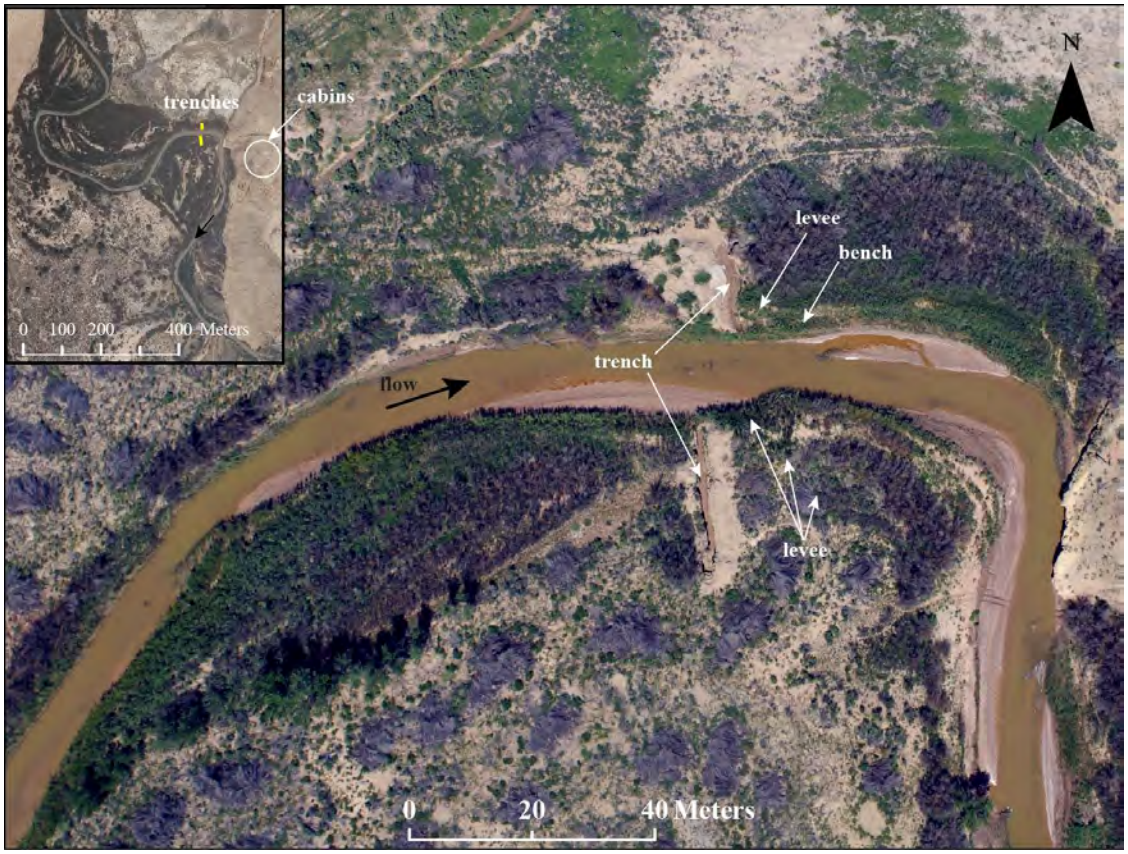

Figure 3.4. Map showing location of Frenchman's Ranch floodplain trench. Aerial imagery was taken in 2010. Basemap in inset is aerial imagery taken in 2009. Tamarisk shrubs were mechanically removed during the time period between the 2009 aerial photograph and the 2010 aerial photograph (note the piles of tamarisk in the 2010 image).

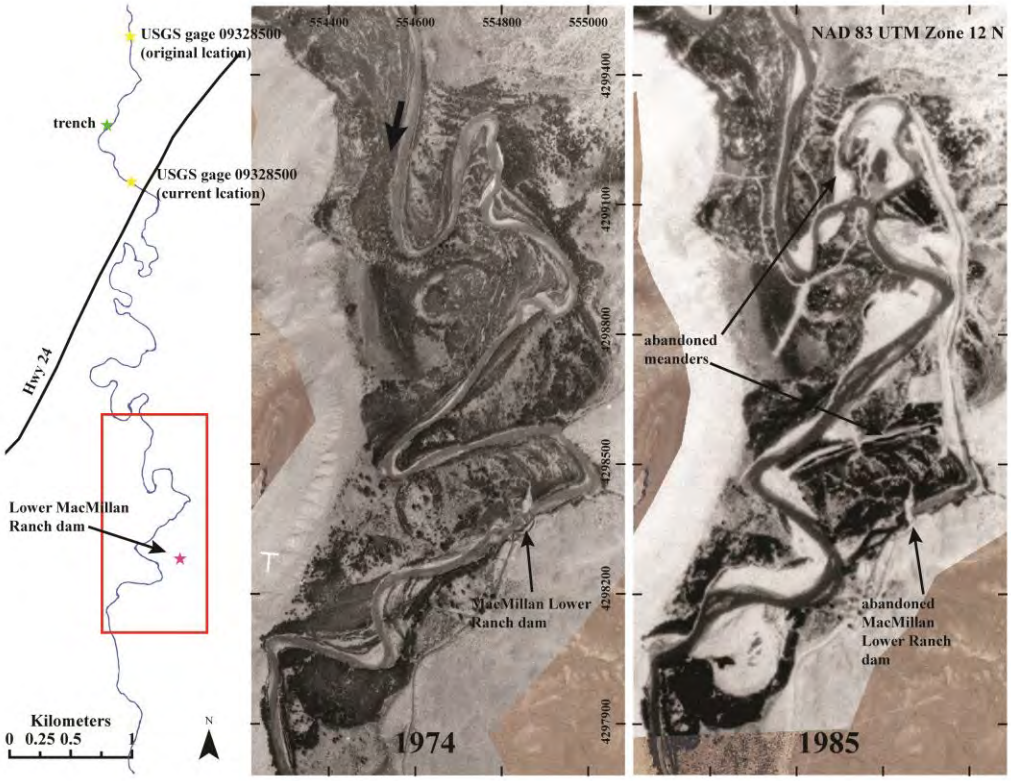

Figure 3.5. Map showing the location of the MacMillan Lower Ranch dam. The 1983 snowmelt flood caused an avulsion which abandoned the meander where the MacMillan Lower Ranch dam was located (identified in both aerial photographs). Another avulsion occurred a short distance upstream, either during the 1983 or 1984 snowmelt flood

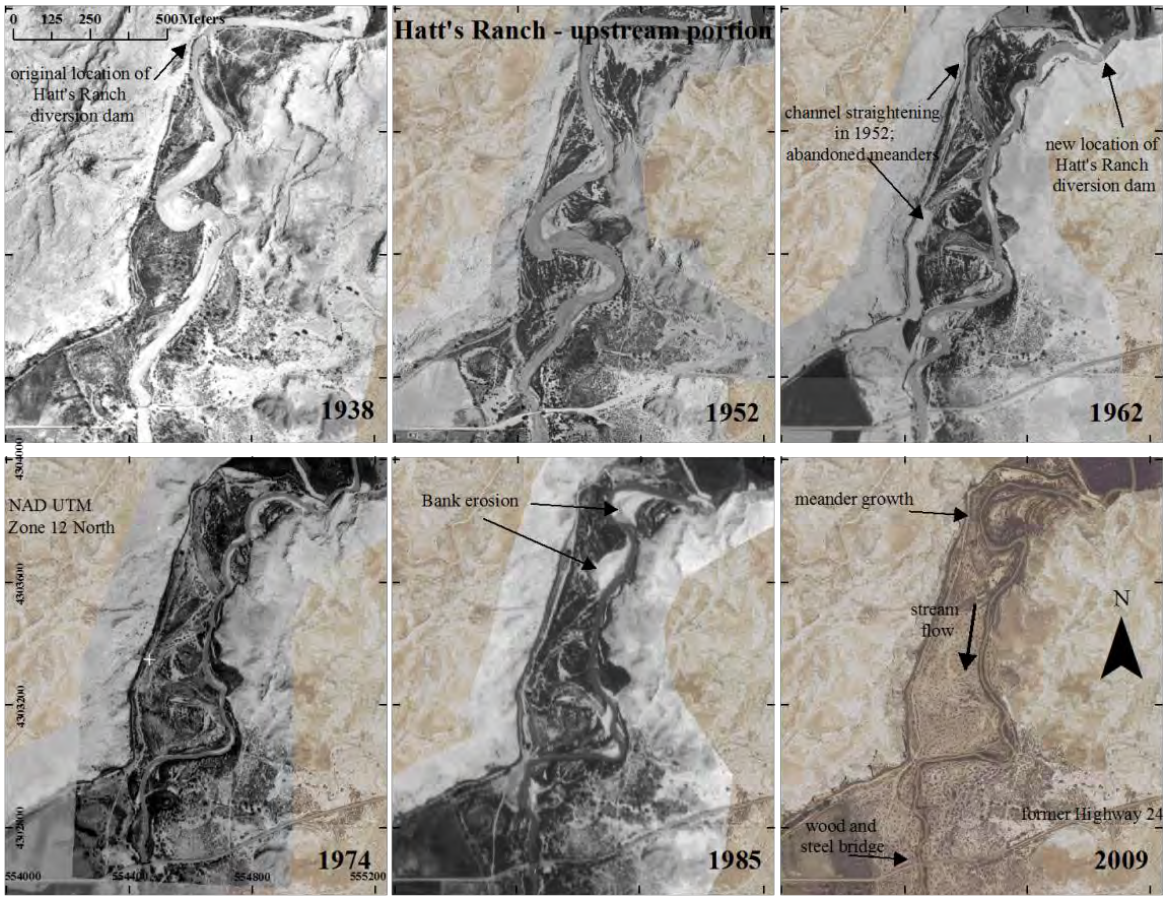

Figure 3.6. Aerial photograph comparison of the upstream portion of Hatt's Ranch. The Hatt's moved the diversion dam to it's current location and straightened the channel in two places in during the winter of 1952/1953, after the aerial photographs were taken in November 1952.

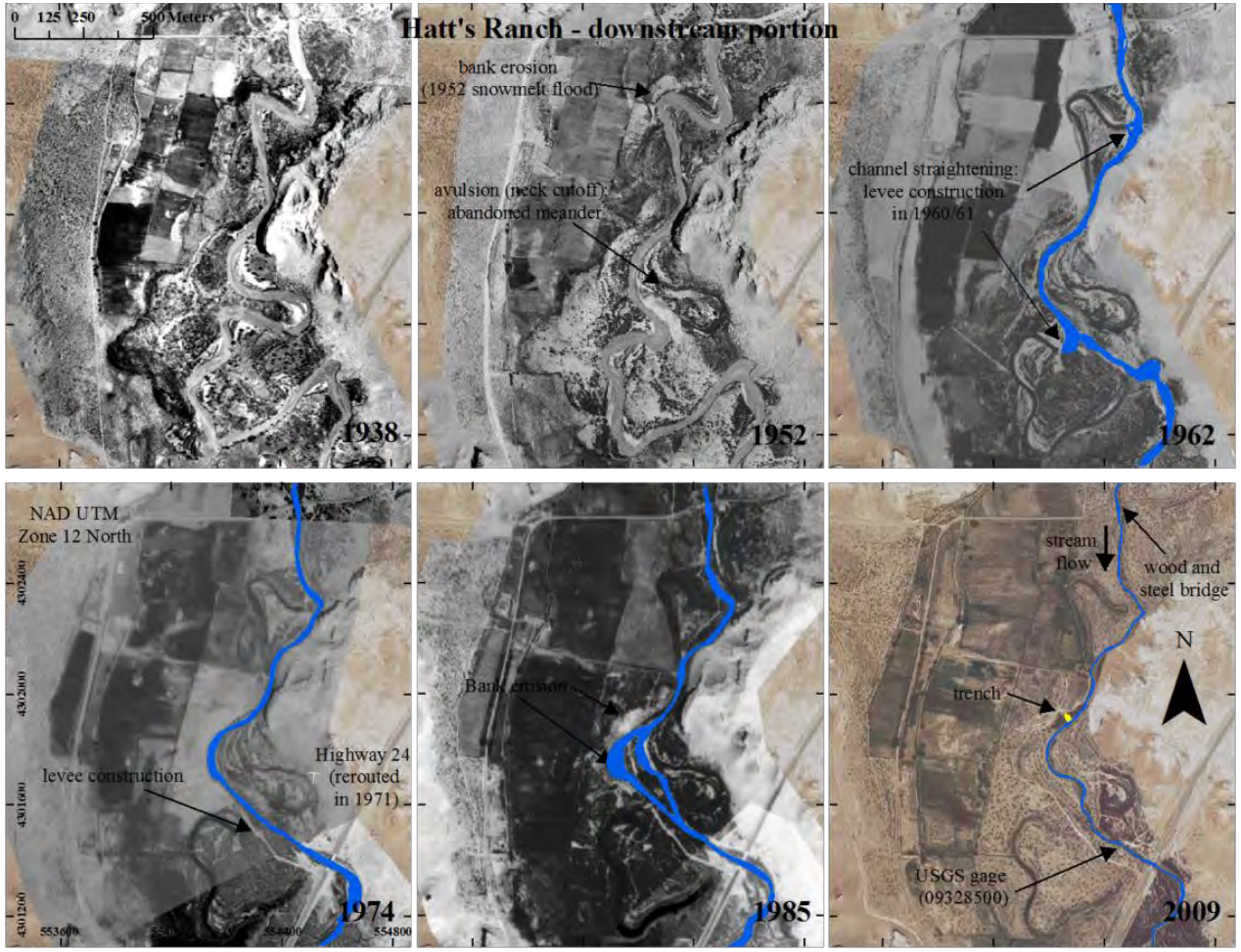

Figure 3.7. Aerial photograph comparison of downstream portion of Hatt's Ranch.

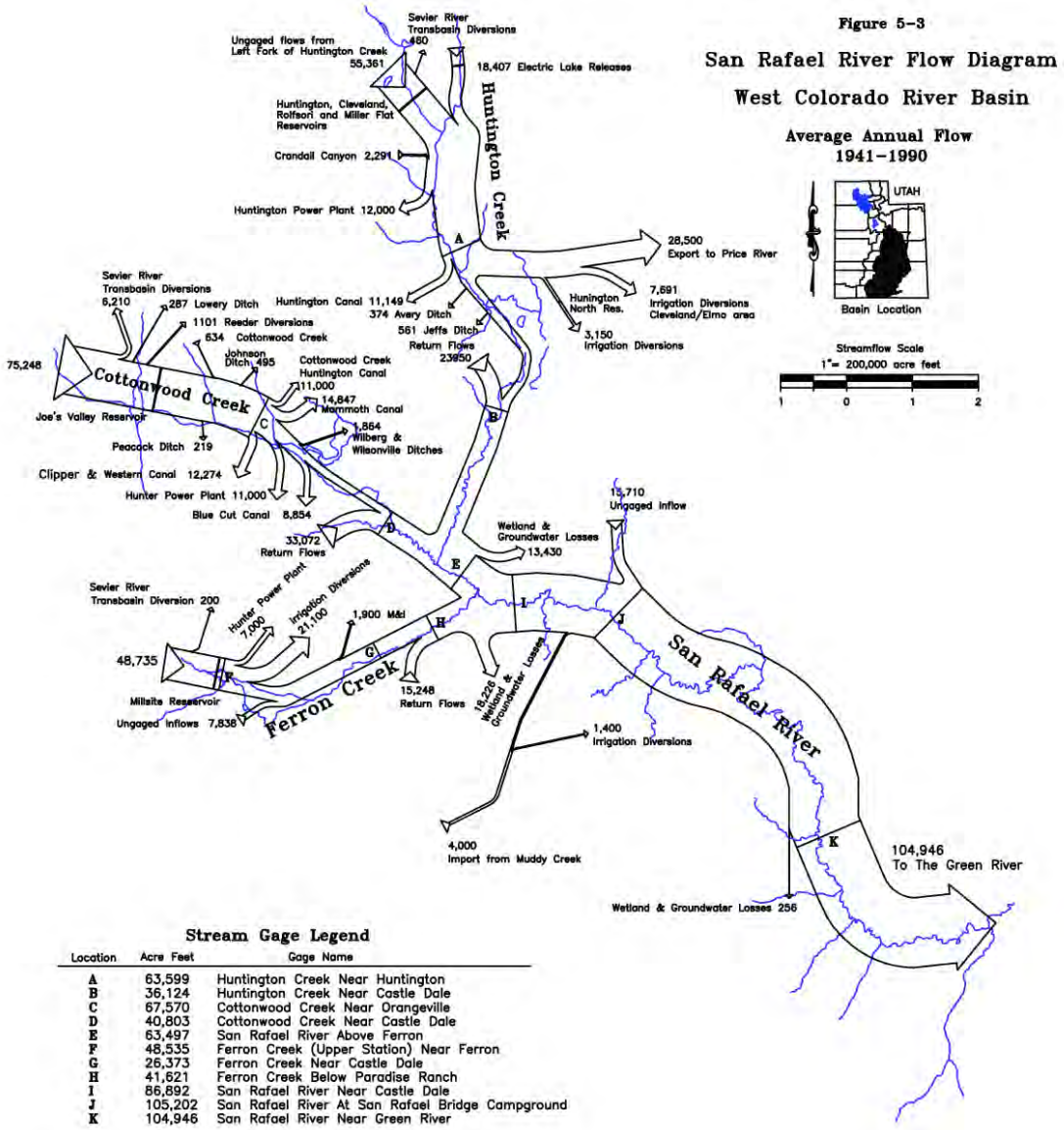

Stream Gage Legend

Location	Acre Feet	Gage Name
A	63,599	Huntington Creek Near Huntington
B	36,124	Huntington Creek Near Castle Dale
C	67,570	Cottonwood Creek Near Orangeville
D	40,803	Cottonwood Creek Near Castle Dale
E	63,497	San Rafael River Above Ferron
F	48,535	Ferron Creek (Upper Station) Near Ferron
G	26,373	Ferron Creek Near Castle Dale
H	41,621	Ferron Creek Below Paradise Ranch
I	86,892	San Rafael River Near Castle Dale
J	105,202	San Rafael River At San Rafael Bridge Campground
K	104,946	San Rafael River Near Green River

Figure 3.8. Map showing the large number of diversions and the average annual stream flow for the San Rafael River between 1941 and 1990. Diversions include both within basin diversions as well as transbasin diversions. Other surface water losses include those to groundwater and wetlands. The size of the arrow in the mainstem river appears unrepresentatively large for the number and magnitude of diversions listed in the figure. Map is copied from UBRW (2000).

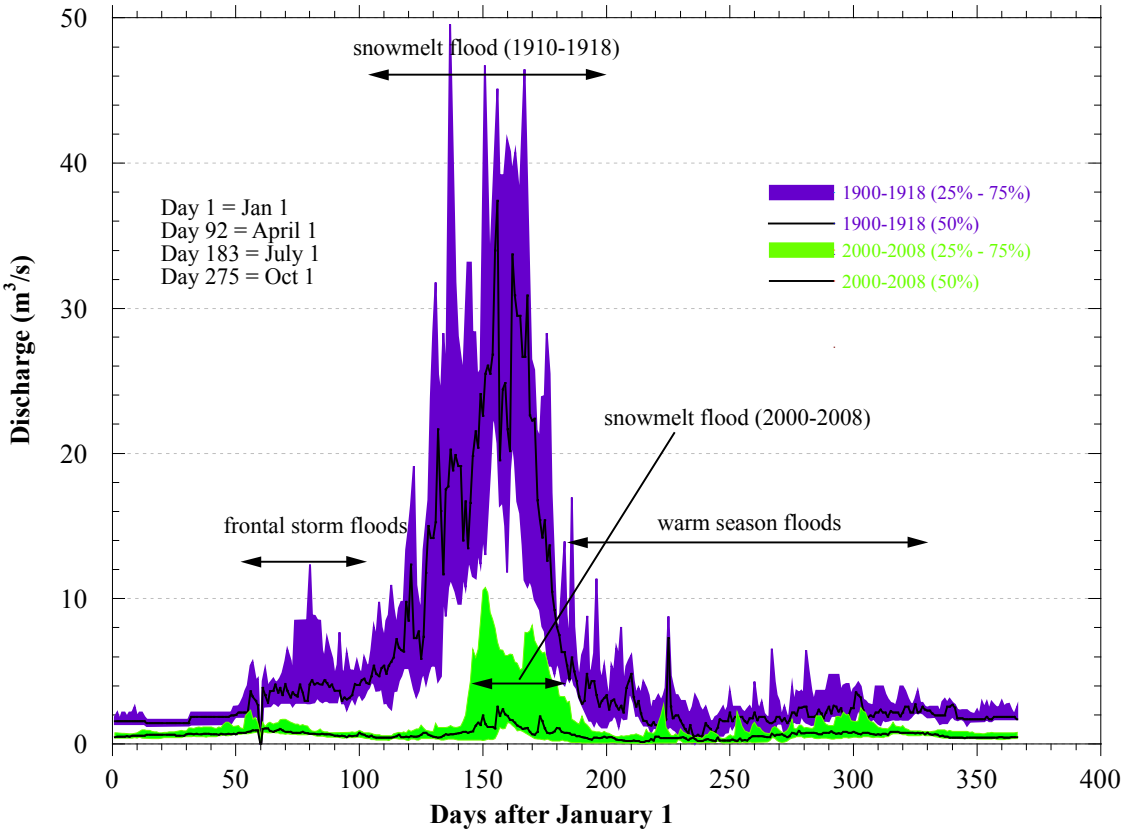

Figure 3.9. Median annual hydrographs for two time periods. The interquartile range for each time period is designated by two colors: purple for 1900-1918 and green for 2000-2008. The black line within each interquartile range is the median stream flow of the time period. There has been a reduction in stream flow between the two time periods for the entire year. The most pronounced reduction in stream flow is evident during the snowmelt flood.

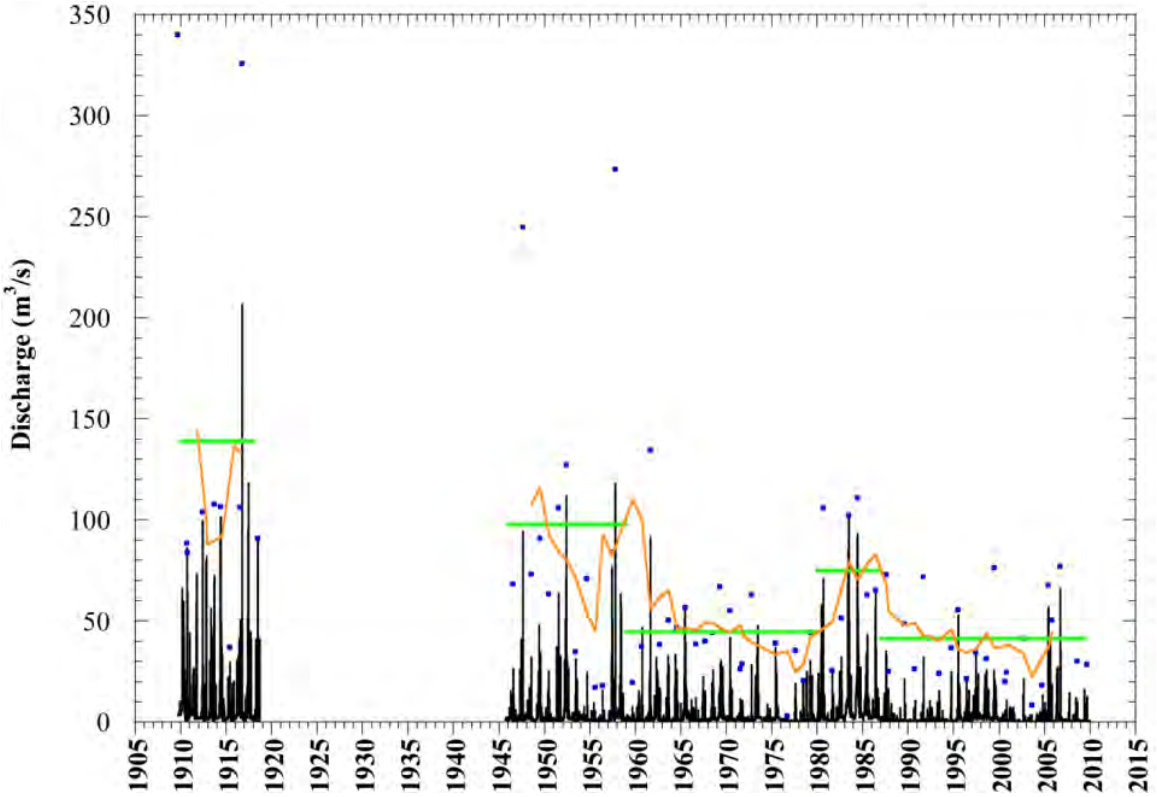

Figure 3.10. Instantaneous annual peak discharge series and mean annual discharge series for the period of record at USGS gage 09328500. Horizontal green lines are the mean annual floods for selected periods. The orange line is a 5-point moving average of the annual peak discharges. Both the moving average and mean annual flood data series indicates a progressive decline in flood peaks over time with the exception of a short period in the 1980s.

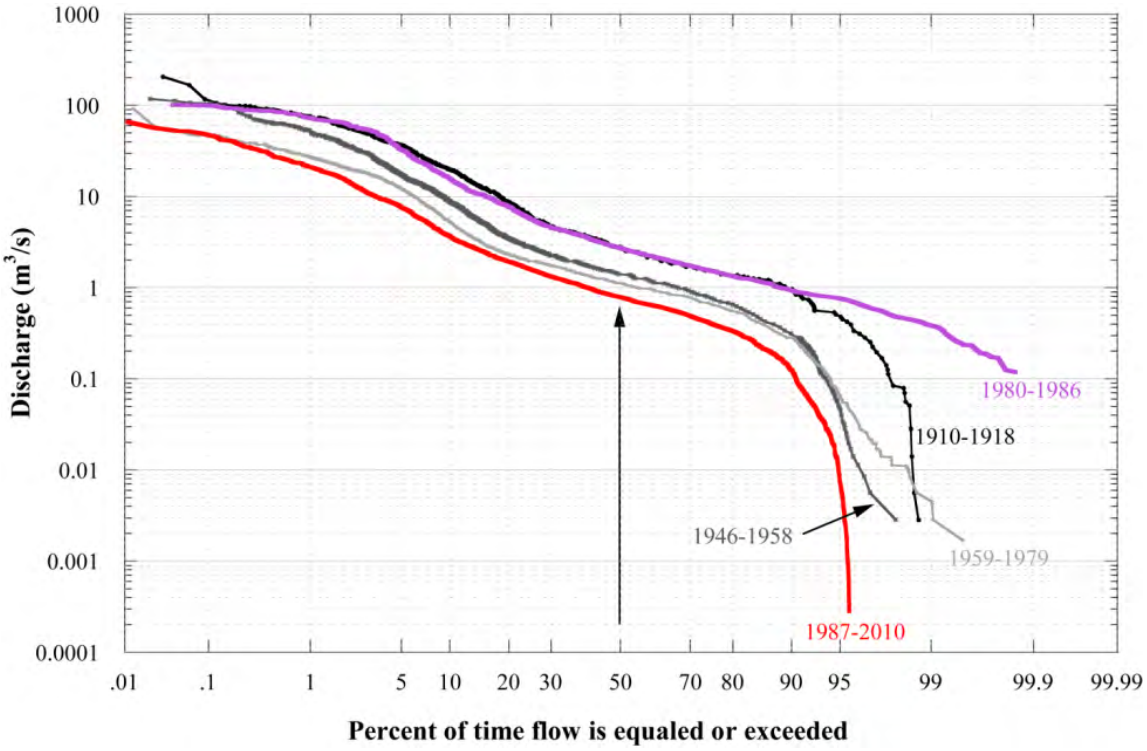

Figure 3.11. Flow duration curves. Curves were calculated using the mean daily stream-flow data at USGS gage 09328500. Between each of the early three time periods, there was a progressive decrease in flow duration at discharges greater than 1 m^3/s. Stream flow increased for the entire proportion of time between the periods 1959-1979 (light grey) and 1980-1986 (purple). In the recent time period, 1987-2010 (red), stream-flow duration was the least for entire proportion of time. The fluctuation of the median discharge is representative of the general trends in the fluctuation of entire flow duration curve between each time period, because the shape of the flow duration curves does not change (except for the range of discharges less than ~1 m^3/s in the period 1980-1986).

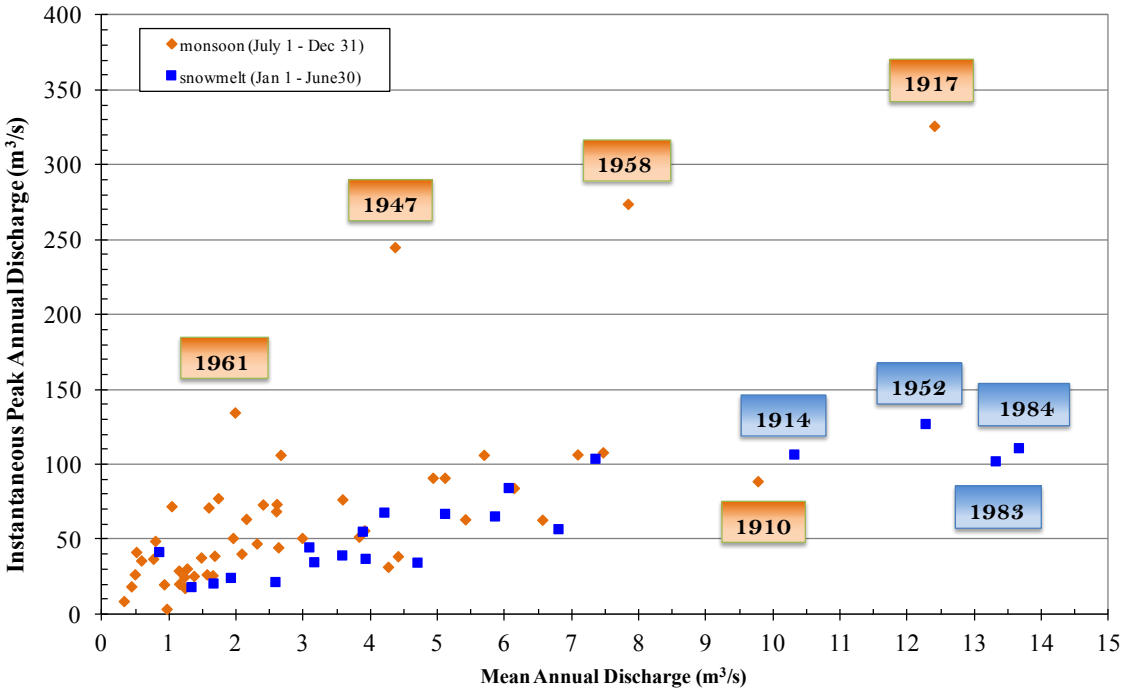

Figure 3.12. Annual peak discharge vs. mean annual discharge. The color of each data point is referenced by the type of flood that produced the largest instantaneous peak during each water year. WY 1909, which includes the largest flood of the period of record, is excluded from this chart, because no mean annual discharge is available for this water year. Note that the largest peak flows were warm season floods. Large snowmelt floods in 1910, 1914, 1917, 1952, 1983, and 1984 resulted in large mean annual discharges.

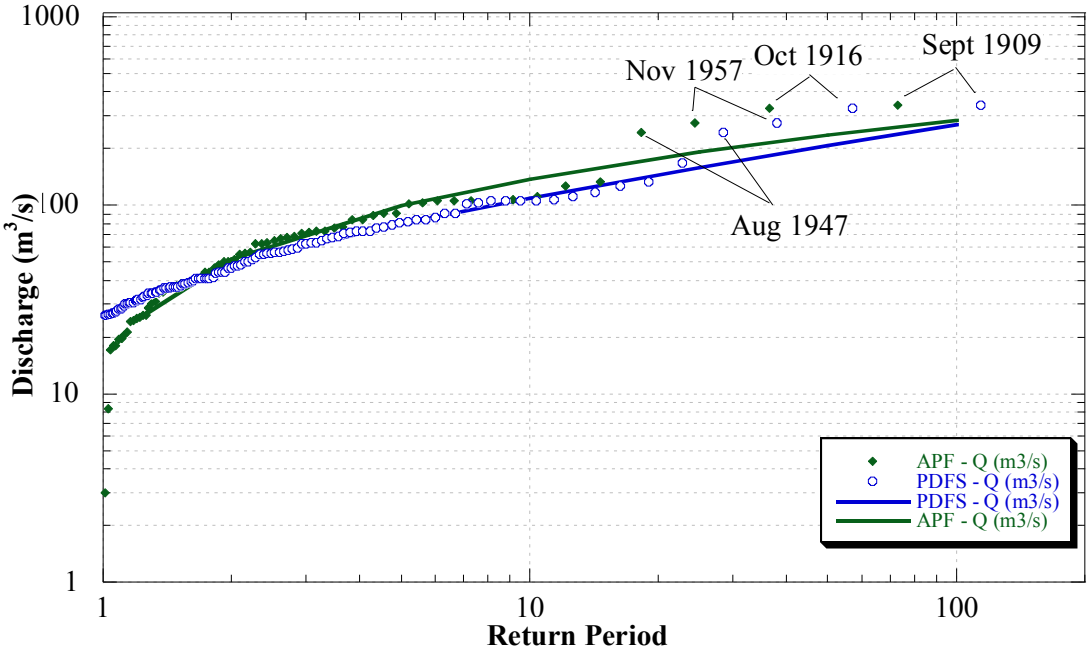

Figure 3.13. Flood frequency at USGS gage 09328500. Flood frequency was computed for both the partial duration flood series (floods greater and equal to 26 m^3/s) and the instantaneous peak annual flood series. The partial duration flood series was created by compiling peak flood discharges from both the mean daily discharge record and the instantaneous peak annual discharge record. Notice that the Log Pearson type III curve computed for all flood magnitudes contained in the instantaneous annual peak flood series overestimates the magnitude of floods above the recurrence interval of 1.6 yrs, and underestimates the magnitude of floods below 1.6 yr RI.

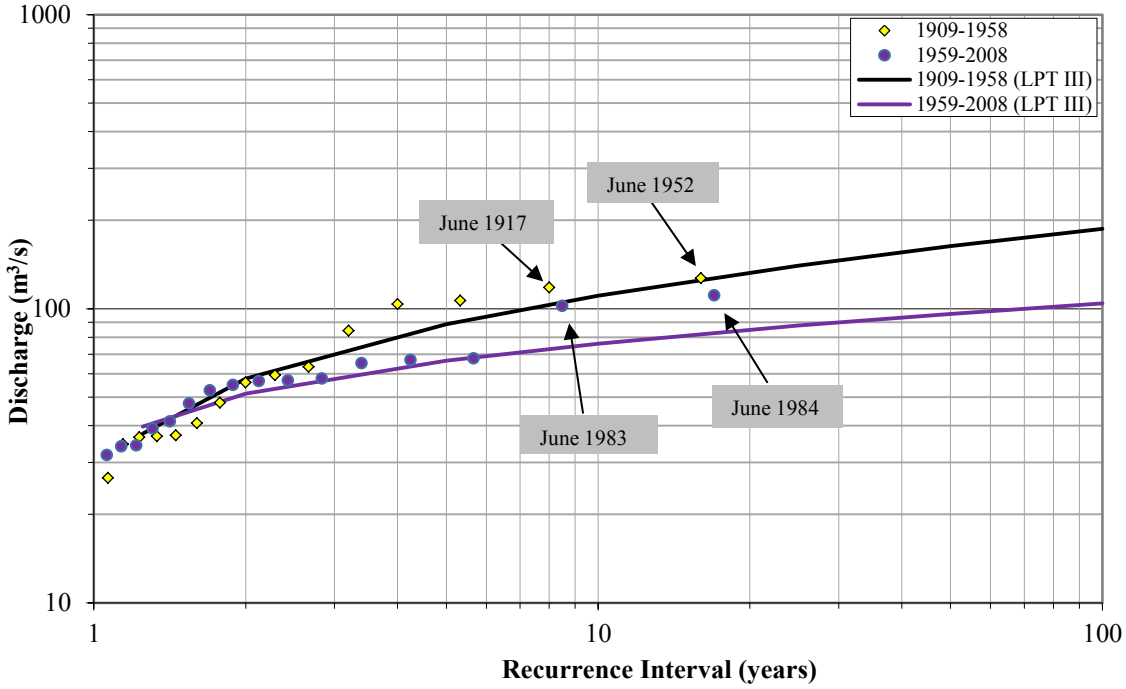

Figure 3.14. Partial duration flood frequency (>26 m^3/s) for snowmelt floods split into two time periods (USGS gage 09328500). Flood magnitudes for the period 1959-2008 are less than the previous period (1909-1958) for all recurrence intervals greater than the 2-yr RI flood.

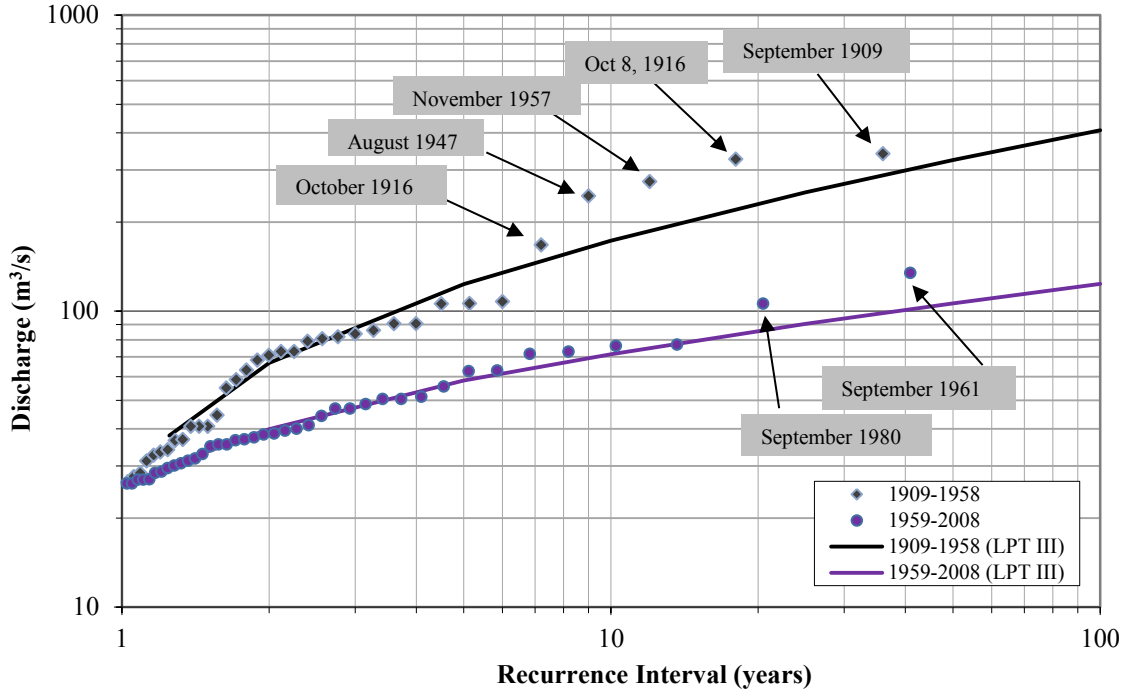

Figure 3.15. Partial duration flood frequency (>26 m^3/s) for warm season floods only, split into two time periods, 1909-1958 and 1959-2008. The discharge data used in this plot was measured at USGS gage 09328500. Flood magnitudes for all recurrence intervals are less for the period 1959-2008 than for the period 1909-1958.

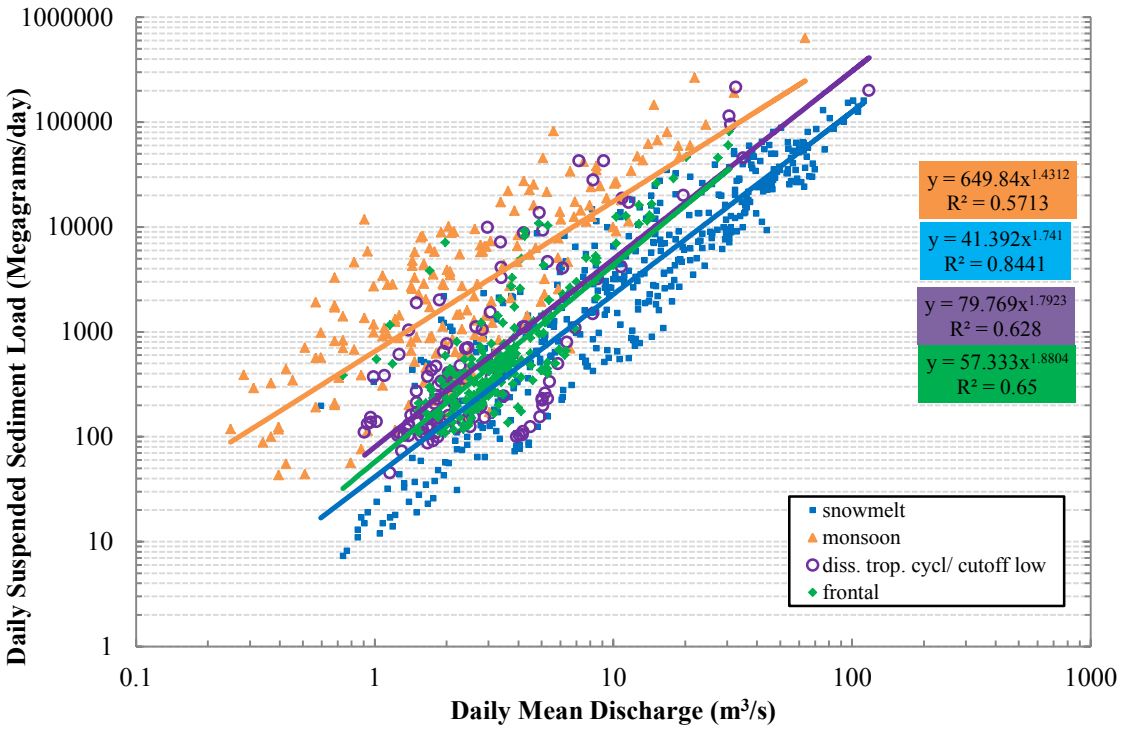

Figure 3.16. Suspended sediment rating curves for four types of floods. Suspended sediment concentrations were measured daily at USGS gage 09328500 during 8 years (1949, 1951-1958). Flood types were distinguished by the combination of season and flood duration. In general, frontal floods occurred in winter and spring, snowmelt floods occurred in spring, monsoon floods occurred in summer, and tropical cyclone/ cut off low pressure floods occurred in fall. However, the seasonal boundaries of each flood types overlapped. For example, winter/spring frontal floods occurred between the December 25 and May 5, snowmelt floods occurred between April 8 and July 28, monsoon floods occurred between July 3 and September 30, and tropical cyclone/ cut off low pressure floods occurred from October 4 to December 2.

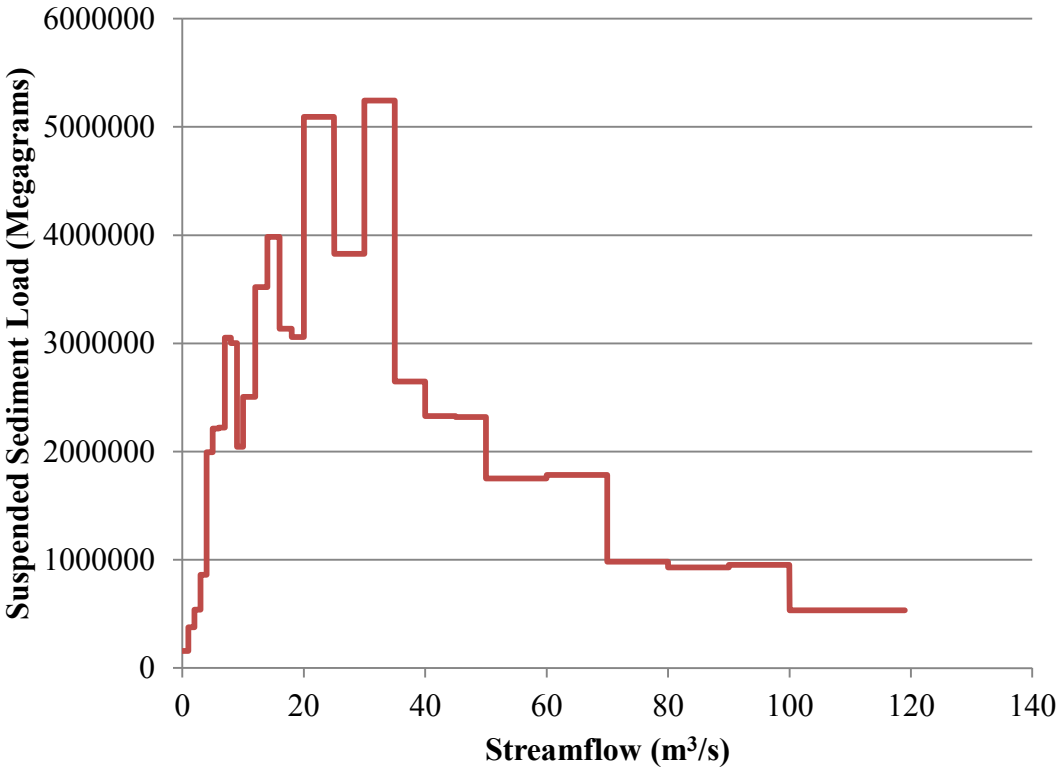

Figure 3.17. Sediment load histogram. The suspended sediment load data and the cumulative distribution of stream flow measured in1949 and 1951-1957 were used to create this histogram. Data were discretized into 26 bins of 5 sizes: 1 m^3/s, 2 m^3/s, 5 m^3/s, 10 m^3/s, 20 m^3/s. The 30-35 m^3/s bin is the peak of the sediment load histogram, and is the effective discharge. The subordinate effective discharge, which is the 20-25 m^3/s bin, transports nearly as much suspended sediment as the primary effective discharge.

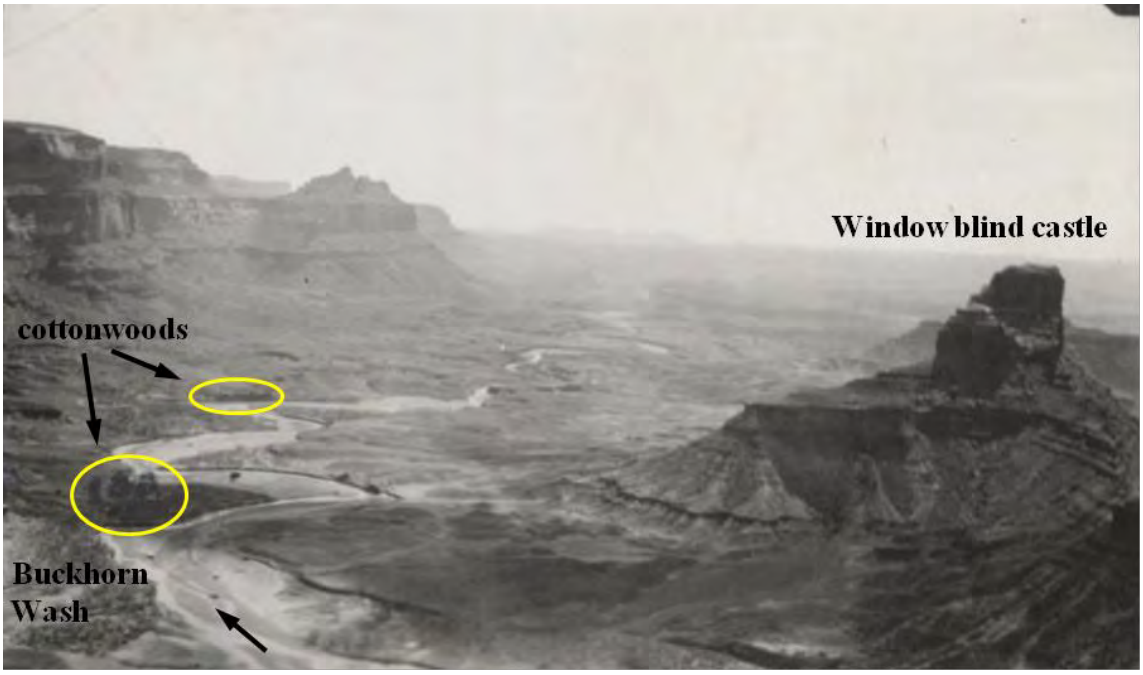

Figure 3.18. Oblique aerial photograph taken in 1928 by Drew Richards. The photograph was taken in the San Rafael Swell, approximately 1 km downstream from the old swinging bridge. View is looking downstream. Buckhorn Wash enters the mainstem on river left in the foreground. Note the apparent lack of vegetation in the wide sandy channel. Cottonwood stands were sparsely scattered along the riparian corridor. Photograph is courtesy of the Emery County Archives and can be found at the online Photograph Collection of the Sheratt Library of Southern Utah University.

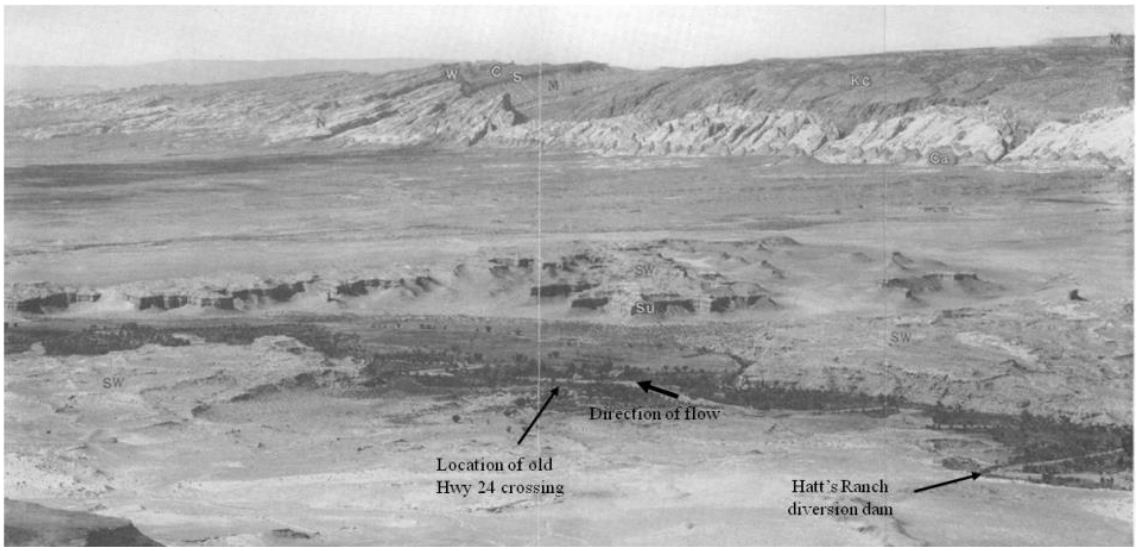

Figure 3.19.Historic oblique aerial photograph of a portion of the study area near the Hatt's Ranch. Photograph was taken sometime in the early 20th century, copied from Baker (1946), and shows the planform of the river before two meander bends were cutoff. Streamflow is from right to left. San Rafael Reef and San Rafael Swell are shown in the background. Numerous cottonwoods occur in the alluvial valley.

Figure 3.20. Photo taken in 1918 by W.B. Emery. The location of the photograph is likely in the vicinity of Gillis' and Frenchman's Ranches. Direction of stream flow is away from viewer. Point bar on the left is comprised of surfaces at multiple elevations, labeled "1", "2", "3", & "4". Cottonwood trees are growing along the right bank in the fine sandy aeolian deposits.

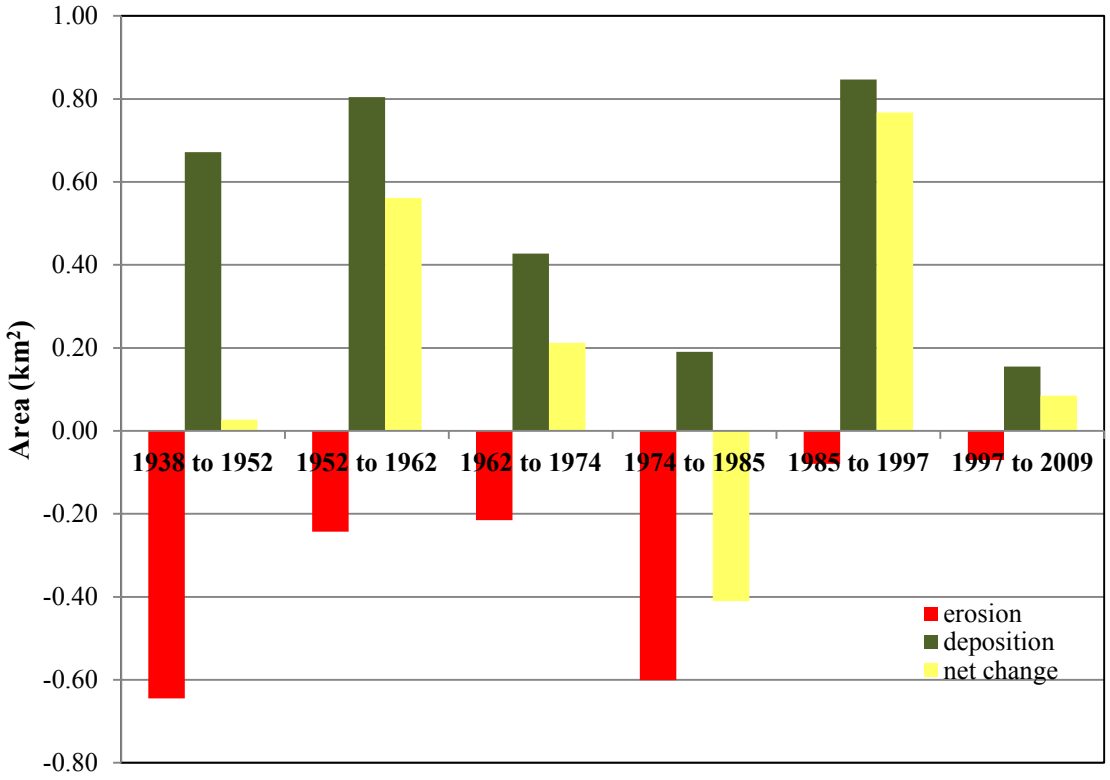

Figure 3.21. Graphical results from a spatial union analysis performed in GIS, of sequential historic aerial photographs. Analysis was conducted for the TbFr segment. Green columns represent the area of floodplain constructed between photograph series'. Red columns represent area of bank erosion. Yellow columns represents the net change (difference between red and green), and may show a net of either floodplain deposition or erosion.

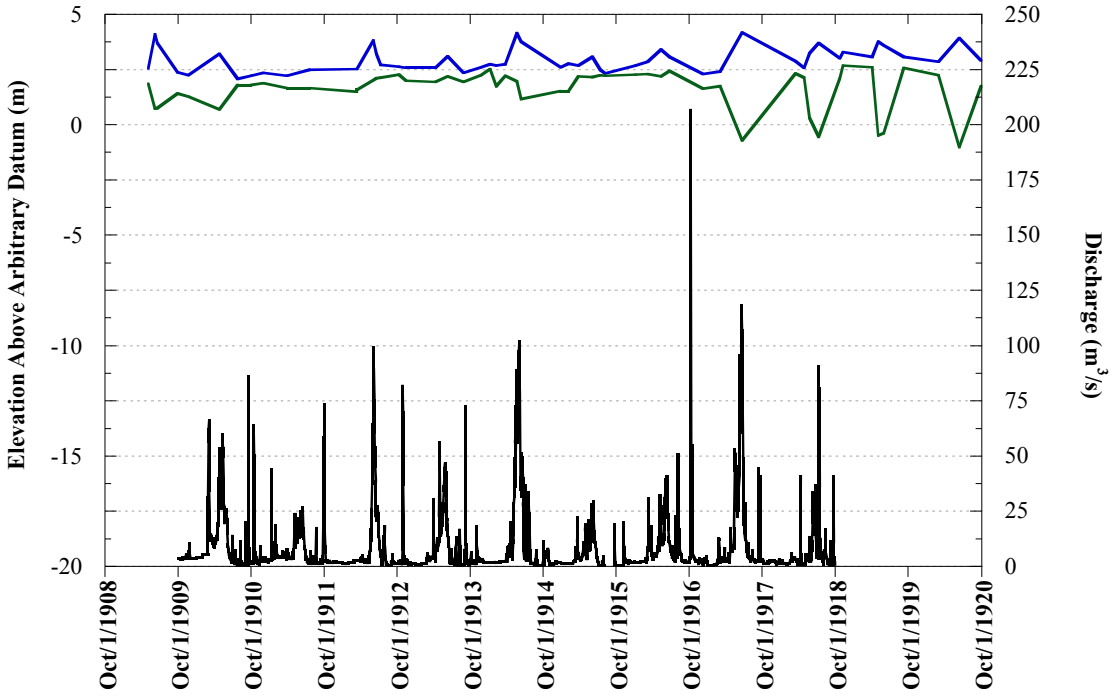

Figure 3.22. Time series of discharge, thalweg elevation and water surface elevation, 1909-1920. Mean daily discharge is shown in black, thalweg elevation is green and water surface elevation is blue. During this time period, 1908-1920, the USGS measured discharge approximately four to five times per year. As a result of the relatively infrequent discharge measurements, the exact magnitude and precise timing of scour and fill during most of the floods is not captured.

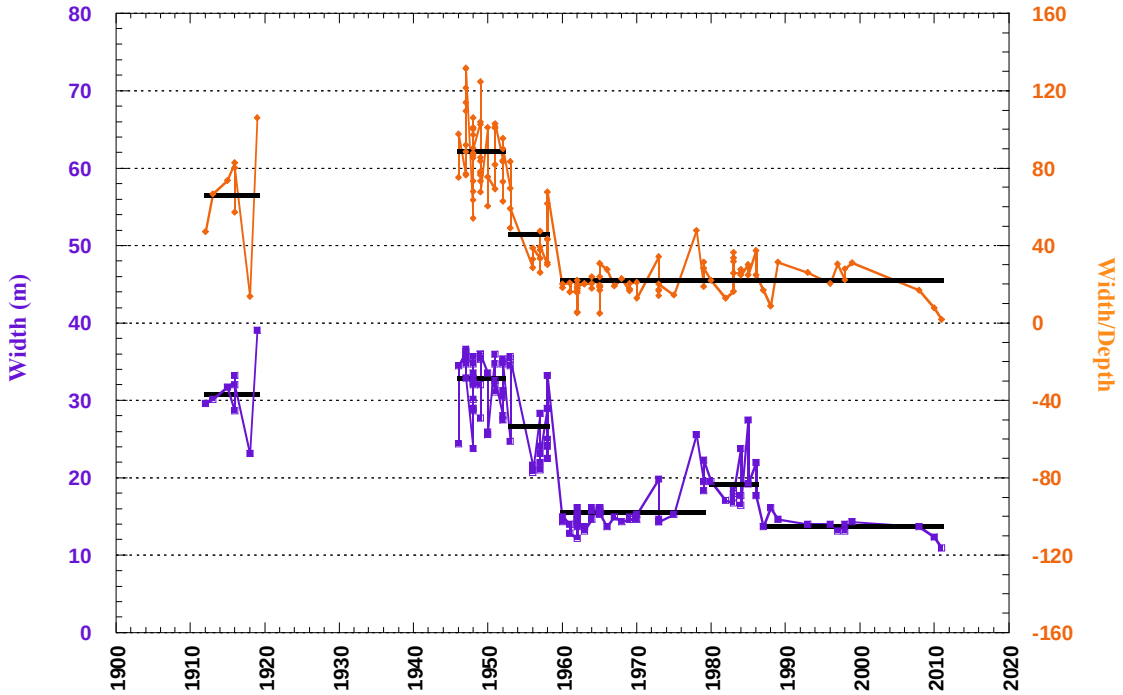

Figure 3.23. Time series of width and width-to-depth ratio for entire period of record. Data was extracted from measurements of discharge at USGS gage 09328500 on the Hatt's Ranch. Only width data measured during stream flows of 7 m^3/s to 28 m^3/s are used in this analysis. Statistics for each of the periods of adjustment in the width-to-depth series and the width series are located in Table 9 and Table 10, respectively. The 1952 snowmelt flood did not significantly widen the channel because the a wide channel had been maintained by regular large snowmelt floods in the 1930s and 1940s.

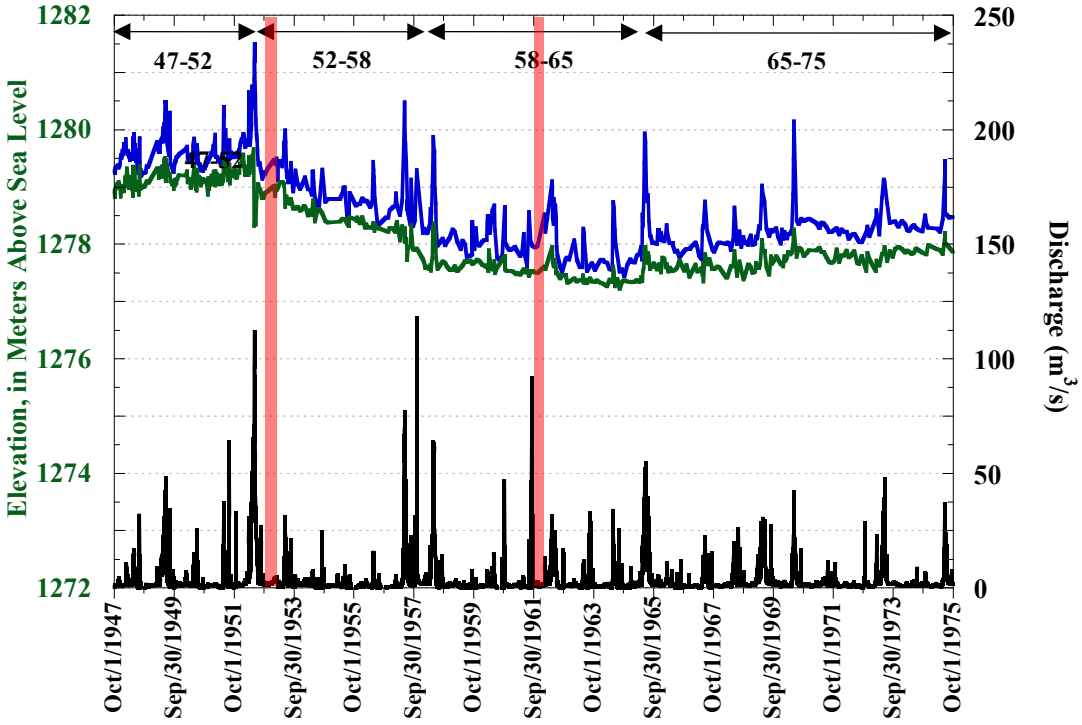

Figure 3.24. Time series of thalweg elevation, discharge, and water surface elevation between 1947 and 1976. This plot reveals four time periods of bed elevation change. Bed incision occurred between 1952 and 1965, which was both preceded and followed by periods of aggradation 1947-1952, and 1965-1976. Vertical red bars indicate the two channel straightening events that occurred on the Hatt's Ranch. In 1952 when the Hatt's moved the diversion dam to it's current location, they cutoff two meander bends located between the current diversion dam and the wood and steel bridge. In 1961/1962 the Hatt's cutoff two meander bends located between the wood and steel bridge and the current Highway 24 bridge. On average, the USGS measured discharge 45 times per year between 1946 and 1965, 20 times per year between 1966 and 1970, and 13 times per year between 1971 and 1976.

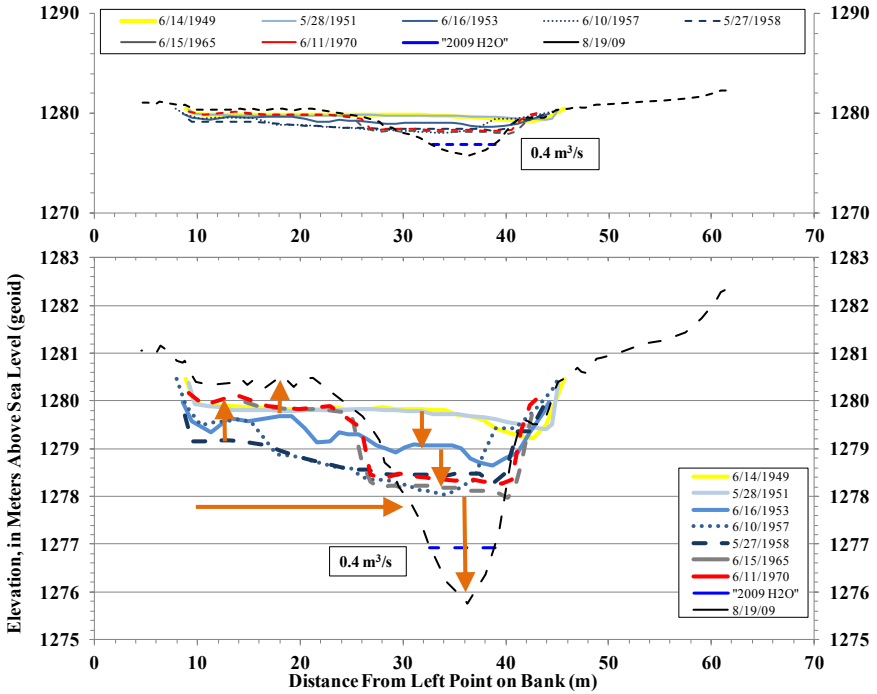

Figure 3.25. Cross sections measured at the abandoned cableway of USGS gage 09328500. The plot of the cross sections at the top does not have vertical exaggeration. The cross sections plotted at the bottom are the same as above but have 2.3 vertical exaggeration. Orange arrows indicate magnitude and direction of changes that occurred between 1949 and 2009. Bed lowering occurred between 1951 and 1953, then again between 1953 and 1958, and again between 1958 and 2009. Channel narrowing occurred between 1958 and 1965 and again between 1970 and 2009. Vertical accretion of the floodplain occurred between 1958 and 1965 and again between 1970 and 2009.

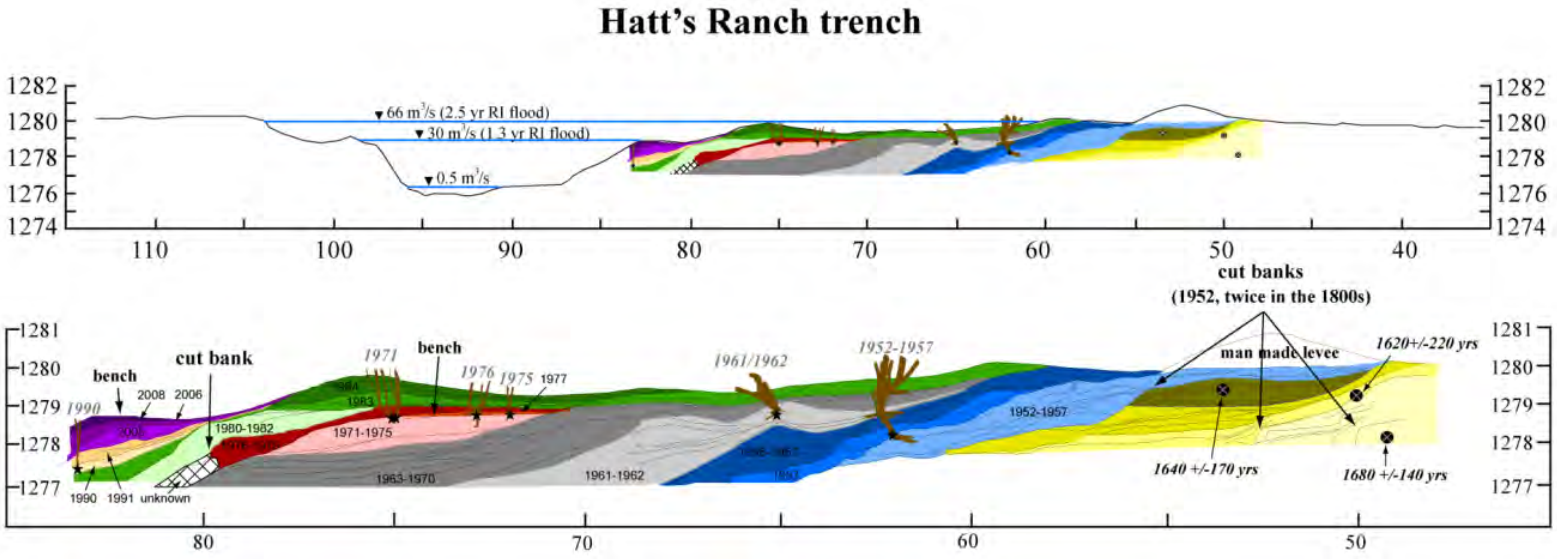

Figure 3.26. Floodplain stratigraphy exposed in trench at Hatt's Ranch. Yellow stars indicate the germination locations of Tamarisk shrubs used in dendrochronologic analyses. Orange and black circles indicates the location where samples were removed for the optically stimulated luminescent analysis. Based on the OSL results, the oldest sediment (shades of yellow and brown packages) was deposited sometime between 1400 and 1840 A.D.

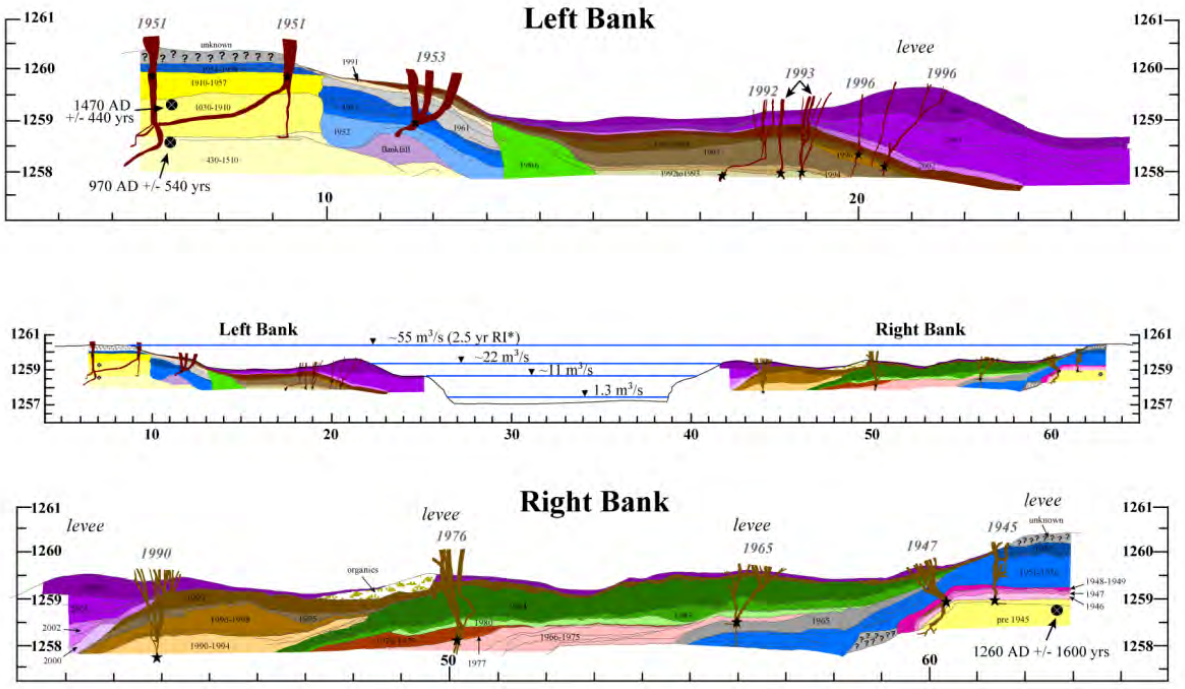

Figure 3.27. Floodplain stratigraphy exposed in the trench on Frenchman's Ranch. Yellow stars indicate the germination locations of tamarisk shrubs used in dendrochronologic analyses. 65.1 m^3/s is the 2.5 yr recurrence interval flood at USGS gage 09328500. The length of river between Hatt's Ranch and Frenchman's Ranch is a losing reach, as determined from the measurement of streamflow at Frenchman's Ranch on April 18, 2011. Assuming that the difference in discharge between the Hatt's Ranch and Frenchman's Ranch is constant at all stream flows, then a flood discharge of 65.1 m^3/s at Hatt's Ranch is approximately 55 m^3/s at Frenchman's Ranch

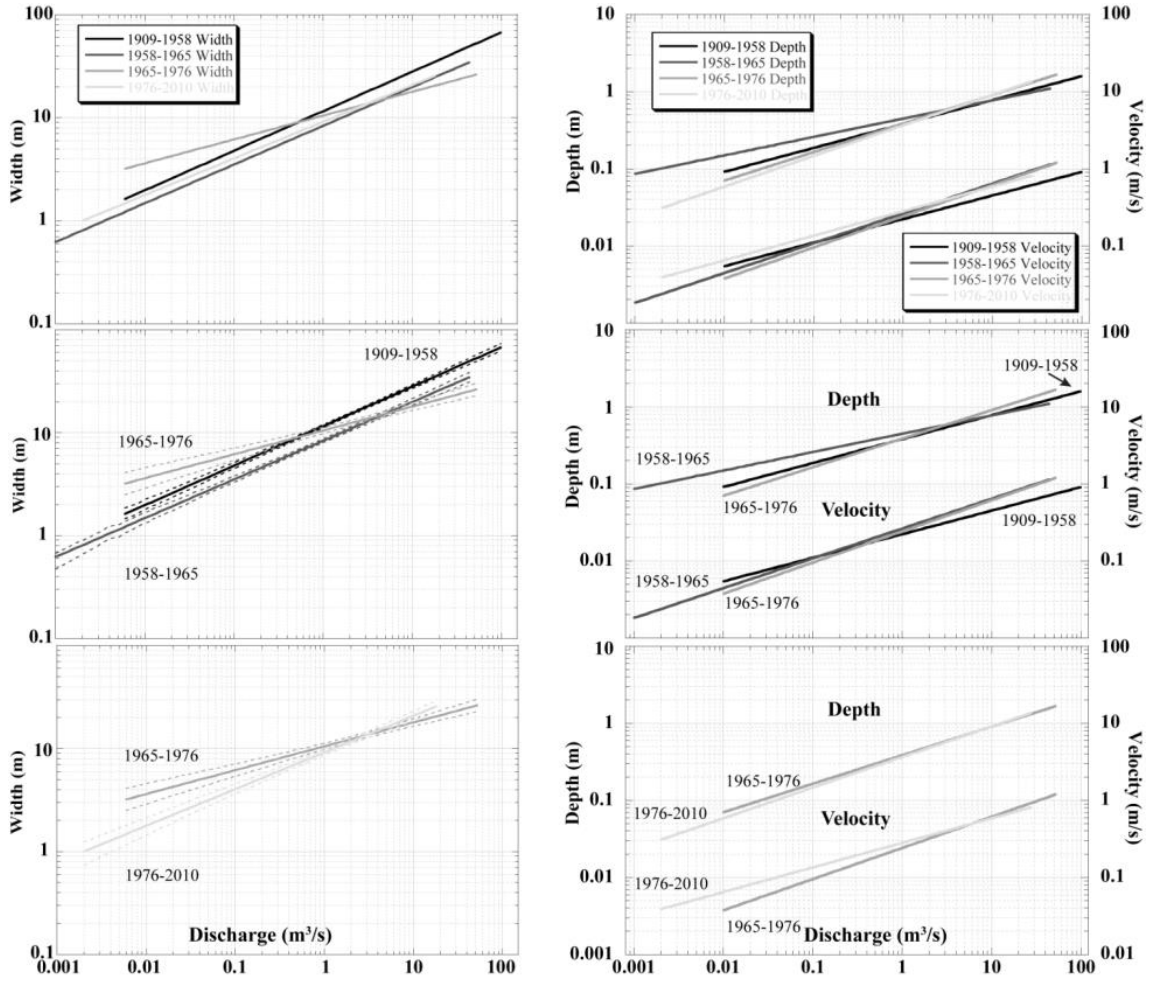

Figure 3.28. Hydraulic geometry relations measured at USGS gage 09328500. The two plots at the top show the hydraulic geometry relations for the entire period of record divided into four time periods, width on left, and velocity and depth on right. The bottom four plots contain the same relationships in the top two plots but the time periods are separated for easier inspection; 95% confidence intervals are plotted for each of the width hydraulic geometry relationships in the bottom two plots in the left column.

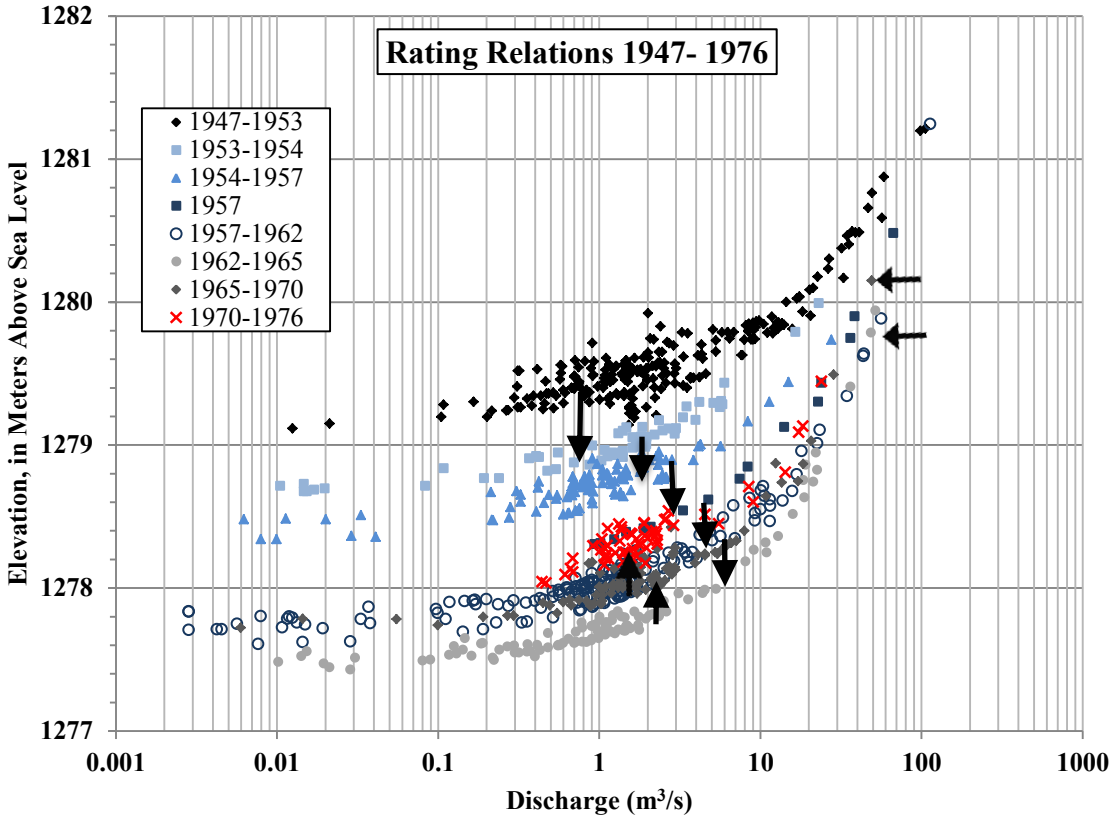

Figure 3.29. Rating relations, 1947-1976, measured at former locations of USGS gage 09328500. Downward shifts in rating relations for discharges less than 10 m^3/s indicate bed lowering between 1947-1953 and 1962-1965. Upward shifts in rating relations for discharges less than 10 m^3/s for the time periods 1962-1965 and 1970-1976 show that the bed aggraded. Increases in stage for discharges greater than 20 m^3/s for time periods 1965-1970 and 1970-1976 are caused by reduction in channel capacity, and means that smaller floods are still capable of spilling over the banks and contributing to vertical accretion of the floodplain.

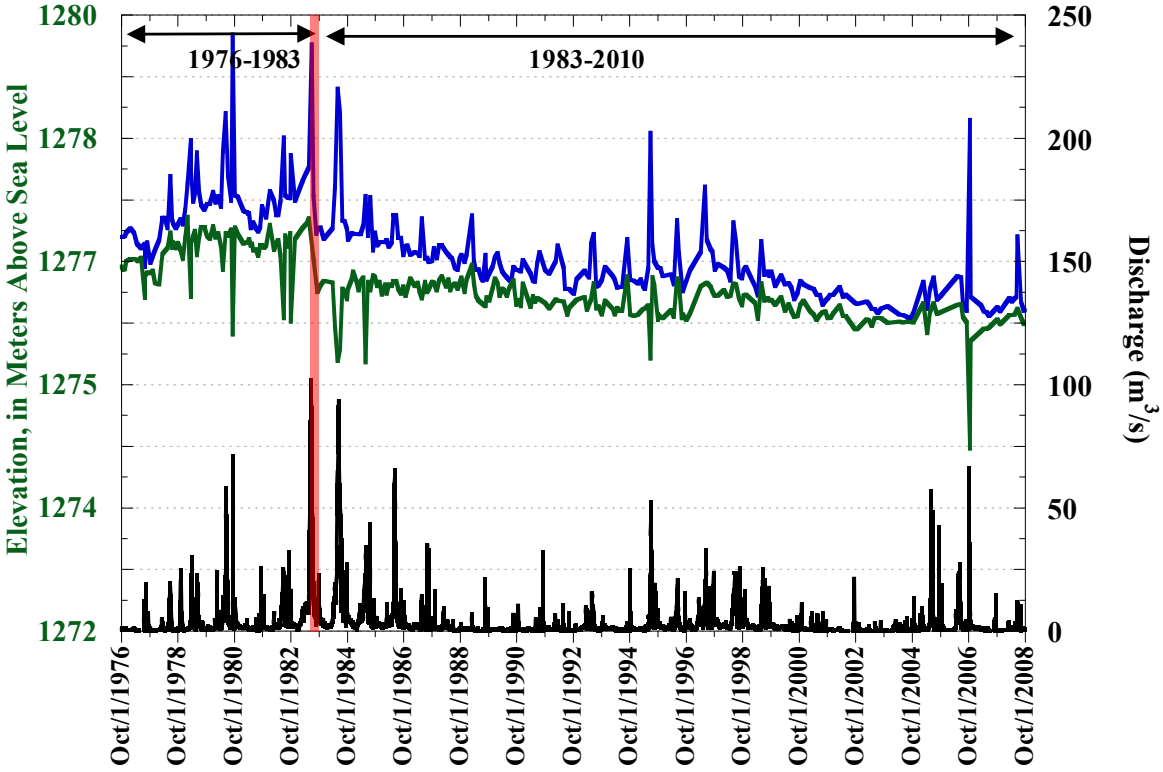

Figure 3.30. Thalweg elevation time series for the time period from 1976 to 2010. The drop in local base level at the downstream location, when the 1983 snowmelt flood bypassed the Lower Macmillan Ranch Dam, is indicated by the red bar. A period of incision from 1983 to 2010 followed the downstream drop in base elevation that occurred during the 1983 snowmelt flood. There is no apparent trend in bed elevation change between 1976 and 1983.

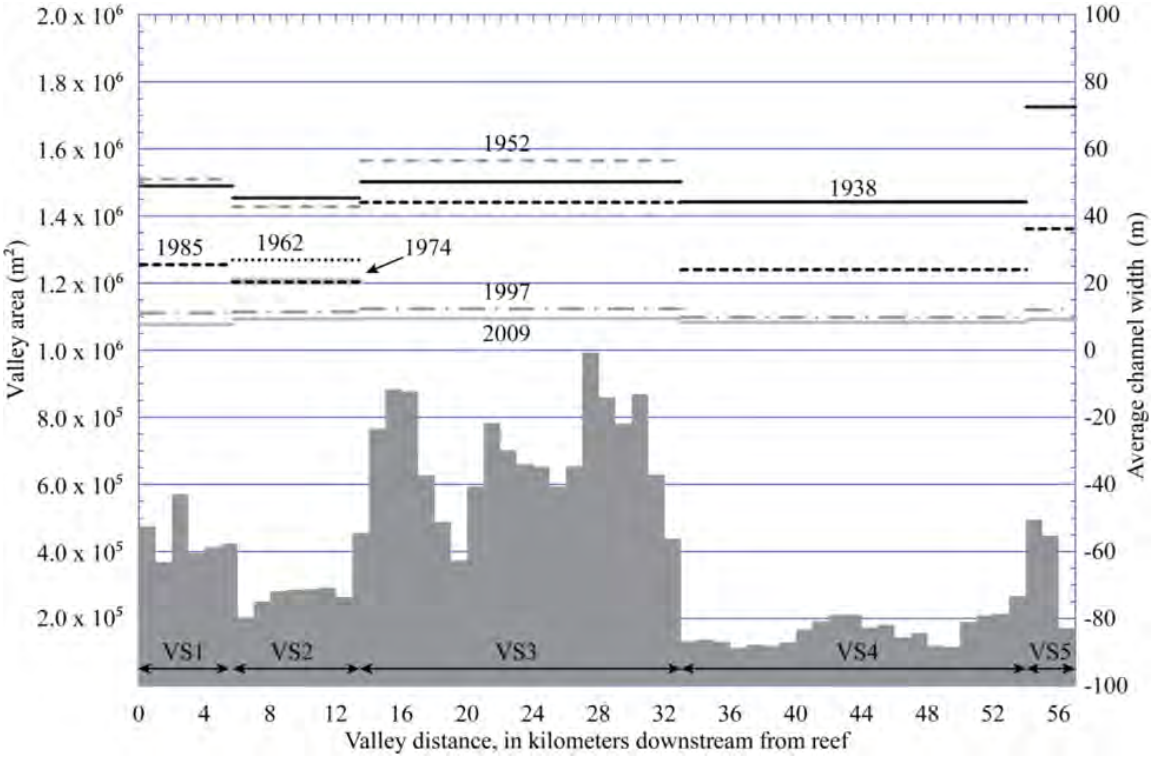

Figure 3.31. Segment average channel width determined from aerial photographs. The average width of the active channel in segment 2 did not change between 1974 and 1985 despite the large snowmelt floods in 1983 and 1984.

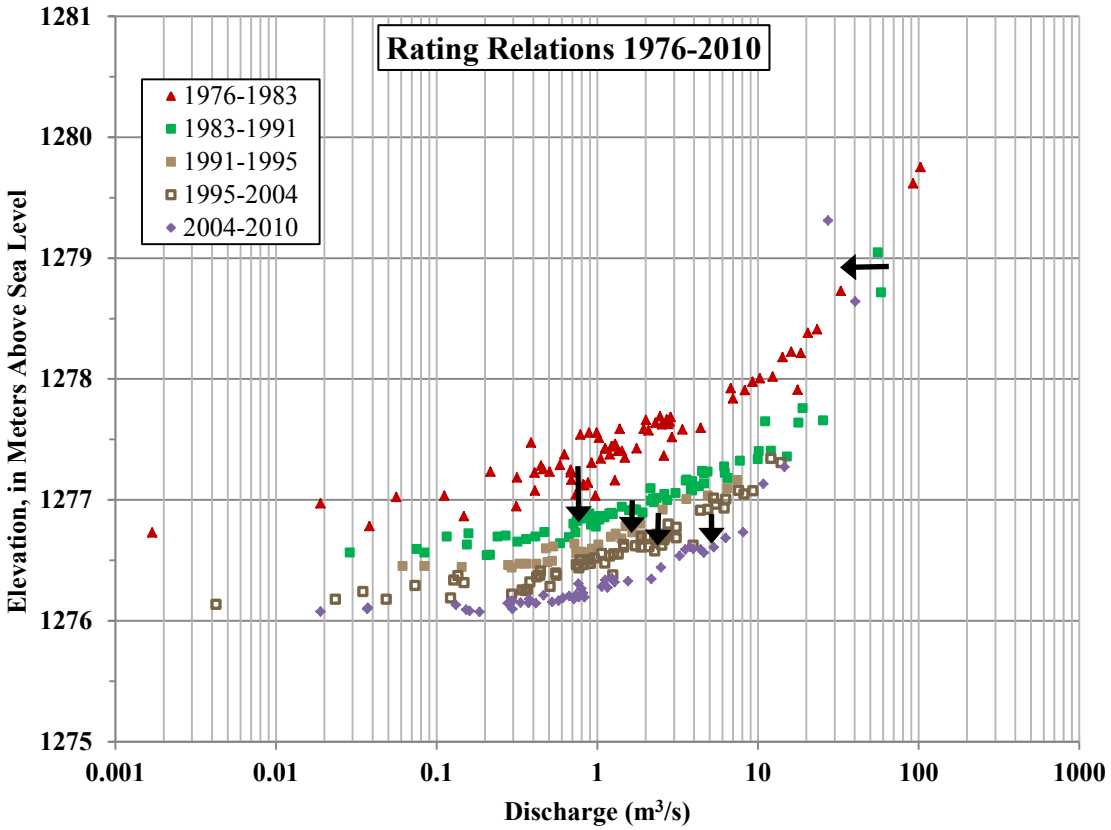

Figure 3.32. Rating relations,1976-2008, measured at the present location of the USGS gage 09328500. Bed elevation decrease is indicated by the downward shift in stage for nearly all discharges. An increase in stage for discharges greater than 30 m^3/s for time periods 2004-2010 is caused by reduction in channel capacity, and means that smaller floods are still capable of spilling over the banks and contributing to vertical accretion of the floodplain.

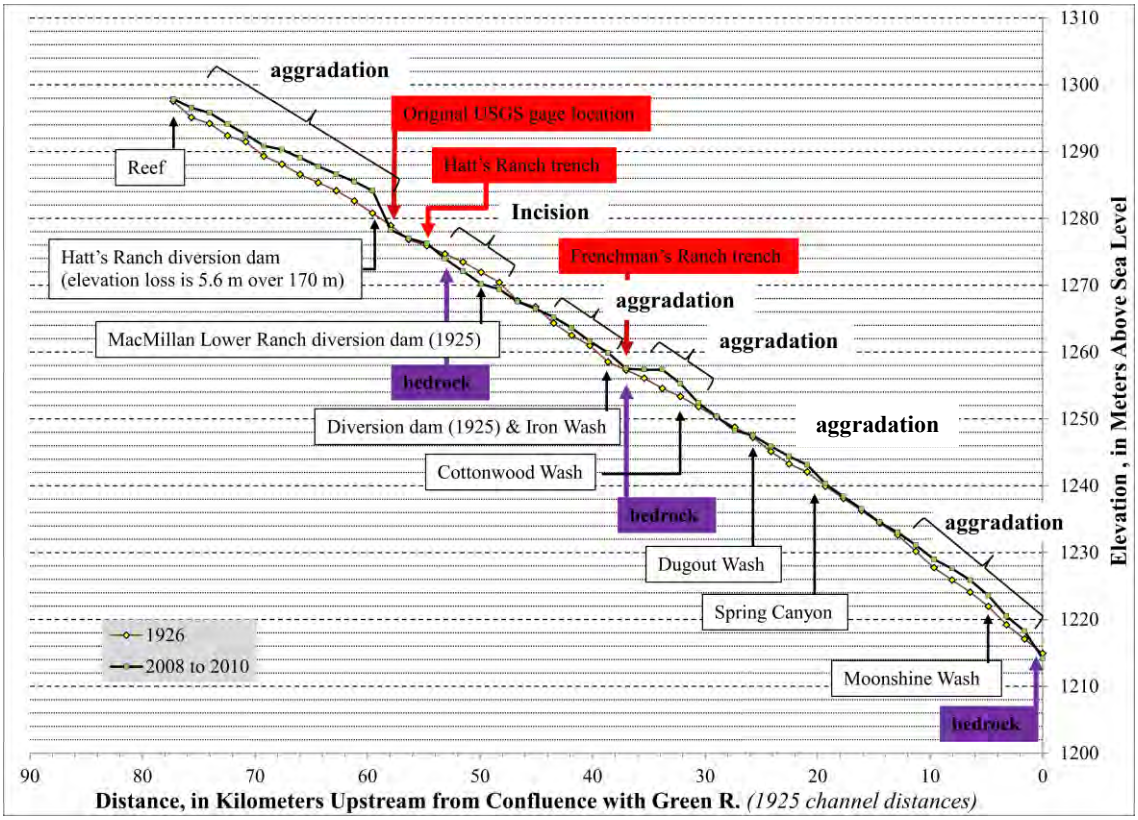

Figure 3.33. Comparison of longitudinal profiles surveyed in 1925 and again in 2008-2010. The long pro comparison shows five segments where aggradation has occurred and one segment where incision has occurred. The 1925 profile was on bedrock in two places and the recent profile is on bedrock in three places.

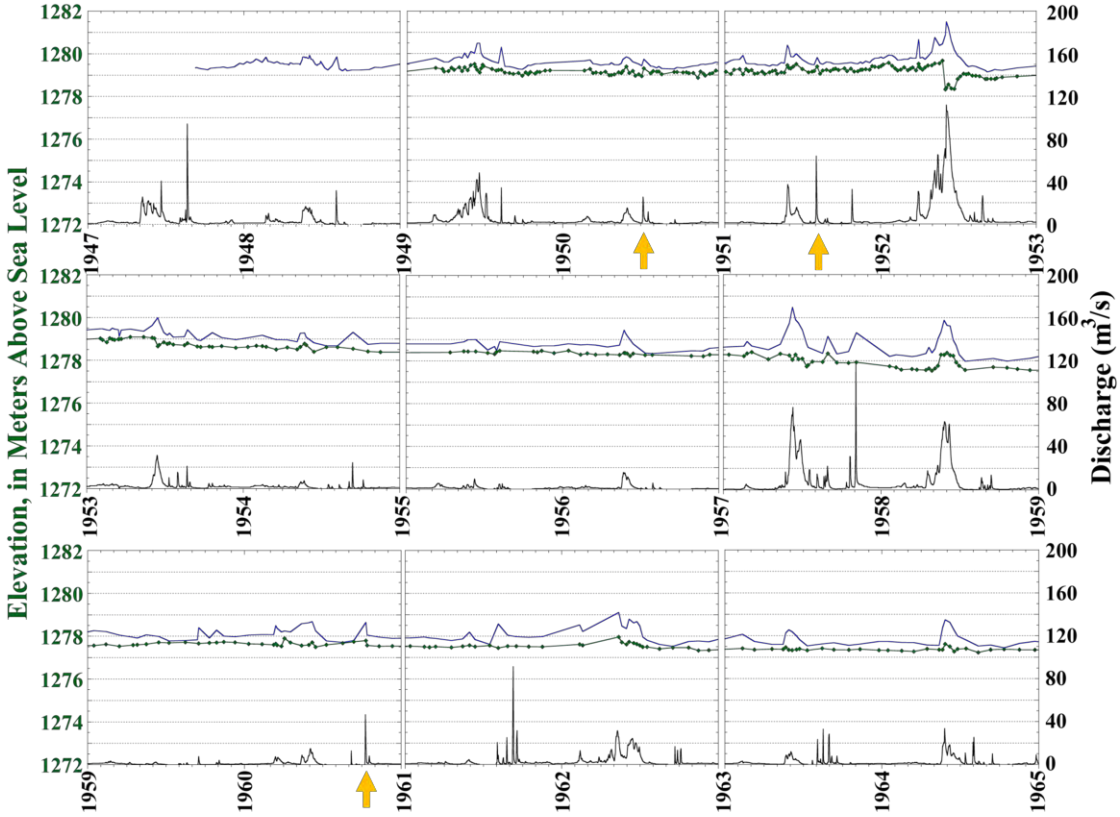

Figure 3.34. Time series of thalweg elevation, water surface elevation and discharge measured at abandoned cableway from 1947 to 1965. The green data series is the thalweg elevation, the blue data series is the water surface elevation, and the black data series is the mean daily discharge. Orange arrows indicate flash floods where bed elevation changes could be determined because of the availability of discharge measurements.

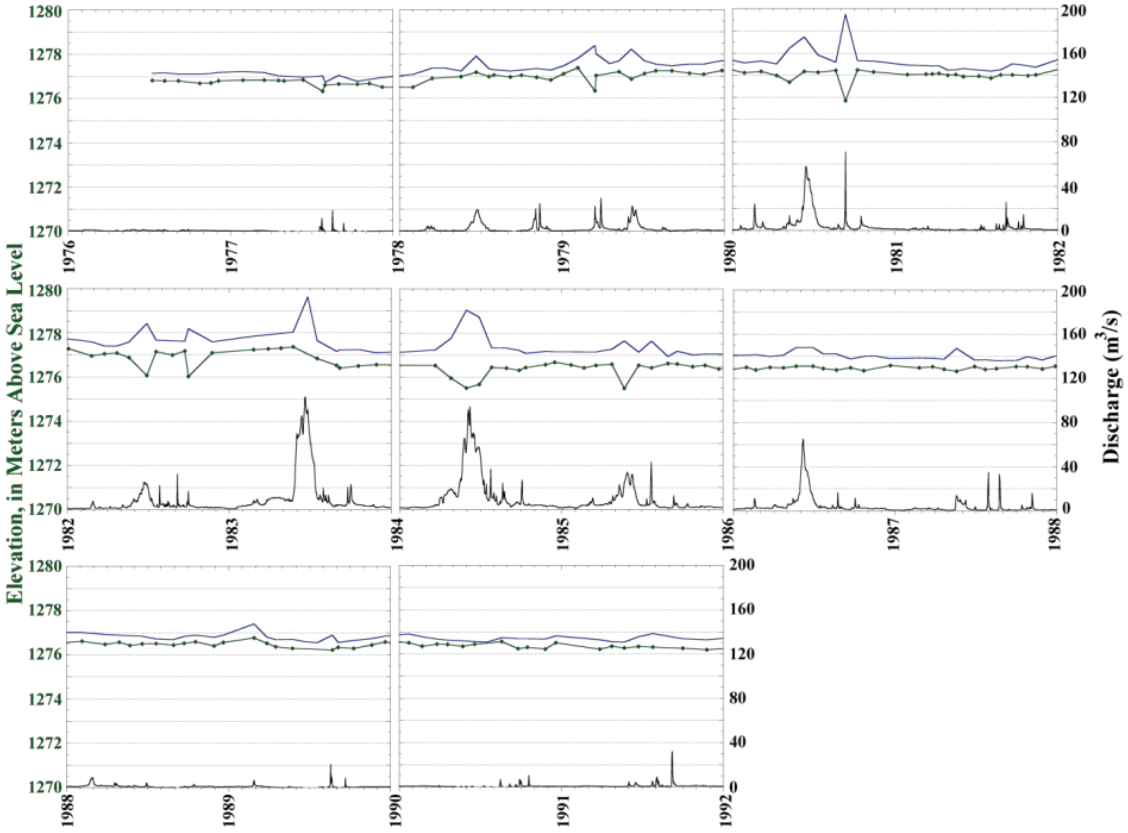

Figure 3.35. Time series of thalweg elevation, water surface elevation and discharge measured from 1976 to 1992. Green data series is the thalweg elevation, the blue data series is the water surface elevation, and the black data series is mean daily discharge.

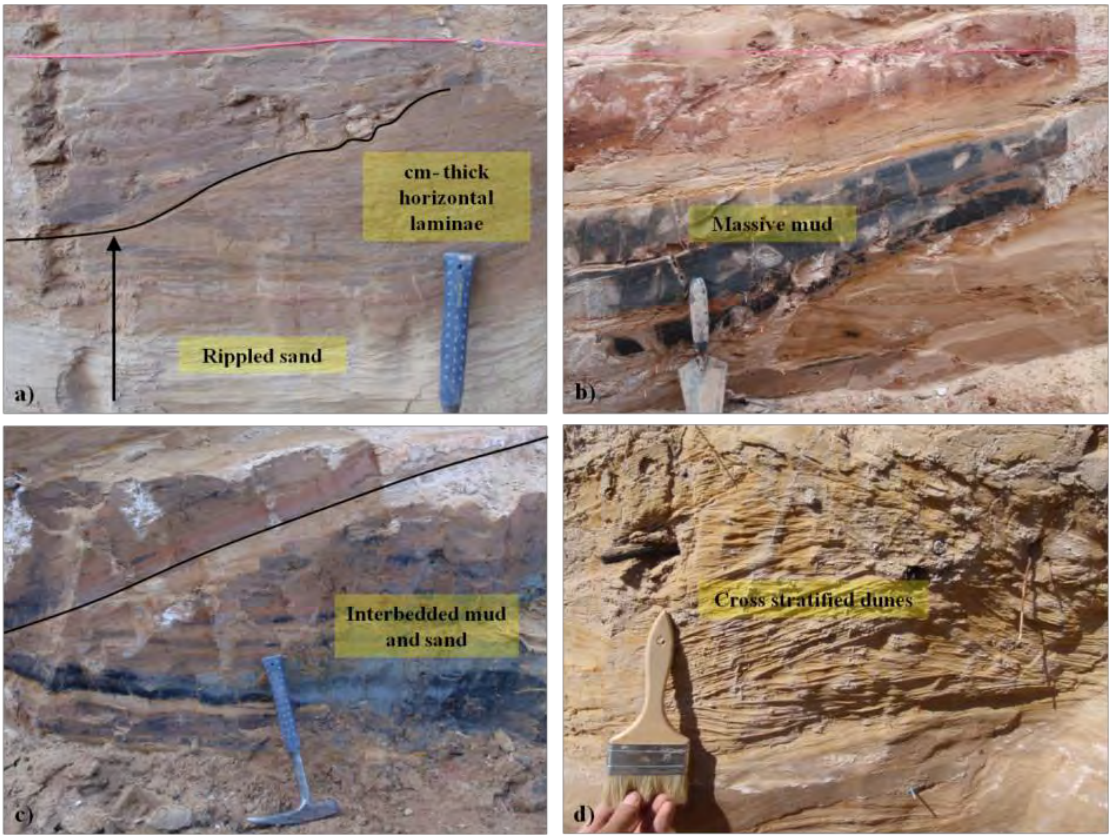

Figure 3.36. Sedimentology of sand bars exposed in Hatt's Ranch trench. Images show the diversity of the sedimentology of sandbars. Sand bars may be comprised of a fining upward sequence of rippled sand and horizontal mud laminae (image "a"), massive mud interbedded with sand (images "a", "b", and "c"), discernible and indiscernible contacts (all images), or dune cross stratified sand with pebbles (image "d"). Note the erosional contact between two sand bar packages in images "a" and "c".

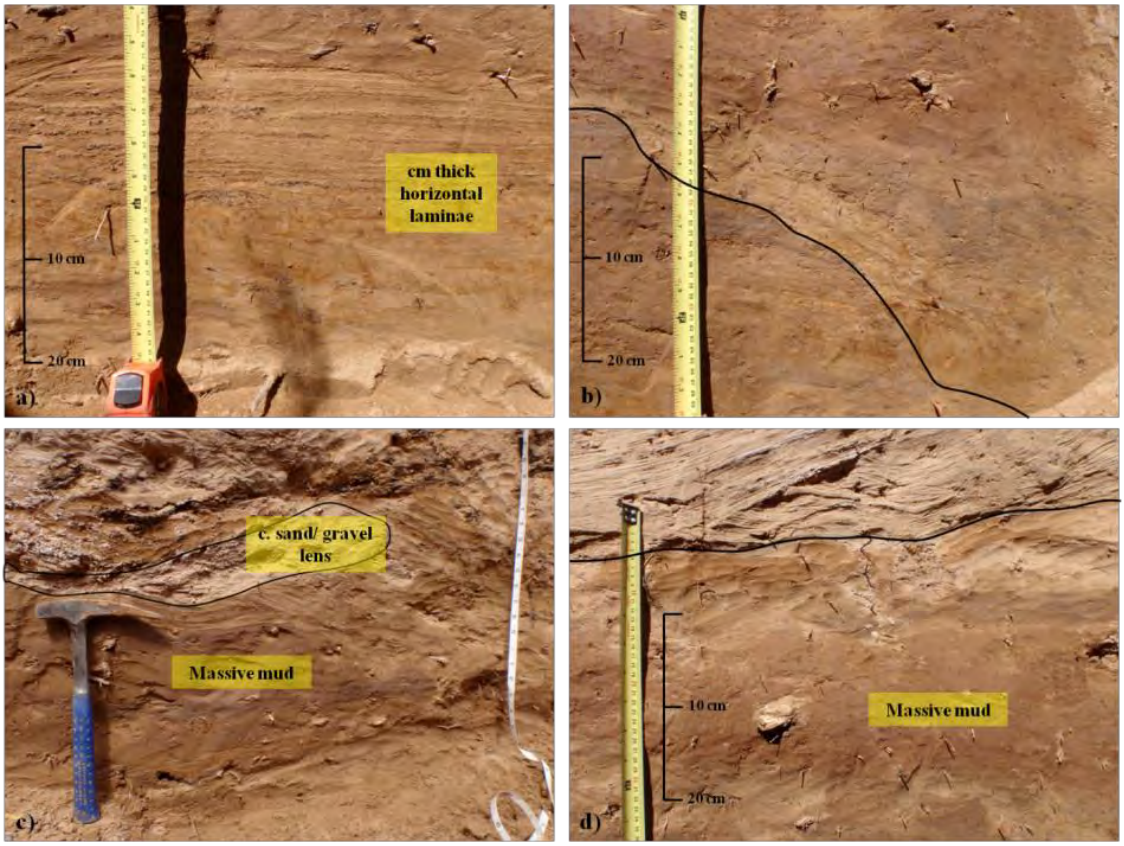

Figure 3.37. Sedimentology of sand bars exposed in right bank trench at Frenchmans's Ranch. Images show the diversity of the sedimentology of sandbars. Sand bars may be comprised of horizontal laminae (image "a"), inclined laminae and massive mud (image "b"), discernible and indiscernible contacts (all images), massive muds (all images), and lenses of coarse sand and gravel (image "c"). Note the erosional contact between two sand bar packages in image "b". In image "d", cross stratified sand overlies the sand bar deposit.

Figure 3.38. Sedimentology of near channel bench exposed in left bank trench at Frenchmans's Ranch trench. The channel is off the right side of the photo.

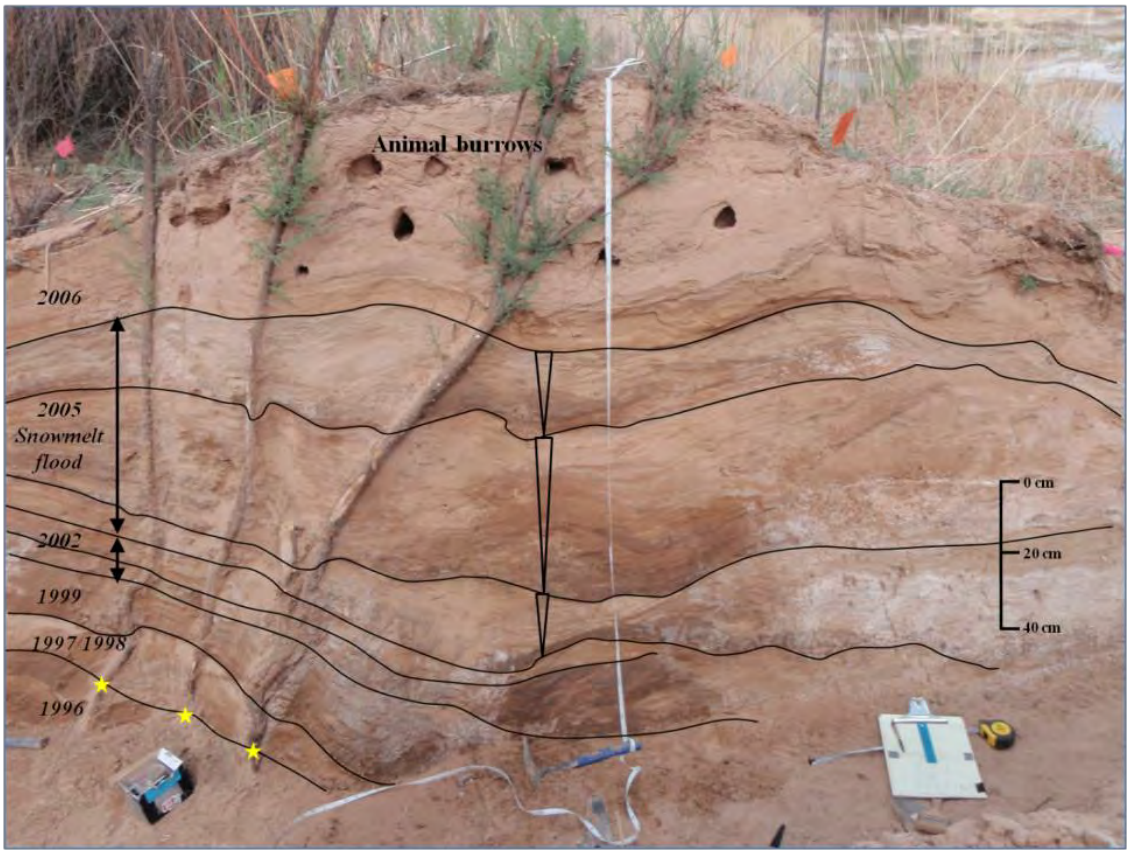

Figure 3.39. Architecture of near channel levee exposed in right bank trench at Frenchmans's Ranch. According to dendrochronologic results, the 2005 snowmelt flood deposited much of the levee as three coarsening upward sequences (identified by vertical triangles in middle of photo). Each coarsening upward sequence correlates to the deposition of sediment during each of the three peaks of the flood. A coarsening upward sequence indicates that fine sediment is in sediment deficit during the falling limb of each flood peak.

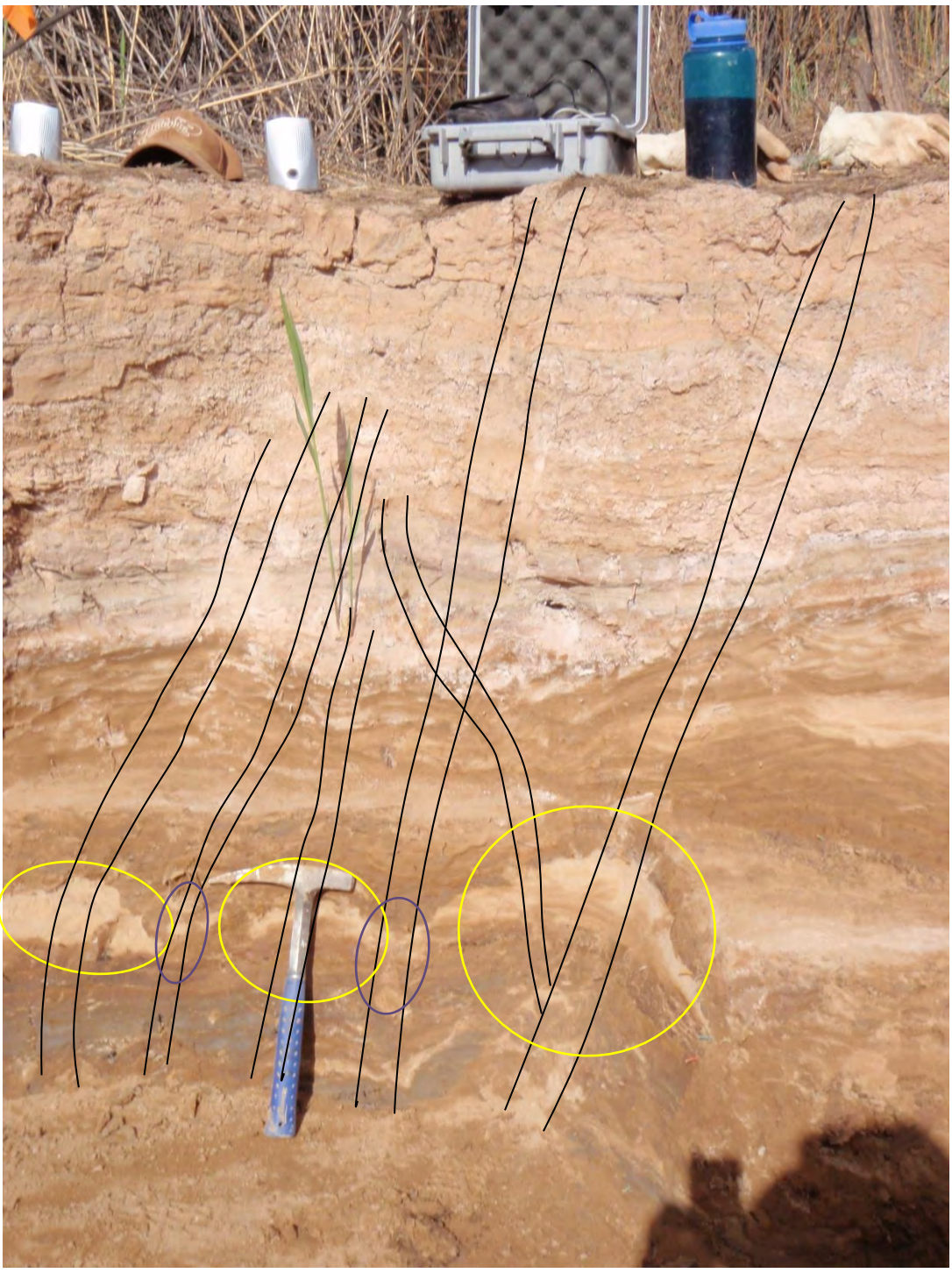

Figure 3.40. Upturned and downturned beds. Upturned beds are shown by yellow ovals and downturned beds are shown by purple ovals.

3.9 Appendix C: Historic Oblique Ground Photos

Figure 3.41. Historic photograph taken some time between 1909 and 1914. Photograph was taken approximately 20 m below cableway that was located approximately 60 m upstream from the old Highway 24 bridge. Photo was taken on right bank looking upstream. This cableway washed out in the floods of 1914. Note the person riding the cable car and the person wading in the river below the cable car. Cottonwoods line the left bank and herbaceous vegetation occupies the sandy surface on river right. An upper geomorphic surface is barely noticeable in the right portion of the photograph. The left bank appears to be eroded in the furthest upstream portion of the photograph. The original photograph is included with the station analysis reports housed at the US Geological Survey national archives.

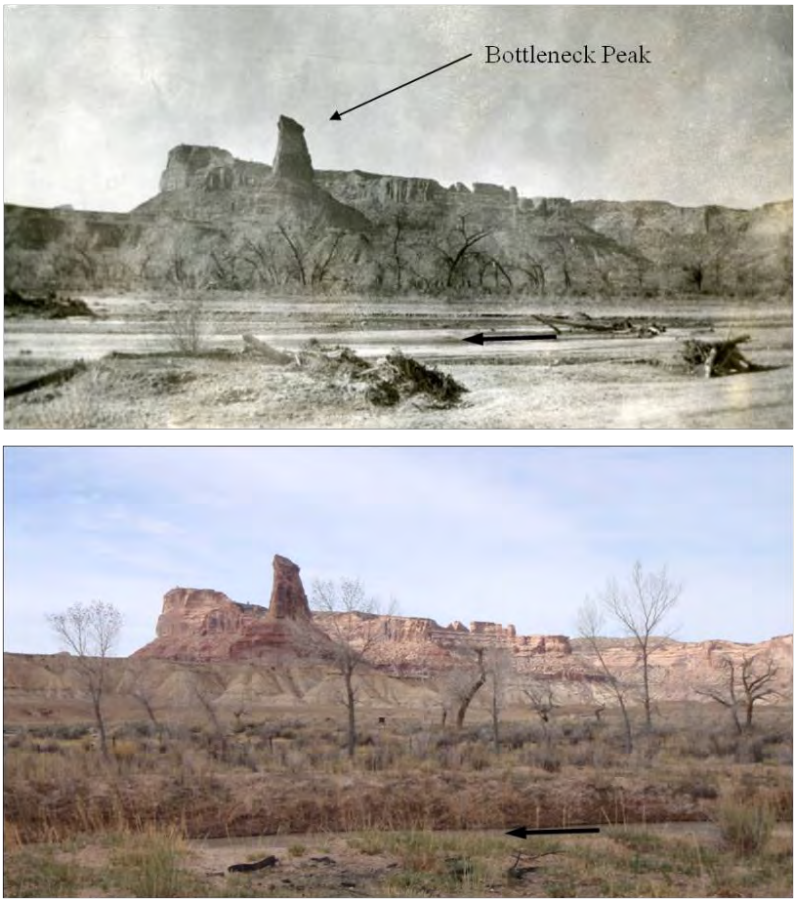

Figure 3.42. Photograph comparison of the San Rafael River in the Swell. Location is approximately 500 m downstream from old swinging bridge at BLM campground. Photographs were taken standing on left bank, looking south across the river. Historic photograph was likely taken in the 1930s, however precise date is unknown (courtesy of Utah State Historical Society, Salt Lake City, digitized online at Southern Utah University Sheratt Library Photograph Collection). The matched photograph was taken on April 20, 2011. Woody debris jams and gently sloping banks are evident in the historic photograph. A grove of cottonwoods that line the right bank in the historic photograph is mostly absent in the present-day photograph. Instead in the present-day photograph, a narrow stand of young cottonwoods, closer to the camera position, line the floodplain at the level inundated by common floods. Inset floodplain deposition has occurred during the time between the dates of the two photographs. The present day photograph was taken after the removal of a grove of tamarisk that once occupied the floodplain surface between the channel and the shrub covered terrace located in the background.

Figure 3.43. Photograph comparison at the old Highway 24 bridge on the Hatt's Ranch, looking upstream. Historic photo was taken sometime between 1910 and 1938 (precise date is unknown). Recent photo, taken on April 19, 2011, shows a newer steel and wooden bridge located in front of the piers of the original highway 24 crossing. The channel in the 2010 photograph is obscured by vegetation including phragmites (*Phragmites australis*), grasses, and tamarisk The present day river channel is not noticeable, because it is has narrowed and incised, and is obscured by the vegetated inset floodplain surfaces in the foreground.

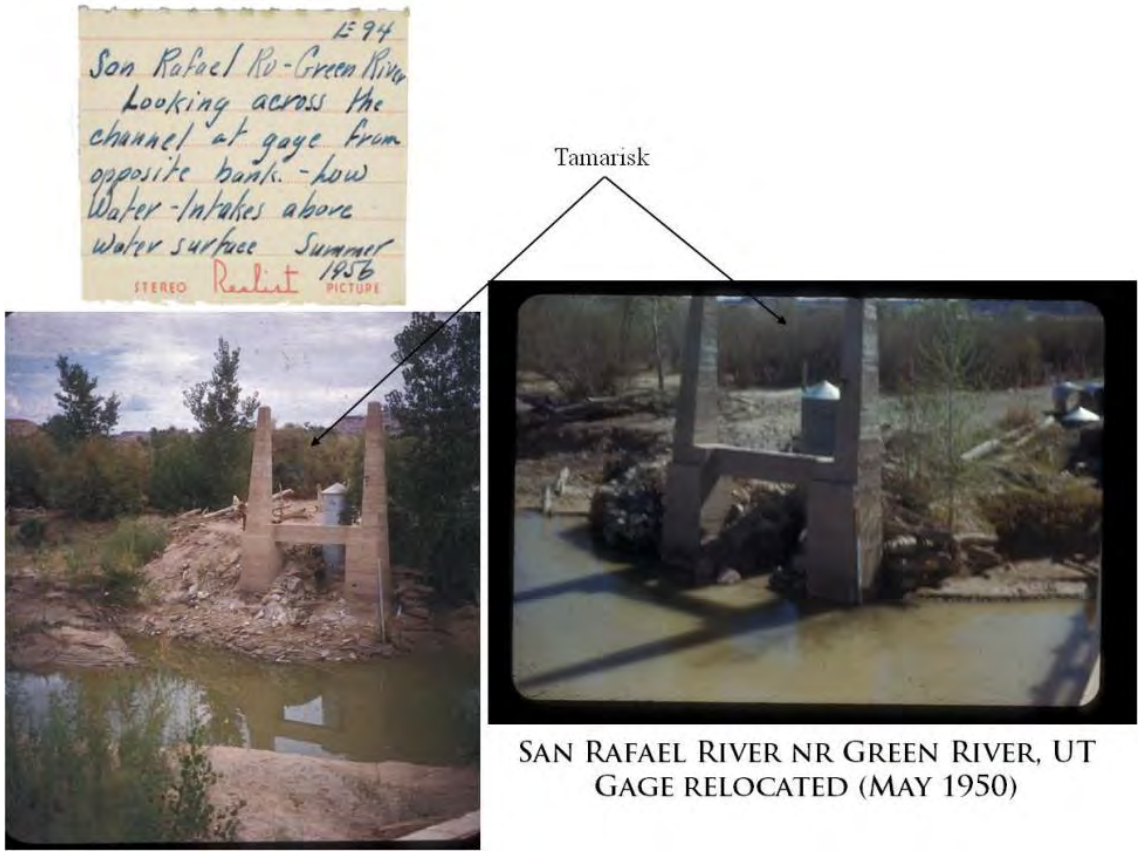

Figure 3.44. Historic photographs taken at USGS gage 09328500. Both photos were taken standing on the right bank. The photo on left was taken in the summer of 1956; the photo on right was taken in May 1950 before seasonal foliage growth. In each photograph, dense stands of tamarisk cover the floodplain surface in the background. Although discharge is not known for either photograph, elevation of the channel bed appears lower in the left photograph. Both photos were scanned from the US Geologic Survey Salt Lake City office library of historic photographs.

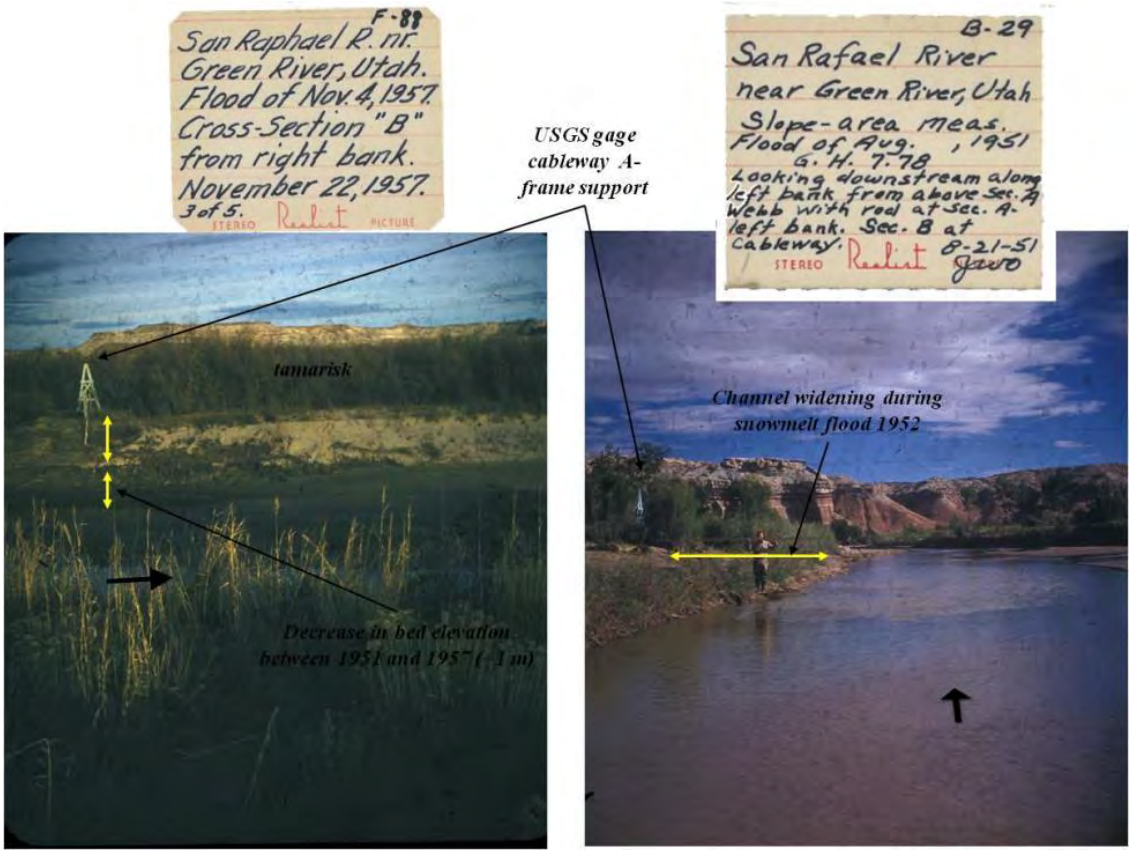

Figure 3.45. Two historic photographs taken at adjacent discharge measurement cross sections at USGS gage 09328500. In the left photo, a dense stand of tamarisk covers the surface on which the cableway A frame support stands. During the time when the two photographs were taken, the river incised approximately 1 m (bottom yellow arrow in left photo) and the river widened (yellow arrow in right photo). Channel widening likely occurred during the 1952 snowmelt flood. Both photos were scanned from the US Geologic Survey Salt Lake City Office library of historic photographs.

Figure 3.46. Oblique aerial photograph of valley segment one, looking downstream. Photograph was taken in August 2010. Tamarisk, which appears brown because of defoliation by the Asian leef beetle (*Diorhabda Elongata*), has colonized much of the entirety of the alluvial valley in this valley segment. Where the alluvial valley bends toward the east, is where I-70 crosses the river.

Figure 3.47. Oblique aerial photograph of valley segment three, looking upstream. Photograph was taken in August 2010. Cottonwood Creek enters the valley just downstream of the photograph. In the photograph, the riparian zone is comprised of a mix of tamarisk and cottonwoods. The defoliated tamarisk shrubs, identified in the photograph as brown/gray, have not colonized the entire width of the valley as they have done in valley segments one and two (Figure 3.46). In the foreground along the left lower corner of the photograph, wind blown sand deposits cover a portion of the alluvial valley where cottonwoods are growing. The San Rafael Swell and San Rafael Reef are seen in the background.

3.10 Appendix D: Additional Figures and Photos Not Discussed in Body of Thesis Chapter 3

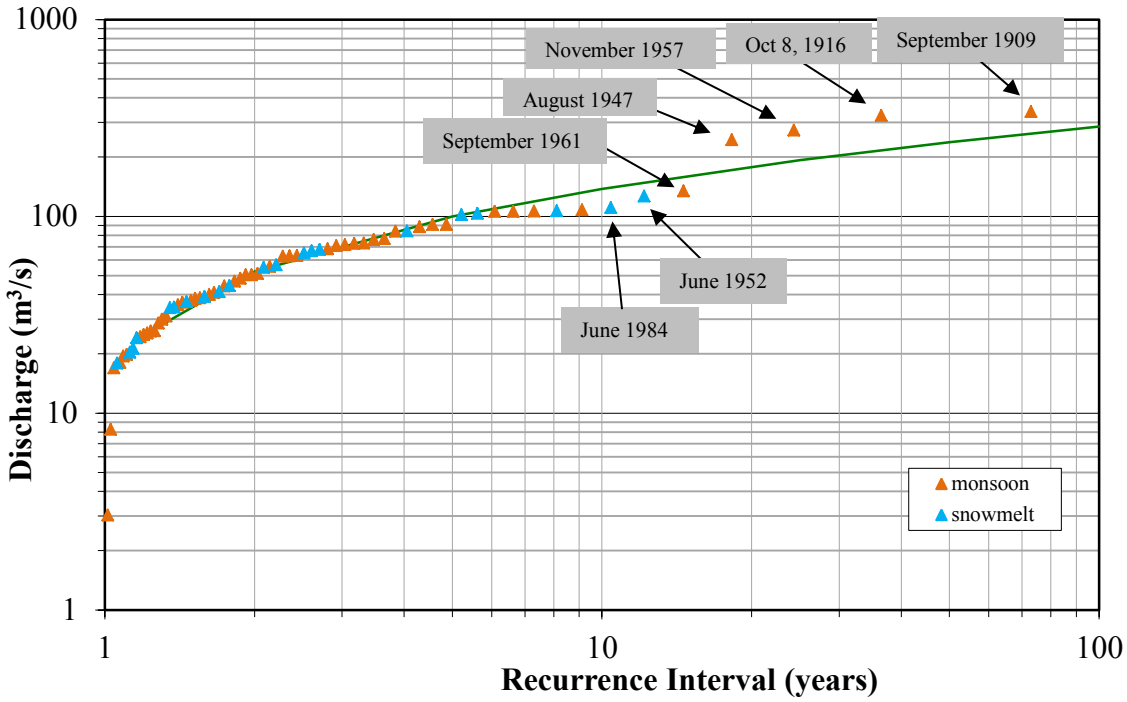

Figure 3.48. Flood frequency at USGS gage 09328500. We calculated the flood frequency shown here using the instantaneous peak annual flood series. Monsoon floods are those that occur between July 1 and December 31. Snowmelt floods occur in April, May, and June.

CHAPTER 4

CONCLUSION

The sediment mass balance of a river is determined by the relationship between sediment supply and transport capacity. Perturbations in the sediment mass balance of a river often result in channel changes. For example, when the capacity of a river to transport the amount of supplied sediment is decreased, a condition of sediment surplus can occur. A positive net change in sediment storage may be manifested as a decrease in channel width, floodplain aggradation, or bed aggradation. On the other hand, when transport capacity exceeds sediment supply, the condition of sediment deficit prevails and incurring channel changes may include bed incision, increase in channel width, or bed armoring.

Depending on the capacity for a particular river reach to adjust, the channel changes that occur as a result of perturbations in the sediment mass balance of suspended load rivers can be very large. These changes may be exacerbated by additional perturbations including invasion of exotic riparian vegetation, land use in the alluvial valley, or direct human modification of the channel-floodplain system. On the Colorado Plateau where the availability of fine sediment is abundant, most rivers during the last 70 years have experienced a reduction in stream flow and have been invaded by tamarisk. This combination has caused a reduction in the width in many of the alluvial rivers of the Colorado Plateau. Of the five rivers that drain the high plateaus of Utah and flow into either the Green River or the Colorado River (Paria, Escalante, Dirty Devil, San Rafael,

Price), the San Rafael River has probably experienced the most significant reduction in stream flow as well as the most significant decrease in channel width. It should be noted that little information is currently available about the geomorphology of the Price River, but future studies may yield similar findings to that of the San Rafael River since it appears to be in a similar condition to the San Rafael River.

During the 20th century, water development in the headwaters has reduced both the magnitude and duration of the annual snowmelt flood in the San Rafael River, by 67% and 93%, respectively. Moreover, water development has had less impact on the annual, short duration floods that occur during the summer and fall seasons. Consequently, these short duration floods continue to deliver large amounts of fine sediment to the San Rafael River. Because of a large reduction in stream flow during the 20th century, yet continued supply of fine sediment, the San Rafael River has become transport limited and thus has been perturbed into sediment surplus. As a result, the width of the channel has decreased significantly. Between 1953 and 2009, the lower 87 km of the San Rafael River narrowed by 82%.

A concatenation of events can explain the process of inset floodplain formation, which is the mechanism of channel narrowing in the San Rafael River. We have shown in Chapter 3 that low to moderate floods, often following a channel-widening flood, deposit sediment on top of active channel surfaces, which are stabilized by vegetation e.g., young tamarisk shrubs. We have observed in some places that tamarisk has actually actively promoted sedimentation. In this manner, inset floodplains have rapidly accreted both vertically and obliquely, thereby diminishing the capacity of the San Rafael River.

Despite the reduction in channel capacity, small to moderate magnitude floods continue to overtop the river's banks and deposit layers of fine sediment on the adjacent floodplains. This observation is similar to what Dean and Schmidt (2011) found in the Rio Grande River in Big Bend National Park. The rapid vertical and oblique accretion of the floodplain including the sedimentation of secondary channels, as well as reach-scale bed elevation changes, have combined to transform the San Rafael River from a wide, laterally-shifting channel to a narrow and deep river resembling an 'irrigation ditch'.

20th century channel changes in the San Rafael River have caused a reduction in both the quality and the quantity of fish habitat. In the early 20th century, reorganization of fish habitat occurred frequently. For example, when cottonwood-lined channel banks eroded, wood fell into the channel and added complexity to aquatic habitat. Furthermore, the river frequently shifted and abandoned old channels and carved new channels. The historic river was comprised of multiple threads, which in combination with a low width-to-depth ratio provided a connection between the active channel and the floodplain. In contrast today, the narrow, single-threaded channel is confined by tall banks that are stabilized by tamarisk, and cottonwoods are less prevalent. Meander migration rates have decreased as well. Compared to historic conditions, the current condition offers less off-channel habitat, less in-stream complexity, and the floodplain is much less connected to the active channel. Despite the stark transformation of the river, three endemic species - the roundtail chub (Gila robusta robusta), bluehead sucker (Catostomus discobolus), and flannelmouth sucker (Catostomus Latipinnis - whose distribution have declined by more than 50% (UDWR, 2006), are still present in the lower San Rafael River. Consequently,

there is an opportunity to intervene and protect, conserve, and manage the San Rafael River for the benefit of the "three species". The management of the river should be guided by an understanding of the geomorphology of the river, which is presented in Chapter 2 and Three, as well as an understanding of the ecology of the river (Bottcher, 2009; Walsworth 2011).

Prior to developing a management plan, goals must be clearly defined. Because of the high demand for the water in the San Rafael River, there exists great potential for there to be a conflict in interests for how to manage the river. For example, a particular management objective will likely benefit one stakeholder but not another. Therefore, objectives will need to be prioritized in ways that considers the interests of all of the stakeholders including agricultural, municipal, and industrial water users; recreationists; and conservationists. Prioritization of objectives of a management plan can be accomplished by utilizing a decision support system (Pieterse et al., 2002; Mysiak, et al., 2005; Kiker, et al., 2005; Matthies et al., 2007; Steel et al., 2008)

Whether or not a decision support system is used, the tradeoffs of each management objective will need to be considered. According to www.google.com, the definition of a tradeoff is the "balance between two desirable but incompatible features; a compromise." For example, a particular management objective may benefit either ecosystem properties, or human needs and desires; conversely, the objective may negatively impact ecosystem properties, or increase pressures on water users or the landscape (Schmidt et al., 1998). Additional things that will need to be considered in a management plan include the feasibility, time, and cost of implementing a plan.

Tradeoffs associated with actions that could be implemented to improve fish habitat are listed in Table 4.1.

Management actions can be categorized into one of four pathways of management (Schmidt et al., 1998). Figure 4.1 illustrates these pathways. The first pathway is no action. Given the evolutionary trajectory of channel changes in the San Rafael River, which has been driven by the reduction in stream flow during the last 80 years as well as the transformation of the native riparian vegetation community to one dominated by the exotic tamarisk shrub, this choice may not be desirable to the future of the "three species". The second pathway, which requires more effort than the 'no action' pathway, is the mitigation of future undesired consequences. In the San Rafael River, possible mitigation measures may include the prevention of further water and resource development or the prevention of the spread of tamarisk into portions of the alluvial valley where it has not yet colonized. Rehabilitation, which is the third option, requires more intervention than mitigation, and is the re-establishment of some attributes of the pre-disturbance condition of the river. The implementation of this management action may require a significant amount of time, effort, and resources, and thus weighing the tradeoffs of the possible rehabilitation action(s) deserves considerable attention. The fourth action is one of complete recovery and restoration of the river to the pre-disturbance condition. For reasons mentioned below, the return of the San Rafael River to the "predisturbance" condition may not be feasible.

There are several reasons why complete restoration and recovery of the San Rafael River is not an option. First, current climate conditions may differ from

"predisturbance" conditions. The earliest data sets that we analyzed in this study - including the USGS gage data from 1909-1918, the 1925 topographic survey, and the 1938 aerial photographs - were collected during a time when precipitation and stream flow may have resembled previous wet periods in the Holocene (Webb et al., 1991; Hereford and Webb, 1992). Therefore, these data sets portray river behavior and character during not only predisturbance times but also elevated precipitation and stream flow regimes. During the 20th century a drier climate developed, as shown by a decrease in the magnitude and the frequency of monsoon floods (see Chapter 3). Our findings support the hypothesis that drier conditions have developed during the 20th century on the Colorado Plateau. Research indicates that dry climatic conditions may continue in the 21st century (Christensen and Lettenmaier, 2007; Seager et al., 2007; Barnett and Pierce, 2009) and perhaps even longer. Furthermore, if the hypothesis that Holocene climate cycles are partly responsible for the decadal to millennial time scale sediment dynamics in Colorado Plateau alluvial valleys (Martin, 1963; Hall, 1977; Love, 1977; Hereford, 2002), then valley alluviation in the San Rafael during the 20th century may have occurred even without the impact of anthropogenic and biological perturbations. Second, the superimposition of human impacts and tamarisk invasion on the climate template may further complicate the possibility of returning the river to a "predisturbance" condition. Third, complete tamarisk eradication has proven to be challenging throughout the American southwest where invasion is widespread (Briggs et al., 1994; Shafroth et al., 2008), therefore restoration of the San Rafael River's riparian community to its predisturbance composition may not be possible. Finally, the dependency on the San

Rafael River for municipal, industrial, and agricultural purposes is strong, and to disrupt this dependency would take a great amount of effort and financial resources.

Since complete restoration of the San Rafael River may not be feasible or even desired, then rehabilitation is the next most efficacious pathway of action. Successful rehabilitation of the San Rafael River requires knowledge of the processes that are responsible for the geomorphology of the river. The environmental history described in Chapter 3 describes the rates, magnitudes, and styles of the channel changes that occurred during the 20th century, and therefore provides insight into the processes that currently govern channel form, and how these process-form relationships have changed over time. This knowledge can then be used to predict the future trajectory of channel behavior.

There are at least five actions that could be considered in a plan to rehabilitate the San Rafael River. These actions are described inTable 4.2. They include environmental flow management, beaver restoration, fish passage improvement, channel and floodplain engineering design, and vegetation restoration. Of these potential management options, environmental flow management has possibly the greatest potential for improving fish habitat, however, these actions may be the most challenging to implement. The San Rafael River is one of the most over allocated rivers in Utah (Walker and Hudson, 2004), and reallocating water rights will require considerable effort and resources.

Environmental flow management requires the knowledge of the biophysical relationships among riparian vegetation, stream flow, and geomorphic processes that are governing river behavior and the distribution of aquatic habitat. In Chapter 3 we have shown that different flood types in the San Rafael River have different transport relations.

In general, snowmelt floods transport lower concentrations of suspended sediment than short duration floods, and can be effective in eroding both the banks and the bed. However, snowmelt floods can also contribute to the construction of floodplains. Knowledge of the characteristics of past snowmelt floods and their influence on channel morphology (see Chapter 2) should inform decisions about stream flow management. Questions to be considered include what years should snowmelt floods be restored? What should be the characteristics of the managed flows e.g., the frequency, timing, rate of increase, duration, and magnitude?

Rather than just choosing one action, implementing a combination of rehabilitation actions may result in more success in improving aquatic habitat; although, the orchestration of multiple actions will need to be well planned. For example, the synchronization of environmental flows with vegetation treatments will increase the likelihood of success in improving aquatic habitat by increasing the probability of bank erosion in areas where tamarisk has been removed. Also, knowledge of the timing of seed dispersal of particular riparian species will improve the effectiveness of vegetation management. For example, cottonwoods and willows have a much shorter seed dispersal window than tamarisk, thus managed environmental flows should be timed to take advantage of the short cottonwood seed dispersal window (Tomanek and Ziegler, 1962; Warren and Turner, 1975; Everitt, 1980).

A management plan will need to consider the spatial extent and location of proposed rehabilitation actions. For example, targeted beaver rehabilitation actions may be best suited in places or types of places where beaver dams have been observed in the

study area. A few of the eight beaver dams that were observed in the study area between 2009 and 2011 were built a short distance upstream of tributary confluences. It is likely that beavers built dams in the vicinity of a tributary confluence to take advantage of the existing hydraulic control there. Furthermore, tributary confluences may be suitable places for channel engineering projects. Also, reaches where the river bed is on bedrock may be suitable places for engineering projects.

Tradeoffs will need to be evaluated when considering the spatial extent of rehabilitation actions. For example, removal of the Hatt's Ranch diversion dam will allow endemic fish species to move more freely between the lower river and the upper river, but it will also allow non-native fish species to colonize upstream areas. Currently, the fish community in the San Rafael Swell is primarily comprised of native fishes, therefore, an increase in the non-native fish population in the upper portions of the river would alter the food web structure and increase predation and competition of the "three species" (Walsworth, 2011).

Finally, a successful management plan should include an adaptive management component. Treating management actions as an experiment can be one of the most valuable things gained from a river management plan (Shafroth et al., 2008). The lessons learned from the success and failures of particular actions should inform and improve future management decisions. In particular, when the impacts of particular actions on biophysical relationships and processes can be determined, then this knowledge can be transferred to similar places that are impacted by similar perturbations.

4.1 References Cited

Barnett, T.P., Pierce, D.W., 2009. Sustainable water deliveries from the Colorado River in a changing climate, Proceedings of the National Academy of Sciences 106 (18), 7334-7338.

Bottcher, J.L., 2009. Maintaining population persistence in the face of an extremely altered hydrograph: Implications for three sensitive fishes in a tributary of the Green River, Utah. (M.S. Thesis), Utah State University, Logan, UT (61 pp.).

Briggs, M.K., Roundy, B.A. Shaw, W.W., 1994. Trial and error: assessing the effectiveness of riparian revegetation in Arizona. Restoration & Management Notes, 12: 160 167.

Christensen N.S., Lettenmaier D.P., 2007. A multimodel ensemble approach to assessment of climate change impacts on the hydrology and water resources of the Colorado River Basin, Hydrology and Earth Systems Sci. 11, 1417-1434.

Dean, D.J., Schmidt, J.C., 2011. The role of feedback mechanisms in historic channel changes of the lower Rio Grande in the Big Bend region, Geomorphology 126 (3-4), 333-349.

Everitt, B.L., 1980. Ecology of saltcedar: a plea for research. Environmental Geology 3, 77-84.

Hall, S.A., 1977, Late Quaternary sedimentation and paleoecologic history of Chaco Canyon, New Mexico: Geol. Soc. Amer. Bull. 88, p. 1593-1618.

Hereford, R., 2002. Valley-fill alluviation during the Little Ice Age (Ca A.D. 1400-1880), Paria River basin and southern Colorado Plateau, United States. Geol. Soc. Amer. Bull. 114, 1550-1563.

Hereford, R., Webb, R.H., 1992, Historic variation of warm-season rainfall, southern Colorado Plateau, Southwestern U.S.A.: Climate Change, 22, p. 239-256.

Kiker, G.A., Bridges, T.S., Varghese, A., Seager, T.P., Linkov, I., 2005. Application of Multicriteria Decision Analysis in Environmental Decision Making, Integrated Environmental Assessment and Management 1 (2), 95-108.

Love, D.W., 1977, Dynamics of sedimentation and geomorphic history of Chaco Canyon National Monument, New Mexico. Socorro, New Mexico Geological Society Guidebook, 28th Field Conference, San Juan Basin III, pp. 291-300.

Martin, P.S., 1963, The Last 10,000 yr, a Fossil Pollen Record of the American Southwest. University of Arizona Press, Tucson, AZ (87 pp.).

Matthies, M, Giupponi, C., Ostendork, B., 2007. Environmental decision support systems: current issues, methods and tools, Environmental Modelling & Software 22 (2), 123-127.

Mysiak, J., Giupponi, C., Rosato, P., 2005. Towards the development of a decision support system for water resource management. Environmental Modelling and Software 20 (2), 203-214.

Pieterse, N.M., Verkroost, A.W.M., Wassen, M., Venterink, H.L., Kwakernaak, C., 2002. A decision support system for restoration planning of stream valley ecosystems, Landscape Ecology 17 (1), 69-81.

Schmidt J.C., Webb, R.H., Valdez, R.A., Marzolf, R., Stevens, L.E., 1998. Science and values in river restoration in the Grand Canyon. BioScience 48 (9), 735-747.

Seager, R., Ting, Mingfang, T., Held, I., Kushnir, Y., Lu, J., Vecchi, G., Huang, H.P., Harnik, N., Leetmaa, A., Lau, N.C., Li, C., Velez, J.,Naik, N., 2007. Model projections of an imminent transition to a more arid climate in southwestern North America, Science 316, 1181-1184.

Shafroth, P.B., Beauchamp, B.B., Briggs, M.K., Lair, K., Scott, M.L., Sher, A.A., 2008. planning riparian restoration in the context of Tamarix control in western North America, Restoration Ecology 16 (1), 97-112.

Steel, E., Ashley, A. Fullerton, Y. Caras, M. B. Sheer, P. Olson, D. Jensen, J. Burke, M., Maher. M., McElhany, P., 2008. A spatially explicit decision support system for watershed-scale management of salmon, Ecology and Society 13(2): 50. http://www.ecologyandsociety.org/vol13/iss2/art50/

Tomanek, G.W., and Ziegler, R.L., 1962. Ecological studies of salt cedar. Unpublished report. Division of biological Sciences. Kansas State College, Manhattan, KS (128 pp.).

UDWR, 2006. Conservation and management plan for three fish Species in Utah. Publication number 06-17. (82 pp.).

Walker, C.A., Hudson, M., 2004. Surveys to determine the current distribution of the roundtail chub, flannelmouth sucker, and bluehead sucker in the San Rafael drainage, during 2003. (Unpublished report). Utah Division of Wildlife Resources, Salt Lake City, Utah (10 pp.).

Walsworth, T.E., 2011. Analysis of food web effects of non-native fishes and evaluation of stream restoration potential for the San Rafael River, Utah. All Graduate Theses and Dissertations Paper 1095. http://digitalcommons.usu.edu/etd/1095.

Warren, D.K., Turner, R.M., 1975. Saltcedar (Tamarix chinensis) seed production, seedling establishment, and response to inundation. J. Arizona Academy of Science 10, 135-144.

Webb, R.H., Smith, S.S., McCord, V.A.S., 1991. Historic channel change of Kanab Creek, southern Utah and northern Arizona: Grand Canyon Natural History Association Monograph, Number 9, (91 pp.).

Table 4.1. Tradeoffs of particular management actions.

Action		Spatial Extent	Time to Implement	Advantages	Disadvantages
1	Environmental flow management	watershed	1 - 100 yrs	• Restores desirable channel processes • Potential for long term success: increase channel width, reconnection to the floodplain.	• Expensive • Seen as undesirable by various stakeholders
2	Beaver restoration	reach, valley segment	1 - 10 yrs	• Upstream of a beaver dam: local aggradation of the bed, local increase in groundwater level • Reconnection to abandoned geomorphic surfaces • Cheap • Downstream of a beaver dam: increase in channel slope and thus increase in pool-riffle habitat heterogeneity.	• If a beaver dam is abandoned or washed away, then there is potential for down-cutting to occur in the recently aggraded area upstream of a dam, which may perpetuate the disconnection of the channel and floodplain.
3	Fish passage improvement	reach, valley segment, watershed	1 - 5 yrs	• Restore access to upstream habitat	• Increases predation and competition from non-native fish
4	Channel design	reach, valley segment	1 - 10 yrs	• short term success i.e., immediate improvement to fish habitat	• Expensive • High potential for failure over long time scales
5	Vegetation restoration	reach, valley segment	1 - 50 yrs	• Reduce bank resistance • The biological control options e.g., tamarisk beetle, are relatively inexpensive	• Both chemical and mechanical treatments options are expensive • chemical treatments degrade the quality of ground and surface water • There are possible negative effects on wildlife species that now utilize the habitat offered by tamarisk stands e.g., southwestern willow flycatcher • Unknown outcomes

Table 4.2. List of management actions.

1	**Environmental flow management**
	• Restoration of a portion of the snowmelt flood, e.g., the magnitude, duration, timing, frequency, and/or rate of change of the flood.
	• Opportunistic restoration of the snowmelt flood i.e., restore some or all of the snowmelt flood, only in years when sufficient water is available in order to reduce the impact on the upstream water users. Or, time the restoration of the snowmelt flood to coincide with complementary rehabilitation actions.
	• Restoration of the complete snowmelt flood, either in some years e.g., years with high annual runoff, or every year.
2	**Beaver restoration:** assist in the construction of beaver dams by installing posts across the width of the channel. Possible location of beaver dam support structures include:
	• At or close to existing beaver dams.
	• At or close to former beaver dams.
	• At hydraulic controls other than beaver dams e.g., tributary confluences
3	**Fish passage improvements:** remove Hatt's Ranch diversion dam
4	**Channel/floodplain design:** reconfigure the channel and/or floodplain. Channel design options are feasible at the reach-scale.
	• Widen the channel.
	• Destabilize channel banks.
	• Excavate abandoned or new secondary channels.
	• Install bed control structures e.g., rock weirs.
	• Remove man-made levees.
	• Gravel augmentation.
5	**Vegetation restoration:** remove non-native tamarisk and restore native cottonwood/willow/grass communities. There are several types of tamarisk treatment:
	• Biological control i.e., facilitate the spread of the Mediterranean tamarisk beetle (*Diorhabda Elongata*), an imported insect that has been proven to defoliate and cause mortality in tamarisk shrubs.
	• Mechanical removal i.e., use of heavy equipment to rip plants from the ground.
	• Chemical treatment i.e., herbicide application.
	The spatial scale of a vegetation treatment vary according to feasibility and desirability and include:
	• Entire length of the river.
	• Selected reaches.
	• Floodplain or in-channel geomorphic unit e.g., channel-proximal floodplain surface, in-channel surface.

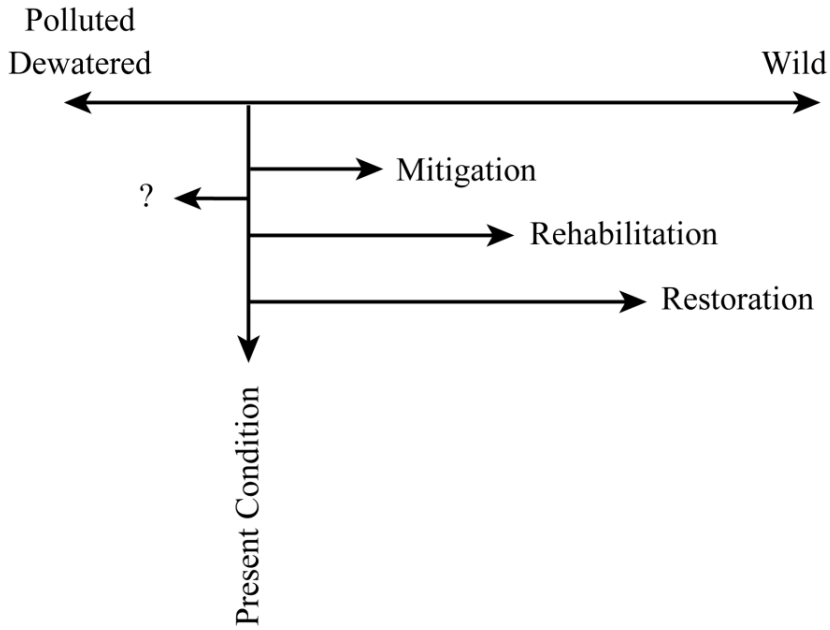

Figure 4.1. Conceptual model of the possible management actions that could be applied to a river that has been significantly perturbed i.e., polluted or dewatered. Restoration is the return of the river ecosystem to its predisturbance, or "wild" condition. Rehabilitation is the reestablishment of some attributes of the river ecosystem to their predisturbance condition. In the case of the San Rafael River, complete restoration may not be possible, therefore policy choices must be made to identify which attributes can and should be rehabilitated.